Ocean Acidification and Deoxygenation in the North Pacific Ocean

Ocean Acidification and Deoxygenation in the North Pacific Ocean

Editors:

James Christian (Canada)   **Tsuneo Ono (Japan)**

Lead Authors: Simone Alin (United States), Wiley Evans (Canada),
Zhongyong Gao (China), Helen Gurney-Smith (Canada),
Kitack Lee (Korea), Pavel Tishchenko (Russia)

Contributing Authors: Nina Bednaršek (United States), Richard Feely (United States),
Masahiko Fujii (Japan), J. Martín Hernández Ayón (Mexico),
Masao Ishii (Japan), Lisa Miller (Canada), Gregor Reid (Canada),
Tetjana Ross (Canada), Heng Sun (China), Shintaro Takao (Japan)

Citation Instructions

The views expressed in this volume are those of the
participating scientists. Contributions were edited for
brevity, relevance, language, and style and any errors that
were introduced were done so inadvertently.

Project Designer
Lori Waters
Waters Biomedical Communications
Victoria, BC, Canada

Feedback

Comments on this volume are welcome and can be sent via
email to: secretariat@pices.int
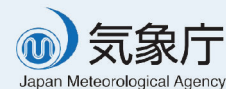
Published by the

Front cover images: top: Moira Galbraith, bottom: Hiroya Yamano.

CONTENTS
Ocean Acidification and Deoxygenation in the North Pacific Ocean

The FUTURE Science Program of PICES

FUTURE (Forecasting and Understanding Trends, Uncertainty and Responses of North Pacific Marine Ecosystems) is an integrative Scientific Program undertaken by the member countries and affiliates of the North Pacific Marine Science Organization (PICES) to understand how marine ecosystems in the North Pacific respond to climate change and human activities, to forecast ecosystem status based on a contemporary understanding of how nature functions, and to communicate new insights to its members, governments, stakeholders, and the public.
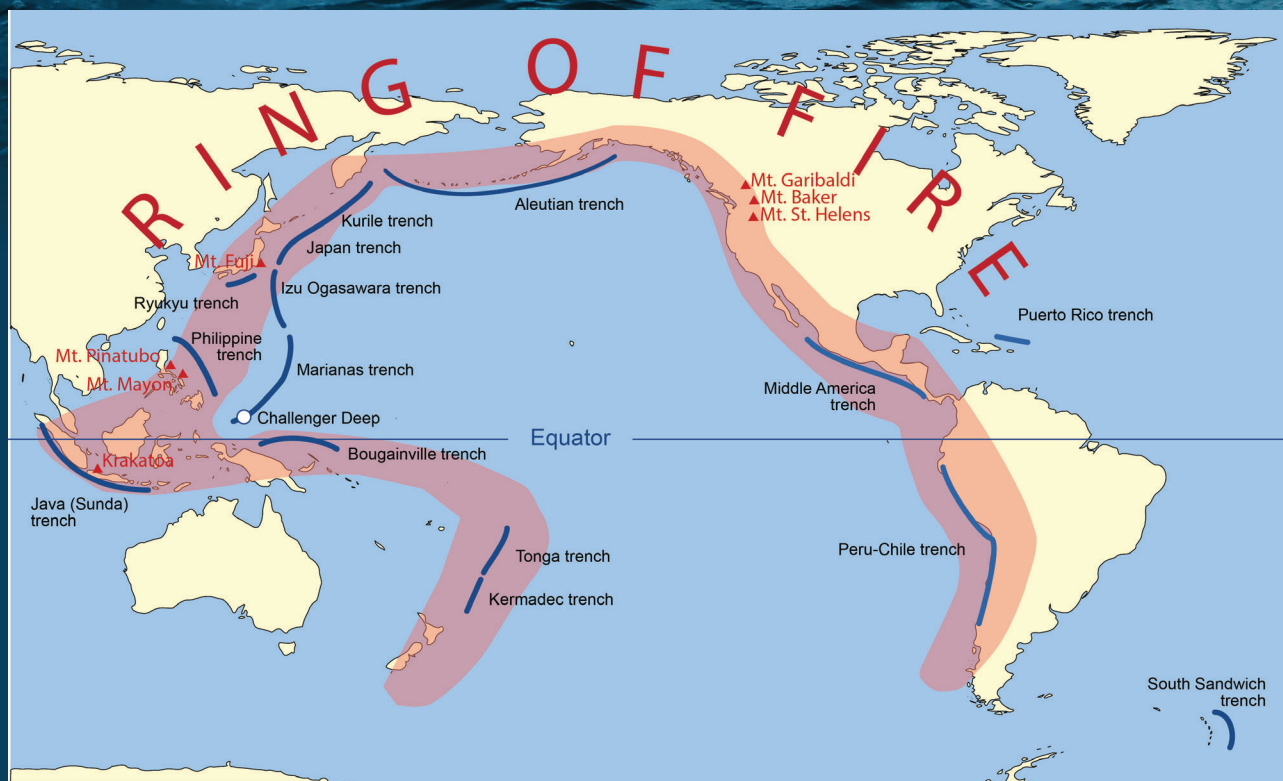
FUTURE evolved from research conducted by its predecessor, the PICES/GLOBEC Climate Change and Carrying Capacity program, which had the goal of increasing understanding of climate influences on marine ecosystems. FUTURE continues a focus on understanding climate impacts on marine ecosystems and places additional emphasis on coastal anthropogenic influences, ecosystem forecasting, and engaging a broad user community with interests in North Pacific ecological and climate information.

This PICES Special Publication on ocean acidification and ocean deoxygenation is an important contribution to FUTURE's principal objective of improving our knowledge and communication of the future of North Pacific ecosystems and the potential impacts of human activities on the North Pacific.

The waters of the Ring of Fire

The North Pacific Ocean is surrounded by the "Ring of Fire": almost all of the coastal regions are mountainous, and volcanoes and earthquakes are plentiful. This might not seem at first glance to have a lot to do with ocean chemistry, but it does. Firstly, the morphology of the ocean basin determines ocean circulation, e.g., there is no exchange between surface and deep waters as there is in the North Atlantic (see Chapter 2). Secondly, the mountains generate huge amounts of precipitation and create cold climates for glacier growth, giving a very different coastal ocean environment than would exist in a less mountainous region. Precipitation also contributes to the strong stratification that prevents exchange between surface and deep waters. Third, partially submerged mountain ranges like the Aleutian and Kuril island chains cause huge amounts of energy associated with tidal currents to be dissipated through mixing, which radically changes water properties throughout the ocean basin (see Chapters 2 and 4). Finally, the topography created by these mountain-building processes created the East Asian marginal seas, a vast region of semi-enclosed basins from which humans have harvested fish and other sea life for millennia.

RING OF FIRE

- Aleutian trench
- Kurile trench
- Japan trench
- Mt. Fuji
- Izu Ogasawara trench
- Ryukyu trench
- Philippine trench
- Mt. Pinatubo
- Mt. Mayon
- Marianas trench
- Challenger Deep
- Krakatoa
- Bougainville trench
- Java (Sunda) trench
- Tonga trench
- Kermadec trench
- Mt. Garibaldi
- Mt. Baker
- Mt. St. Helens
- Puerto Rico trench
- Middle America trench
- Peru-Chile trench
- South Sandwich trench

Equator

[7]

[1] Ocean acidification and deoxygenation
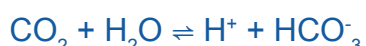
- Ocean acidification is caused by uptake of excess carbon dioxide (CO_2) from the atmosphere. CO_2 reacts with seawater (H_2O) to produce carbonic acid, which undergoes dissociation, producing excess protons (acidity).

- Ocean acidification results in an ocean more undersaturated with respect to the calcium carbonate minerals that marine animals use to build their shells and exoskeletons. This means that the energy cost of creating these structures increases, and in extreme cases shells can dissolve.

- Ocean deoxygenation is caused by increasing sea surface temperature. Because the solubility of oxygen (O_2) is lower in warmer water, a warming ocean means that water transported into the ocean interior (oxygen is effectively saturated at the surface) will have less oxygen at the beginning of its transit than it would have in a cooler climate.

- Warming of surface water causes stratification of the upper ocean and thus reduces transport of surface water into the ocean interior (ventilation). This increases deoxygenation in the ocean interior where organisms consume oxygen by respiration of organic matter.

Anthropogenic CO_2

In preindustrial times, the concentration of CO_2 in the atmosphere was about 280 parts per million (ppm), and this concentration had remained stable for thousands of years. Over the previous million years or so, the concentration fluctuated between about 180 ppm (glacial) and 280 ppm (interglacial), as the 100,000 year glacial-interglacial cycle dominates recent Earth history (Imbrie et al., 1992). So when anthropogenic CO_2 emissions began on a large scale, the concentration was already at its highest point in recent Earth history. It has increased exponentially since, reaching 400 ppm for the first time around 2012 (the global annual mean did not exceed 400 ppm until 2016). Of the approximately 600 petagrams (one petagram = one billion metric tonnes) of cumulative human carbon emissions since 1800, about one third is now dissolved in the oceans.

Ocean carbon chemistry

The key equilibria of ocean carbon chemistry are:

$$CO_2 + H_2O \rightleftharpoons H^+ + HCO_3^-$$

$$HCO_3^- \rightleftharpoons H^+ + CO_3^{2-}$$

i.e., when CO_2 dissolves, it reacts with water to form bicarbonate (HCO_3^-) which further dissociates to form carbonate (CO_3^{2-}), each step releasing one H^+ (acidity). CO_3^{2-} combines with Ca^{2+} ions to form $CaCO_3$, which is the key biogenic mineral in the shells of bivalves and other calcareous organisms. The measurable parameters of ocean carbon chemistry are dissolved inorganic carbon (DIC), total alkalinity (TA), pH, and dissolved CO_2 concentration.
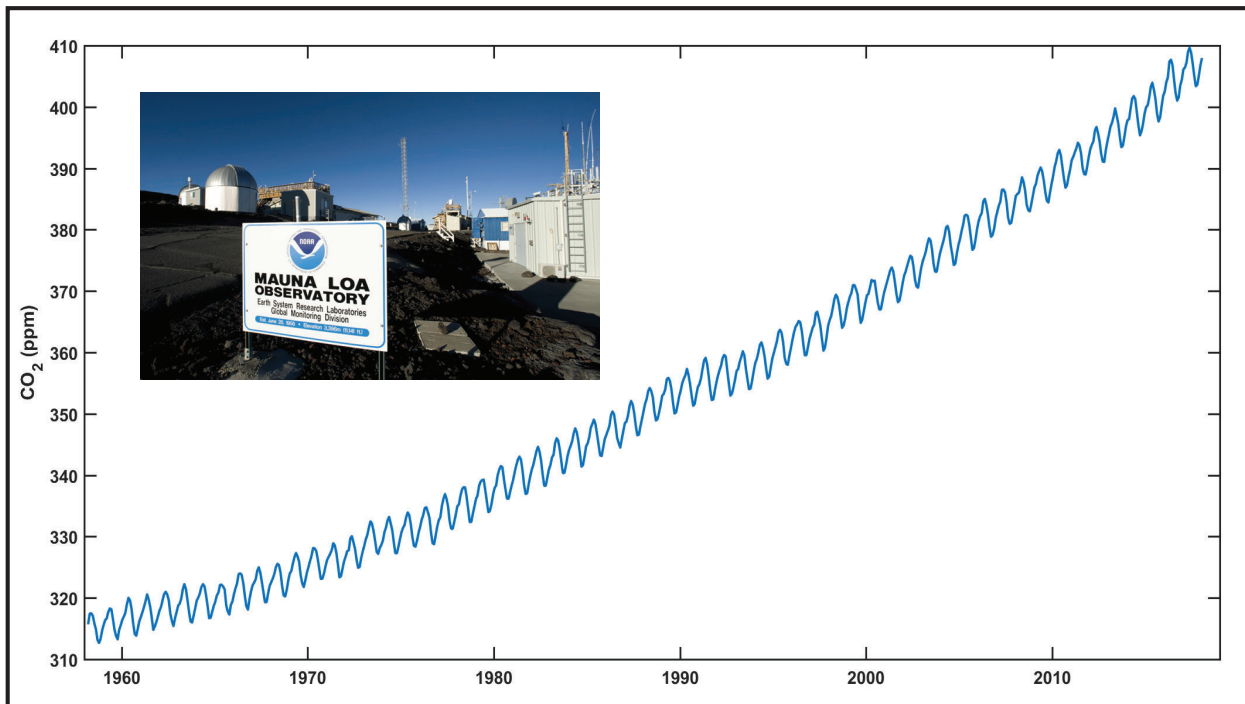
$$DIC = CO_2 + HCO_3^- + CO_3^{2-}$$

DIC is about 90% HCO_3^-, 10% CO_3^{2-}, and 1% dissolved CO_2. As the total DIC increases and the ocean becomes more acidic, the fraction of HCO_3^- increases and that of CO_3^{2-} decreases, with the net result that the concentration of CO_3^{2-} decreases even as the total DIC increases. It is primarily the loss of CO_3^{2-} that stresses calcareous organisms. Naively, one might assume that adding CO_2 would increase CO_3^{2-}, but actually the opposite is true.

DIC is produced in the ocean interior from respiration of organic carbon and dissolution of carbonate minerals, and at the surface from air-sea exchange of atmospheric CO_2.

Alkalinity is a measure of the charge balance of seawater (difference between total proton donors and total proton acceptors) and is often considered a measure of 'buffering capacity', i.e., the higher the alkalinity, the more acid you would have to add to change the pH by, e.g., 0.01 unit. Alkalinity is removed from seawater when carbonate minerals precipitate and is added when they dissolve.

[9]

[Figure 1-1] Atmospheric CO_2 concentration measured at Mauna Loa, Hawaii. Data courtesy of National Oceanic and Atmospheric Administration (US) Earth System Research Laboratory. Inset: Mauna Loa Observatory, Hawaii.

Much of the variation of DIC and alkalinity at the surface is related to fresh water fluxes (i.e., addition of freshwater from rain or runoff, or loss of freshwater to evaporation). Therefore, DIC and TA are sometimes expressed as their values normalized to constant salinity of, e.g., 35.

$$nDIC = DIC \times 35/S$$
$$nTA = TA \times 35/S$$

(Salinity (S) is the mass of salt in a volume of water expressed in kg of salt per cubic metre (1000 kg) of water; open ocean water usually has a salinity of 32-35.)

This helps us to understand net biological sources and sinks, which may be much smaller locally than the change due to concentration/dilution.

If you know any two of DIC, TA, pH, and pCO_2, plus the temperature (T) and salinity (S), you can calculate the other two, and the carbonate system is said to be 'closed', e.g.,

$$[CO_2] = f\,(T, S, DIC, TA)$$
$$DIC = f\,(T, S, [CO_2], TA)$$
$$TA = f\,(T, S, [CO_2], pH)$$

6.023×10^{23}

Avogadro's Number The concept of a 'mole' is fundamental to chemistry, because it relates the number of molecules actually present to the more familiar, measurable quantities like mass and volume. Avogadro's number (6.023×10^{23}) expresses the number of individual atoms or molecules in a mole of a substance. For example, a mole of water (H_2O) contains one mole (6.023×10^{23} atoms) of oxygen and two moles of hydrogen, and weighs 18 g because oxygen and hydrogen have atomic masses of 16 and 1, respectively. In ocean chemistry it is usual to express concentrations in moles per litre or moles per kg of solution rather than, e.g., in grams per litre. The symbol M indicates moles per litre, so, for example, a nitrate concentration of 30 µM implies 3.0×10^{-5} moles per litre. The mole is one of the seven 'base' units of the Système Internationale (SI).

SI Units The Système Internationale of units of measurement prescribes the kilogram (kg) as the basic unit of mass and the metre (m) as the basic unit of length. Volume is measured in litres which is a derived unit (one litre = 1000 cubic centimetres). In this publication we are mostly discussing molar concentrations or seawater densities in kg m^{-3}. SI prefixes indicate increments of 1000 or 1/1000, such that one microgram (µg) is 10^{-6} g and one petagram (Pg) is 10^{15} g.

Current human emissions of CO_2 are around 10 Pg of carbon or 36 Pg of CO_2 per year. There are 1000 kg in a metric ton, so a Pg of emissions is often colloquially referred to as a 'gigaton'. There are about 750 Pg of carbon currently in the atmosphere and about 38,000 Pg dissolved in the ocean.

Name	Symbol	Power
atto	a	-18
femto	f	-15
pico	p	-12
nano	n	-9
micro	µ	-6
milli	m	-3
kilo	k	3
mega	M	6
giga	G	9
tera	T	12
peta	P	15
exa	E	18

Amedeo Avogadro, Italian Scientist (1776 - 1856) and creator of Avogadro's Law. *Portrait courtesy of Edgar Fahs Smith Memorial Collection, Kislak Center for Special Collections, Rare Books and Manuscripts, University of Pennsylvania.*

[11]

Carbonate minerals

The "saturation state", or Ω, of a carbonate mineral, (e.g., calcium carbonate or $CaCO_3$) is the ratio of the concentrations of its constituent ions in situ to their concentrations at saturation, which is represented by the conditional solubility product, K_{sp}^*.

$$\Omega = \frac{[Ca^{2+}]\,[CO_3^{2-}]}{K_{sp}^*}$$
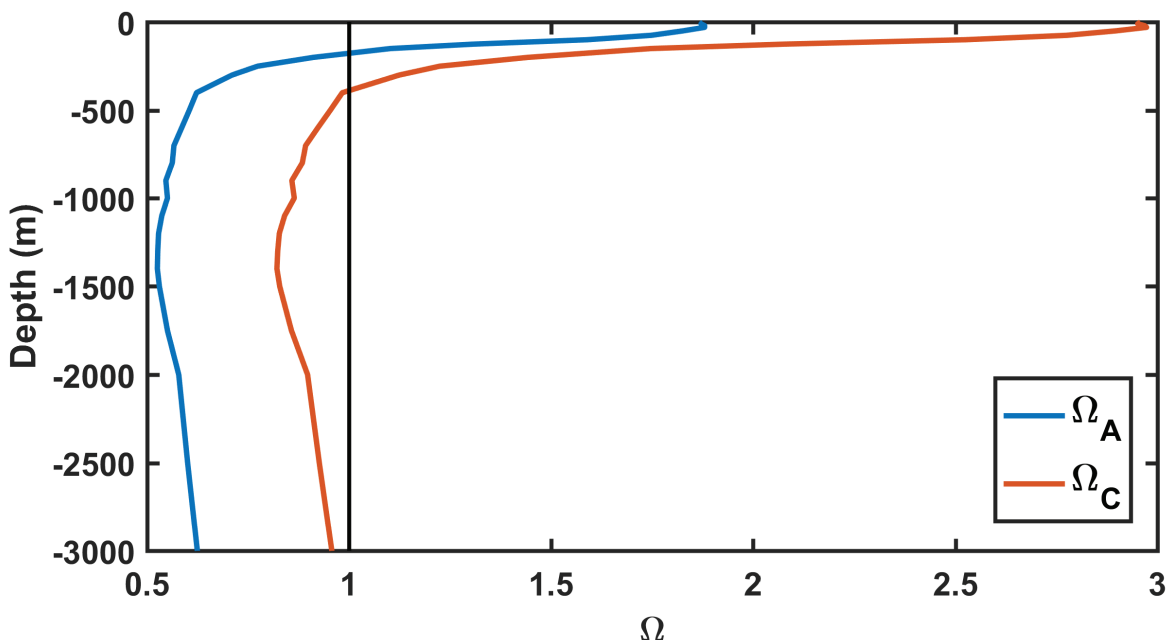
The conditional solubility product is an inherent property of water of a specific temperature, salinity, and pressure (depth), independent of the in situ concentrations.

In theory, minerals precipitate when $\Omega > 1$ and dissolve when $\Omega < 1$. In practice, many organisms have evolved in an environment with much higher Ω, and as Ω declines they become stressed even at values much greater than one. Conversely, some organisms with carbonate minerals in their shells and skeletons can exist for extended periods in environments where $\Omega < 1$ (Maas et al., 2012).

In general, the deep ocean is undersaturated with respect to $CaCO_3$ ($\Omega < 1$), while the surface ocean is supersaturated ($\Omega > 1$). The depth at which $\Omega = 1$ is often referred to as the saturation depth, or saturation horizon. The saturation horizon is much shallower in the North Pacific than in most other parts of the world ocean. Calcite and aragonite are two forms of $CaCO_3$ with the same chemical composition but distinct mineral crystal structures. Most organisms form one or the other. For example, reef-building corals are aragonitic while most bivalves are calcitic. In general, the saturation horizon is deeper for calcite, i.e., calcitic organisms can tolerate a lower CO_3^{2-} concentration than aragonitic ones.

[Figure 1-2] Example profiles of the saturation state of seawater with respect to calcite (Ω_C) and aragonite (Ω_A) at Ocean Station PAPA (50°N, 145°W). Data from GLODAP2 and World Ocean Atlas 2013 courtesy of National Centers for Environmental Information (US).

Ocean deoxygenation
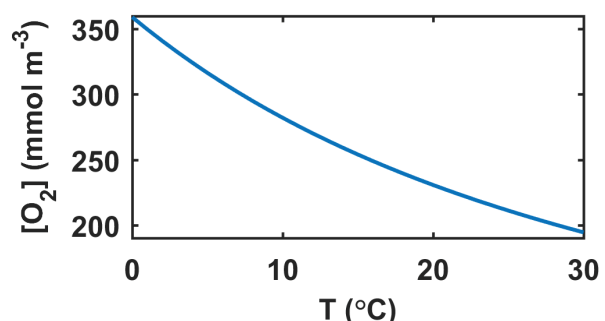
The ocean becomes deoxygenated mainly by increasing surface ocean temperature, with localized contributions from increased rates of oxidation (respiration) of organic matter. Global ocean deoxygenation is a very different process than the localized formation of 'dead zones', e.g., near the mouth of the Mississippi River, which are mostly a consequence of anthropogenic nutrient inputs from land.

Once surface water is transported into the ocean interior, it loses oxygen over time due to respiration. It can only gain oxygen by mixing with other water masses, i.e., there is no net gain to the ocean as a whole.

The important controlling parameter is the temperature at the sea surface when the water was last at the surface (time zero). When the water begins its transit through the ocean interior, the oxygen concentration will be near the saturation concentration.
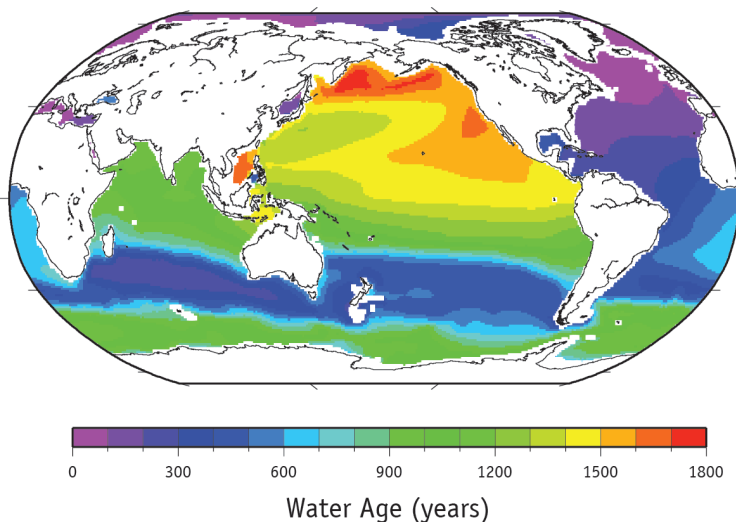
$$O_2sat = f\,(T, S)$$

[Figure 1-3] Saturation concentration of dissolved oxygen in seawater as a function of temperature, for a constant salinity of 35. Calculated according to Weiss (1970).

[13]

[Figure 1-4] Distribution of water age at a depth of 1000 m from an ocean general circulation model simulation. "Ideal age tracer" (England, 1995) concentration after 8000 years of simulation with climatological atmospheric forcing, normalized to a maximum value of 1700 years. Data courtesy of the Canadian Centre for Climate Modelling and Analysis.

Water Age (years)

Because sea surface temperature is increasing globally, if other factors remain the same the oxygen concentration in the ocean interior will decline, because the time zero concentration is less and the rate at which oxygen is lost is about the same.

Changes in the spatial or vertical distribution of organic matter respiration can cause localized deviations from this trend, but globally the amount of organic matter respiration is unlikely to change much (the most likely scenario is that it will decline slightly, e.g., Christian (2014)).

North Pacific oceanography in relation to acidification and deoxygenation
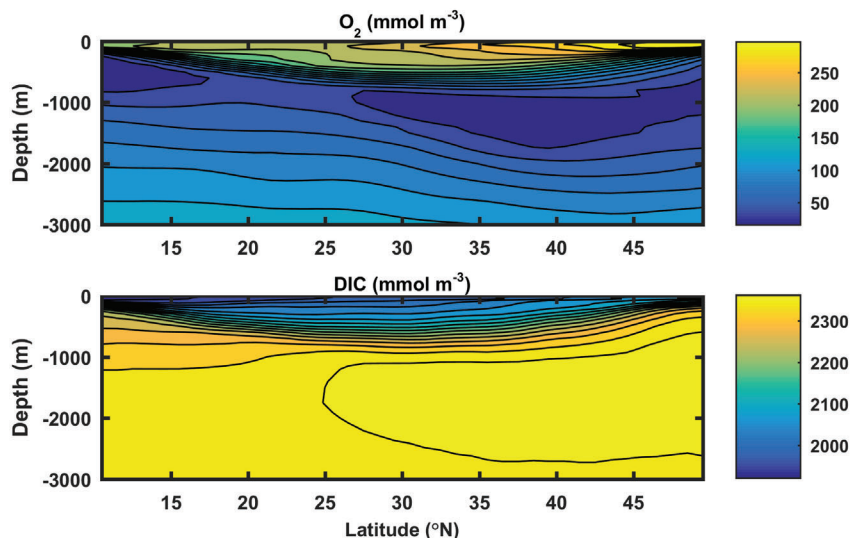
The North Pacific Ocean is unique among the major ocean basins in a number of ways. The subsurface waters are very old, i.e., the time that has passed since the water was last at the surface is much longer than in most others parts of the ocean. This is particularly true in the mid-depth waters, e.g., 200-1200 m. Somewhat counterintuitively, abyssal waters (> 3000 m) are not as old as mid-depth waters, because they are constantly (albeit slowly) renewed with cold, dense, oxygen-rich waters that sink to the abyss in the high latitudes of the Southern Ocean.
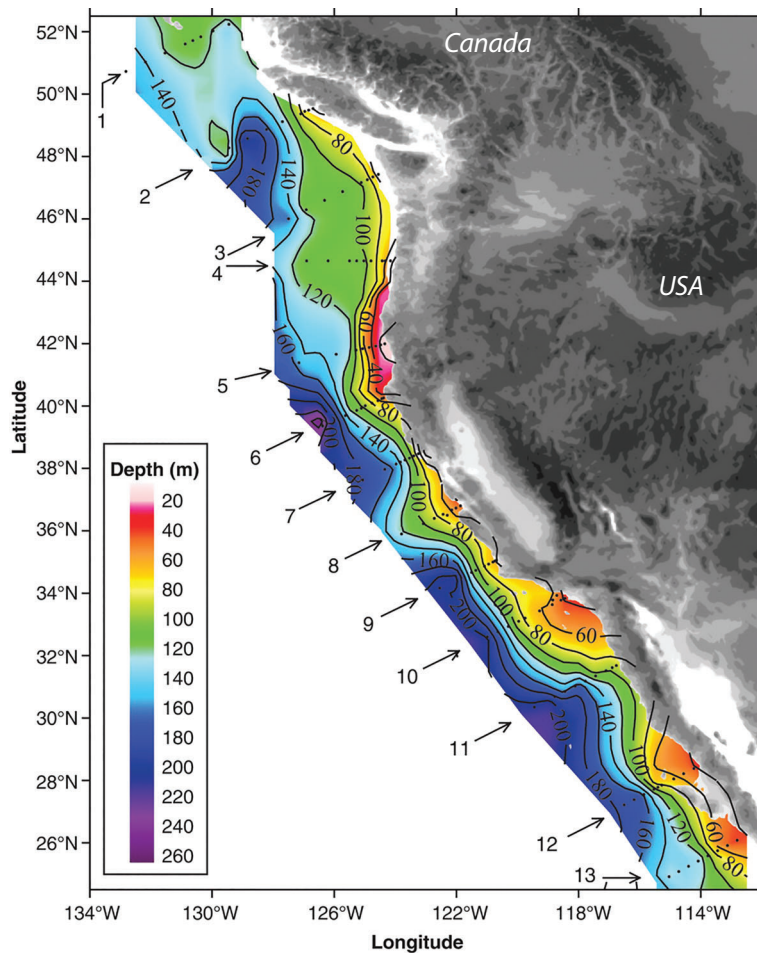
These mid-depth waters are particularly low in O_2 and rich in DIC, i.e., acidic and corrosive to $CaCO_3$ shells. This corrosive water upwells onto the continental shelf along the west coast of North America, and the upper boundary of the corrosive zone is gradually getting shallower because of anthropogenic CO_2.

Surface waters of the northern North Pacific are also fresher than is usual for open ocean waters (high rates of precipitation). Fresher waters have a more limited 'buffering capacity' than saltier ones, meaning that the saturation state will decline more rapidly for a given increase in DIC.

Ocean acidification and deoxygenation are global problems. PICES member countries have responsibility for assessing their extent and effects in the North Pacific Ocean and its marginal seas.

[Figure 1-5] Distribution of dissolved oxygen and total dissolved inorganic carbon (DIC) along 160°W. Data from GLODAP2 and World Ocean Atlas 2013 courtesy of National Centers for Environmental Information (US).

[Figure 1-6] Minimum depth of undersaturated water ($\Omega_A < 1$) on the North American continental shelf in summer 2007. Black dots represent sampling locations. Reproduced with permission from Feely et al. (2008).

"The realization that future global warming might significantly impact ocean O_2 distributions is very recent, dating back only a decade. The science of ocean deoxygenation is thus in its early stages, and progress to date has mostly involved clarifying what is possible or conceivable within large uncertainties." (Keeling et al., 2010)

[15]

What is pH?

A deceptively simple concept that turns out not to be simple at all on close examination. We are all taught in school that lemon juice and vinegar are acidic (pH<7) and ammonia basic (pH>7), while pure water has a pH of 7. But what exactly does pH mean in a complex medium like seawater that contains thousands of different ions, some of them at very high concentrations?

How much salt is there in seawater?

Seawater has a salinity of around 35 kg of salt per 1000 kg (1 cubic metre) of water. The unit is sometimes referred to as 'per mil' (‰) (equivalent to percent, but per thousands rather than hundreds) or simply as 'parts per thousand'. But how do we know much salt there is? Early attempts to determine the salinity of seawater tried to simply evaporate away the water and weigh the salt. But this does not work. How can we be sure we have removed all of the water? If you heat the sample enough to be certain, you will volatilize some of the salts as well.

Today, salinity is normally measured by conductivity: a solution with lots of charged ions will conduct electricity better than a dilute solution. So salinity is often expressed on an operational scale called 'practical salinity units' (psu). For most purposes, the differences among these measures are unimportant and we simply refer to 'salinity',

which has a value of 32-35 in the open ocean, and is near zero in lakes and rivers (anything above 0.5 is considered brackish). Estuaries, of course, can be anywhere in between.

The dependence of electrical conductivity on salinity, or more generally on the ionic strength of a solution, is also the key to why the pH of seawater is hard to measure. Classical methods used for low-ionic-strength solutions do not work for seawater, because the sea salt interferes with the baseline electrochemical potential, which should be both low and stable so you can measure differences from it.
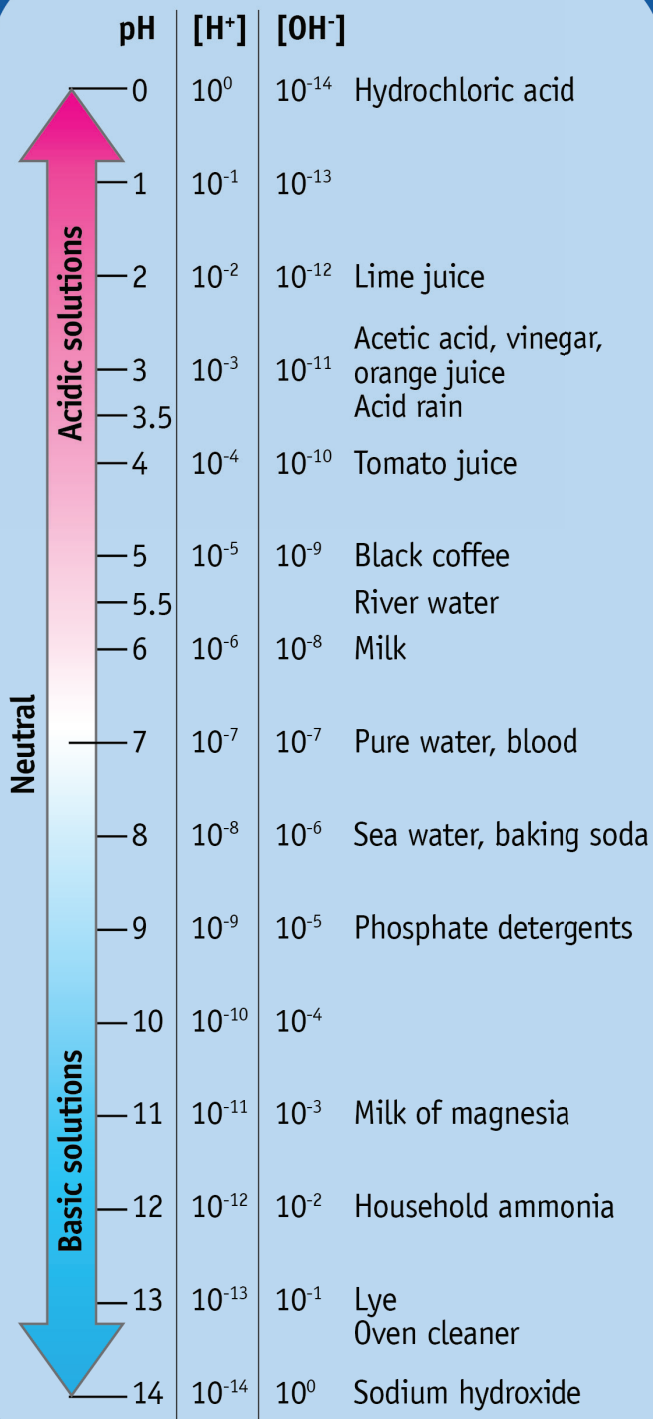
Another method that has been developed for measuring seawater pH employs an indicator dye whose colour changes with the pH of the solution (the same basic principle as litmus paper, but much more precise). This method has been employed extensively by oceanographers since the 1990s. There are two important limitations to this method. The first is that samples must be analyzed immediately: they can not be preserved and stored like samples for DIC or alkalinity. The second is that while the method is very precise, it is not necessarily very accurate.

This is an important distinction in environmental chemistry: precision expresses how noisy your method is; accuracy expresses whether your method actually gives the correct number. Let's say the pH of a sample is 8.100. A method that produces repeat measurements of 8.101, 8.102, and 8.009 is both precise and accurate. A method that generates 8.201, 8.202, and 8.199 is precise, but not accurate, and a method that generates 8.11, 8.12, and 8.09 is accurate but not precise.

The truth is, both salinity and pH are operationally defined. There isn't necessarily a 'true' concentration, as for the total concentration of a specific element like calcium or iron. Modern methods can be both precise and accurate, but real skill and effort are required to realize their full potential.

Biological processes in closed systems can cause very big pH changes, and most of these issues are not important if you are just trying to keep your swimming pool, aquarium, or possibly even fish farm in balance. However, when trying to look at changes in the ocean, including anthropogenic ocean acidification, extremely precise and accurate analyses are required in order to confidently identify the relatively small changes occurring. Surface ocean pH is thought to be changing, on average, at a rate of about 0.002 per year. The standard electrochemical method for seawater has an optimum precision of 0.004, while the colourimetric method is at about 0.001. A typical $500 pH meter intended for use in low-salinity waters will have a precision of about 0.01. Lower precision methods can exhibit trends, but only after many data are collected over many years (see Chapter 4c). The pool kit or the cheap hand-held pH probe does not give meaningful pH numbers in seawater.

Credit: creative commons

pH	$[H^+]$	$[OH^-]$	
0	10^0	10^{-14}	Hydrochloric acid
1	10^{-1}	10^{-13}	
2	10^{-2}	10^{-12}	Lime juice
3	10^{-3}	10^{-11}	Acetic acid, vinegar, orange juice
3.5			Acid rain
4	10^{-4}	10^{-10}	Tomato juice
5	10^{-5}	10^{-9}	Black coffee
5.5			River water
6	10^{-6}	10^{-8}	Milk
7	10^{-7}	10^{-7}	Pure water, blood
8	10^{-8}	10^{-6}	Sea water, baking soda
9	10^{-9}	10^{-5}	Phosphate detergents
10	10^{-10}	10^{-4}	
11	10^{-11}	10^{-3}	Milk of magnesia
12	10^{-12}	10^{-2}	Household ammonia
13	10^{-13}	10^{-1}	Lye / Oven cleaner
14	10^{-14}	10^0	Sodium hydroxide

Acidic solutions

Neutral

Basic solutions

[2] ⌈The open ocean⌋

- The Pacific is the largest ocean basin on Earth. The North Pacific represents about 25% of the total ocean area and volume.

- The North Pacific is uniquely vulnerable to ocean acidification and deoxygenation because its large oxygen minimum zone (OMZ) has naturally low O_2, high DIC, and low $CaCO_3$ saturation states due to accumulated respiration of organic carbon. The waters of the North Pacific OMZ are the oldest in the world ocean (up to 1700 years since last contact with the atmosphere).

- The North Pacific can be roughly divided into the subtropical gyre and the eastern and western subarctic gyres. The circulation and biogeochemistry of the eastern and western subarctic gyres are quite different. The western gyre experiences much deeper convective mixing in winter and much greater seasonality of phytoplankton production and CO_2 concentration. The eastern gyre experiences permanent stratification similar to the subtropical gyre, with convective mixing rarely exceeding 100 m.

Aragonite Saturation Depth

Calcite Saturation Depth
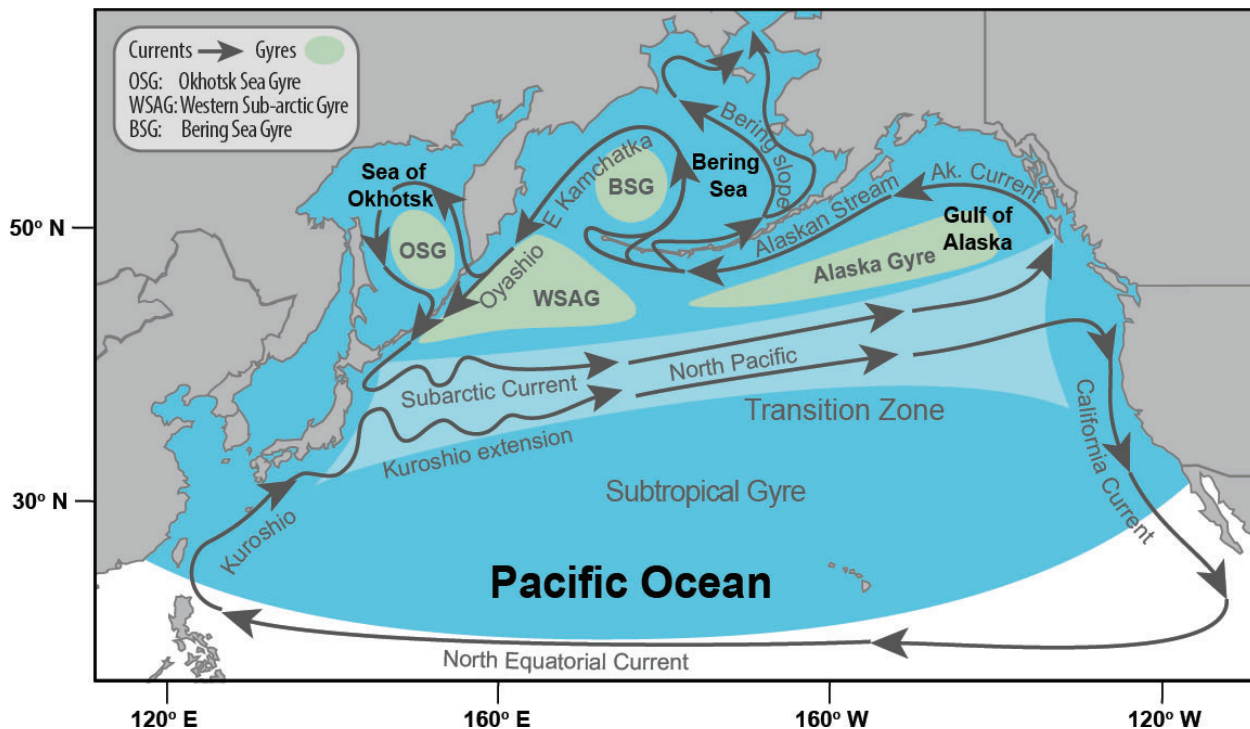
[Figure 2-1] Depth (m) of the saturation horizon (depth at which $\Omega = 1$) for calcite and aragonite. Reproduced with permission from Feely et al. (2004).

Introduction
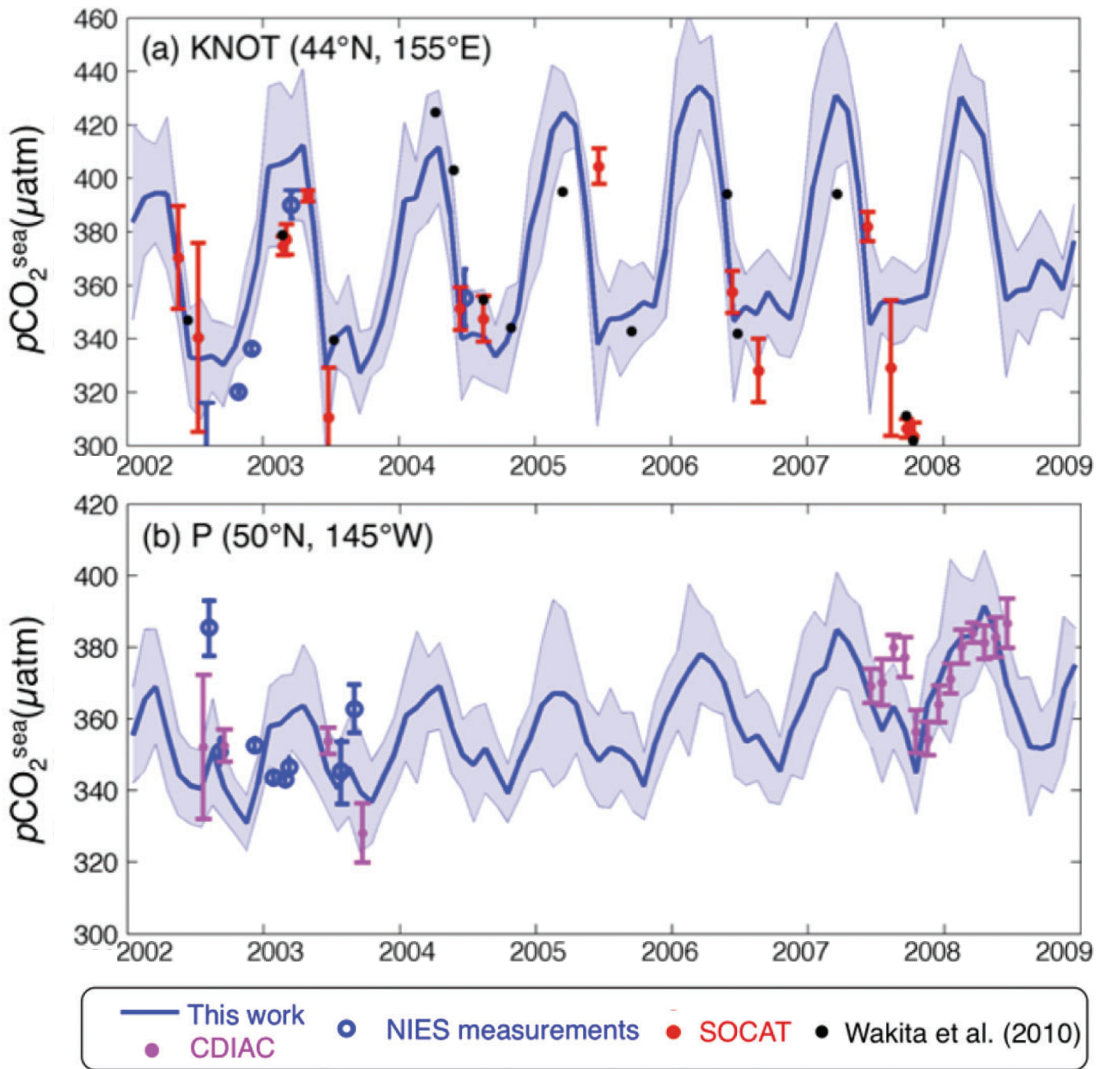
The North Pacific Ocean contains the largest area and volume of low oxygen waters of any major ocean basin. Low oxygen waters are also rich in DIC and have low $CaCO_3$ saturation states (see Chapter 1). As a result, the saturation horizon is much shallower in the northern North Pacific than elsewhere (Figure 2-1).

[19]

[Figure 2-2] Map of the North Pacific and key oceanographic features, including major currents (arrows) and sub-polar gyres (green shaded areas). Modified from Holsman et al. (2018).

The largest part of the North Pacific resides in the subtropical gyre, which has a high saturation state (Ω) in surface waters and a deep thermocline (the thermocline separates surface waters in recent contact with the atmosphere from subsurface waters ranging in age from years to hundreds of years since last contact). The surface waters are warm (>20°C) and salty (more evaporation than precipitation). The seasonal cycle of CO_2 uptake and outgassing in the subtropical gyre is primarily driven by temperature. On top of this seasonal cycle, there is a small net uptake driven by increasing atmospheric CO_2 due to anthropogenic emissions.
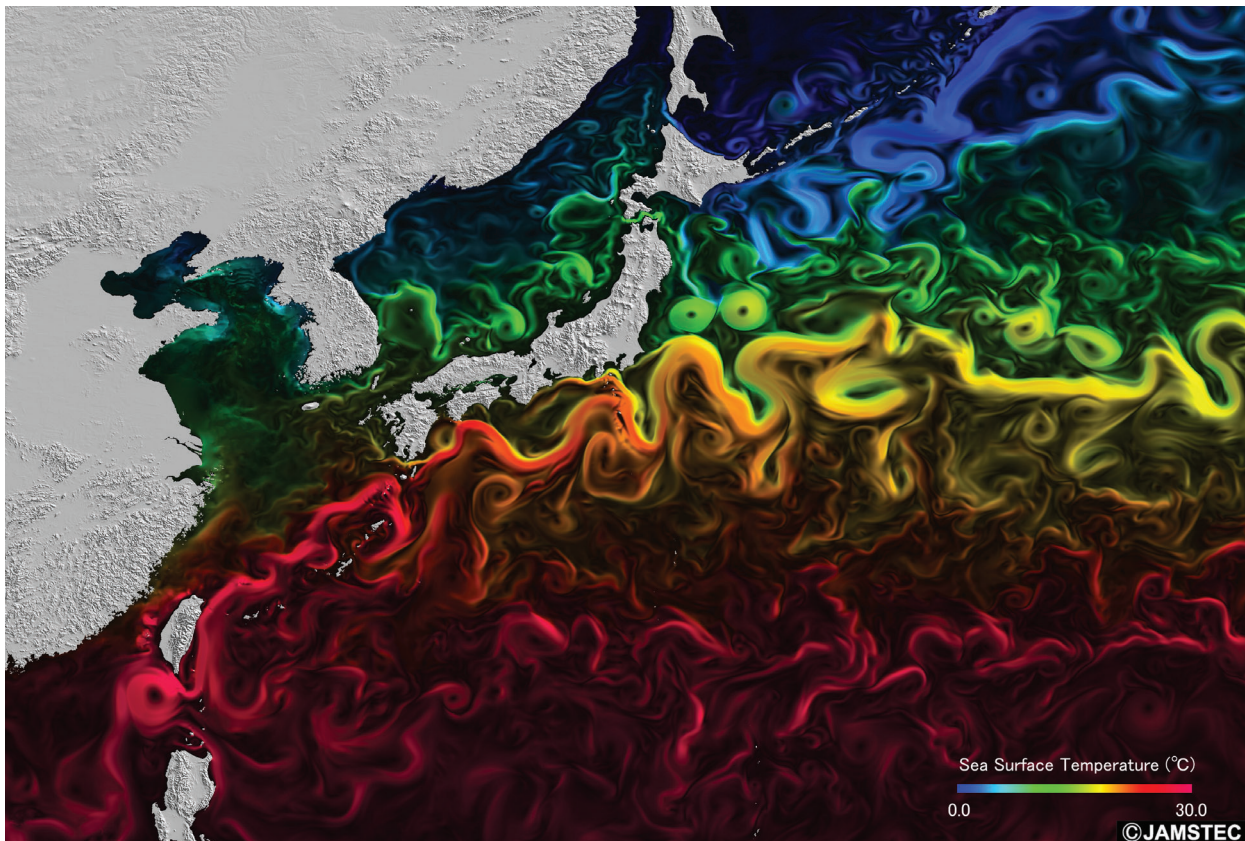
The subarctic gyres represent a smaller region with greater productivity, greater seasonality, and a more spatially complex circulation. The subtropical gyre flows clockwise, and the net vertical flow in the centre is downward, resulting in a deep thermocline and low productivity. The subarctic gyres flow counterclockwise and the net vertical flow is upward, bringing nutrients and DIC to the surface. The eastern (Alaska) gyre nonetheless has a strong, permanent halocline (equivalent to a thermocline, but primarily a gradient of salinity rather than temperature) and relatively low productivity. The western gyre has weaker stratification

[Figure 2-3] Annual cycles of surface ocean pCO$_2$ at Station KNOT in the northwestern North Pacific and Station PAPA in the northeastern North Pacific. Reproduced with permission from Nakaoka et al. (2013).

and much deeper convective mixing in winter, which in turn leads to greater seasonality of productivity, surface CO$_2$ concentration and flux, and CaCO$_3$ saturation state (Figure 2-3). The Kuroshio current, in the western subtropics, is the Pacific equivalent of the Gulf Stream, and brings warm, salty water from the subtropics. The Oyashio, by contrast, brings cold water from the Bering Sea and the Alaska Stream. The meeting of these two currents creates a region of great spatial complexity (Figure 2-4) and high productivity. Japanese fishers in particular have fished these waters for generations.

[21]
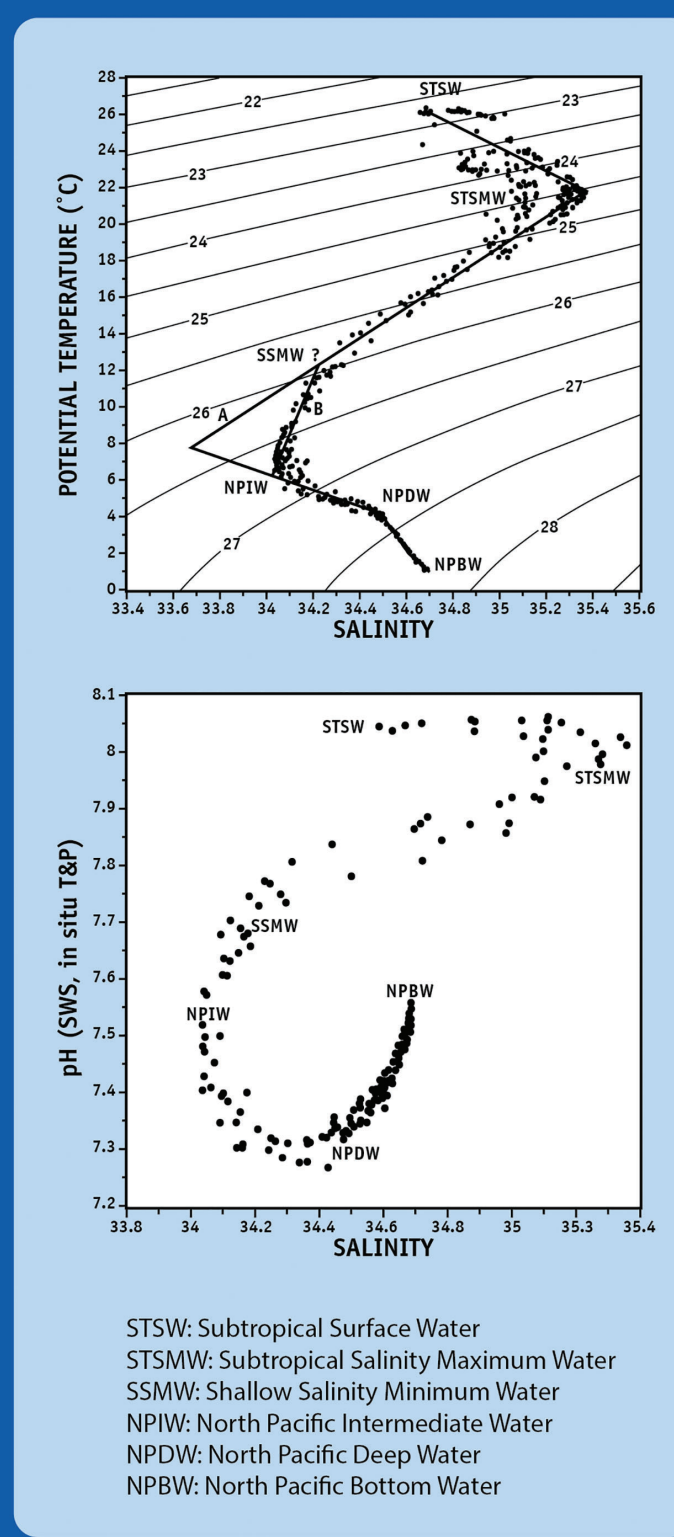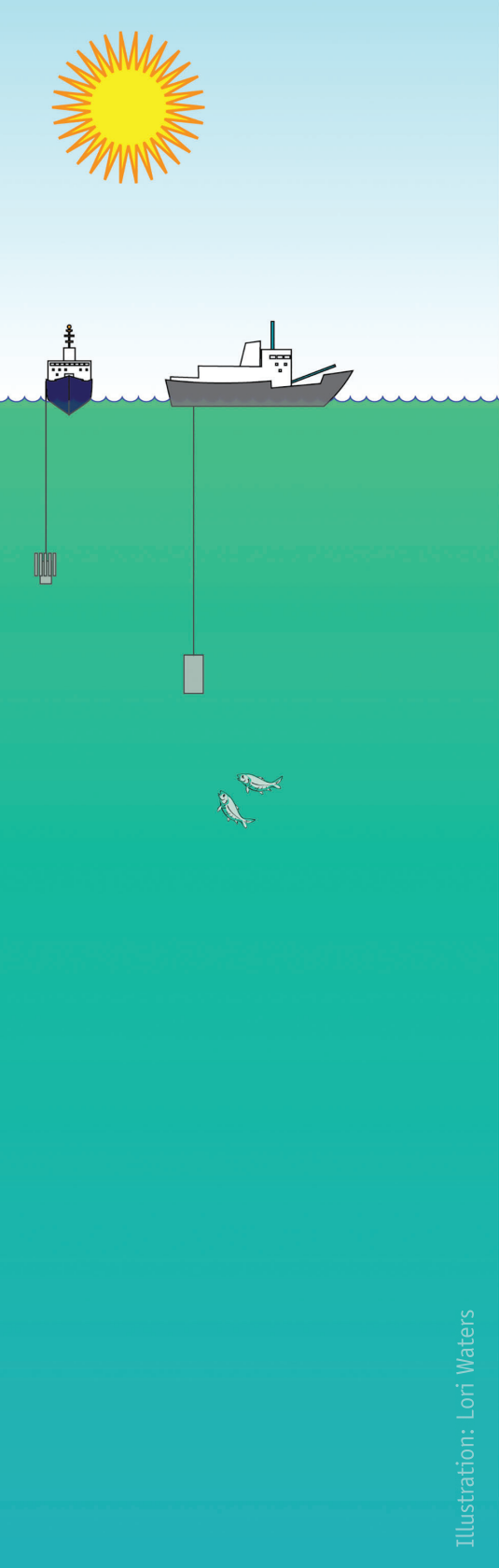
[Figure 2-4] Sea surface temperature in the Kuroshio extension region on April 1, 2001 in a high resolution (1/30°) ocean model simulation. Colour scale is sea surface temperature and colour intensity is proportional to surface current speed. Data from Japan Agency for Marine-Earth Science and Technology (JAMSTEC).
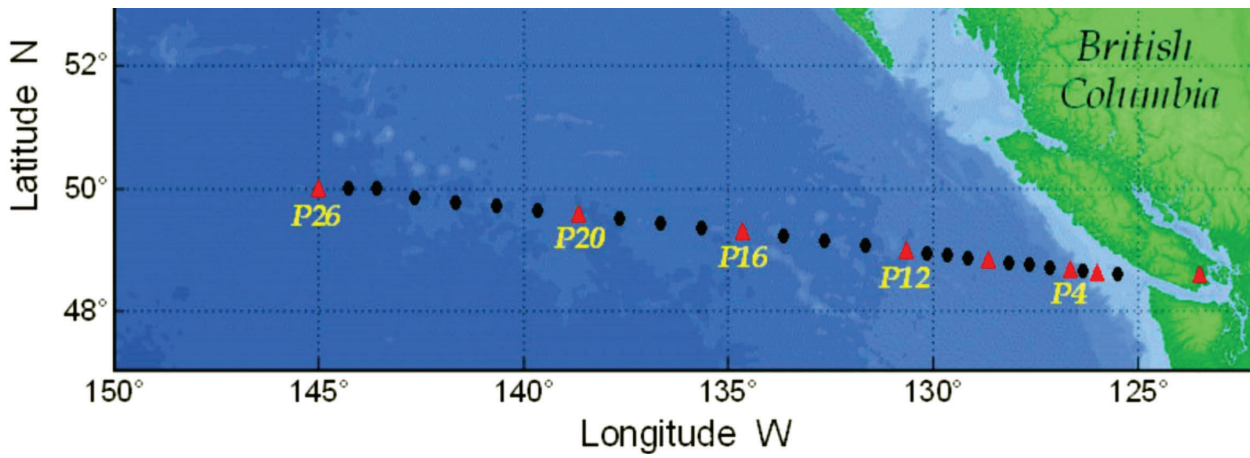
Vertical structure and water masses

The water masses of the North Pacific and their associated chemistry are well illustrated by full depth profiles from Station ALOHA (22°45' N, 158°W) (Figure 2-5). The bottom depth at this location is around 4850 m. North Pacific Intermediate Water is the deepest water that has recently been in contact with the atmosphere, and has higher oxygen and pH than would otherwise be the case at this depth. Subtropical Salinity Maximum Water is also recently ventilated, due to excess evaporation in the subtropics. So at the latitude of Station ALOHA, we see both a salinity maximum (density of about 1024.5 kg m^{-3}, or about 200 m depth) and a salinity minimum (density of about 1026.7 kg m^{-3}, or about 500 m), both of which are 'young' waters, rich in O_2 and poor in DIC. pH declines over this depth range and reaches a minimum in between North Pacific Intermediate Water and North Pacific Deep Water, i.e., the deeper waters are younger than the intermediate ones. The OMZ occurs at a depth of about 700 m at this location (pH minimum of ~7.3 at S~34.35).

STSW: Subtropical Surface Water
STSMW: Subtropical Salinity Maximum Water
SSMW: Shallow Salinity Minimum Water
NPIW: North Pacific Intermediate Water
NPDW: North Pacific Deep Water
NPBW: North Pacific Bottom Water

Illustration: Lori Waters

[Figure 2-5] Depth profiles collected at Station ALOHA (22°45′N, 158°W) illustrate the main water masses of the North Pacific. The upper panel shows where each water type is located in temperature-salinity space (the contour lines are water density: lower values indicate shallower depths). The lower panel shows pH as a function of salinity, indicating how it declines with depth and then increases again in the deepest waters. Reproduced with permission from Sabine et al. (1995).

[23]

[Figure 2-6] Map of sampling stations along Line P in the northeastern North Pacific. Line P is maintained by Fisheries and Oceans Canada and is the longest continuous oceanographic time series in existence. P26 is the long-term observation station elsewhere referred to as Station P or Station PAPA.
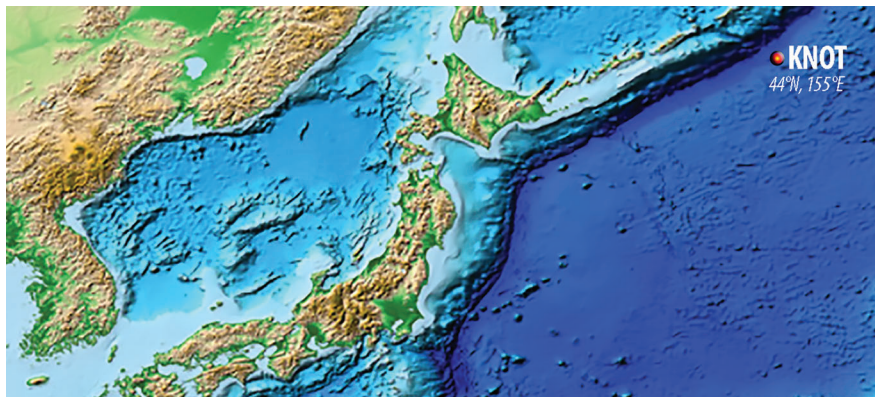
Historical data and trends

Carbon system observations have been made in the open Pacific since the 1970s, but the era of modern methodologies dates to the 1980s, (e.g., Johnson et al., 1985). The 137°E Line (Japan), Line P (Canada), and HOT (United States) are some of the longest running ocean time series programs, and have been making high quality carbon system observations since 1983, 1985, and 1988 respectively. Time series observations have also been made along A-line (1987-2007) and at Station KNOT/K2 (1992-present) in the northwestern Pacific.

The earliest observations are not adequate to fully constrain the carbon system and, e.g., calculate $CaCO_3$ saturation states. For example, on Line P, DIC data date from 1985 but alkalinity only from 1992, and the quality of the alkalinity data is poor before about 2000 (Suzuki et al., 2013).

HOT data have been featured, e.g., in IPCC assessment reports, as the combination of high quality data, frequent sampling (~ 10 times per year), and a long continuous time series clearly indicates the anthropogenic trend. DIC and pCO_2 increase and pH and saturation state decline, with continuous, approximately linear trends over nearly 30 years of observations (Dore et al., 2009; Bates et al., 2014). The subtropical gyre is an environment of relatively low natural variability compared to the subarctic, so the anthropogenic signal is more readily apparent over shorter periods of time (Christian, 2014).

Ocean CO_2 time-series sites have been established at stations KNOT (44°N, 155°E) and K2 (47°N, 160°E) in the western subarctic gyre (Figure 2-7). The annual mean pH in the surface mixed layer at K2 decreased significantly during 1999-2015 at rates of 0.025 ± 0.010 per decade (Wakita et al., 2017). Below the surface mixed
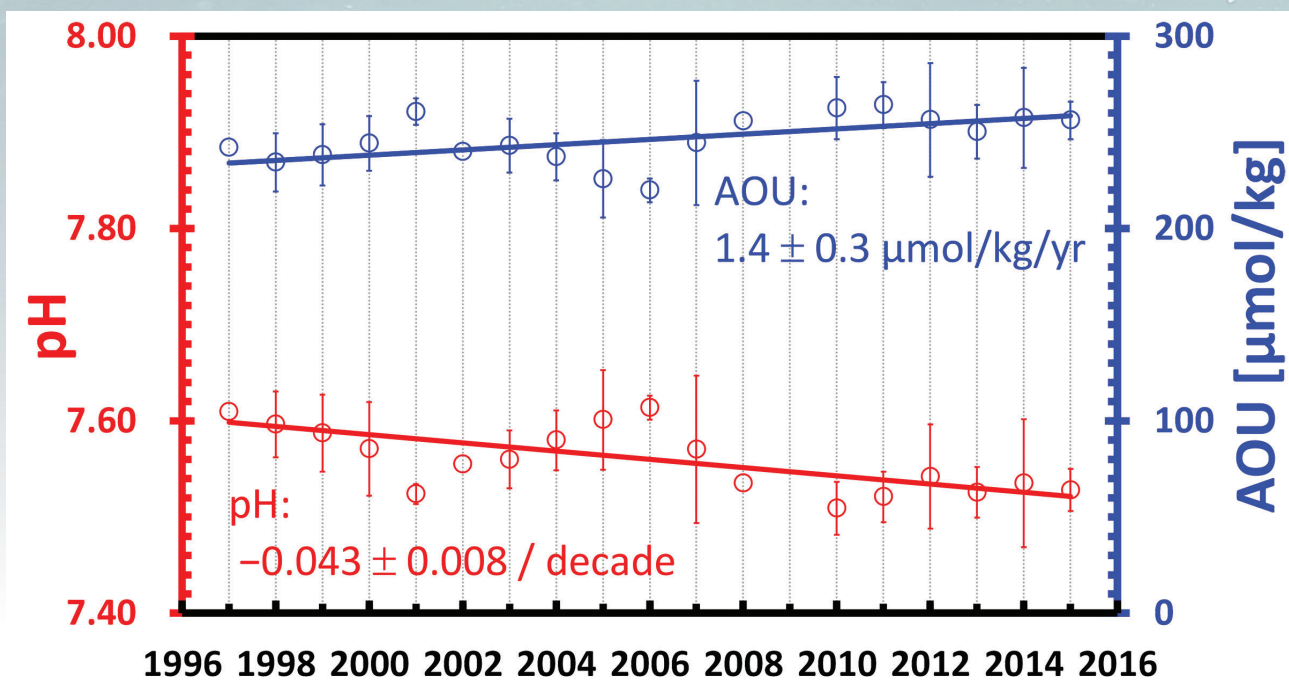
[Figure 2-7] Map illustrating the location of Station KNOT in the northwestern North Pacific. Time series observations are no longer made at Station KNOT but oceanographic cruises occupy it regularly on an opportunistic basis.

layer, pH decreased at a rate of 0.043 ± 0.008 per decade at about 200 m depth (Figure 2-8). This rate is the largest ever reported in the open North Pacific (e.g., Dore et al., 2009). The enhanced pH decline reflects not only ocean uptake of anthropogenic CO_2 but also the increase in remineralization of organic matter, as indicated by the loss of oxygen.
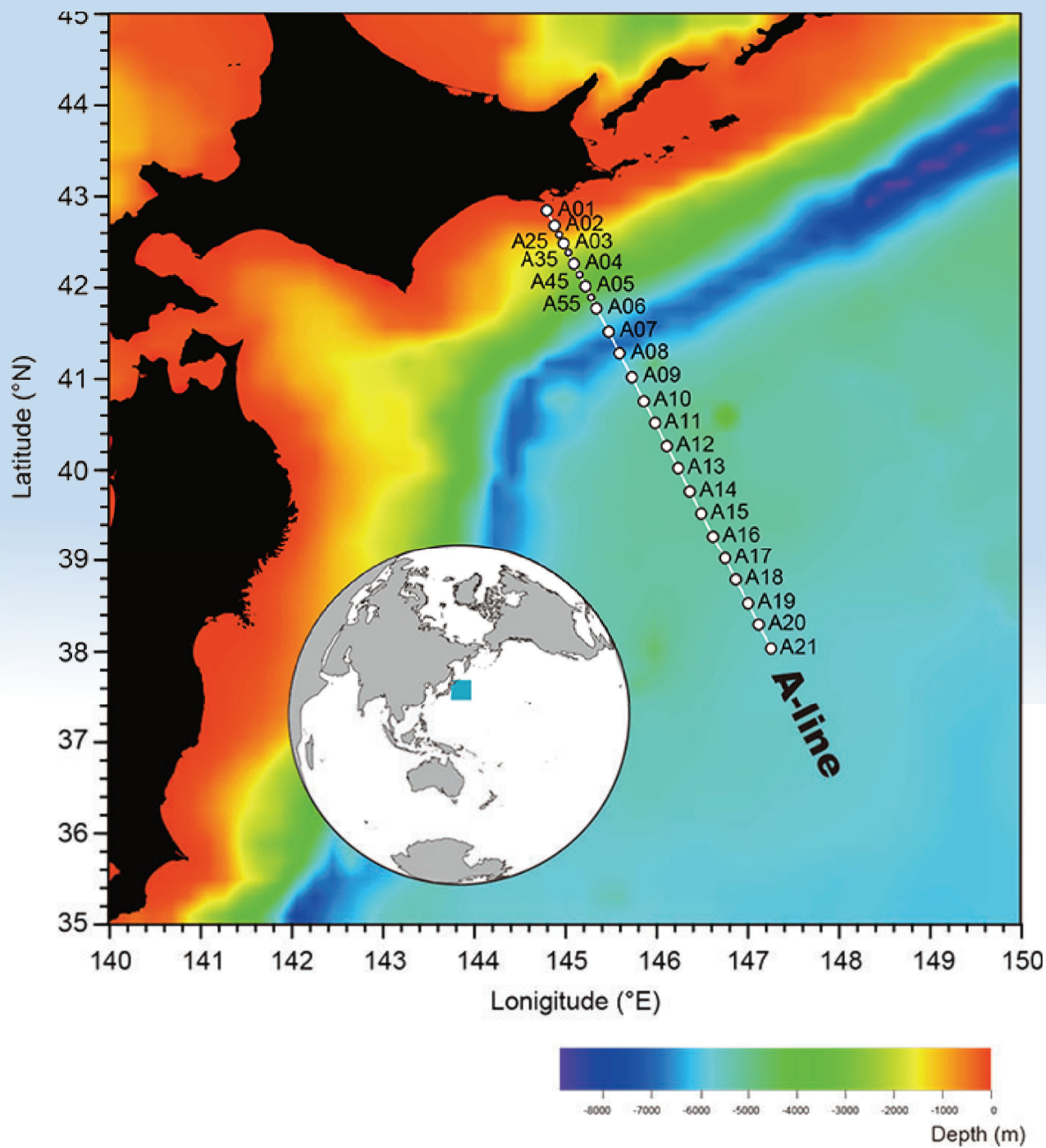
The Japan Meteorological Agency (JMA) has measured CO_2 concentration in surface waters since the 1960s, and DIC since the 1990s. From these data, trends in pH and Ω_A can be estimated. At 137°E, the results show a clear acidification signal, with pH decreasing at rates ranging from 0.015 to 0.021 per decade in winter and from 0.008 to 0.019 per decade in summer. Basin-scale trends in pH can be estimated using pCO_2 data from the Surface Ocean CO_2 Atlas (SOCAT). Iida et al. (2015) constructed equations for global-scale estimation of surface

pCO_2 using SOCAT data. Surface alkalinity in the Pacific can be estimated by using the equation of Takatani et al. (2014), which was estimated from alkalinity data collected in the PACIFICA database (Suzuki et al., 2013). Reconstructed monthly pH of Pacific surface water since the 1990s shows a basin-scale pH trend of -0.016 per decade.
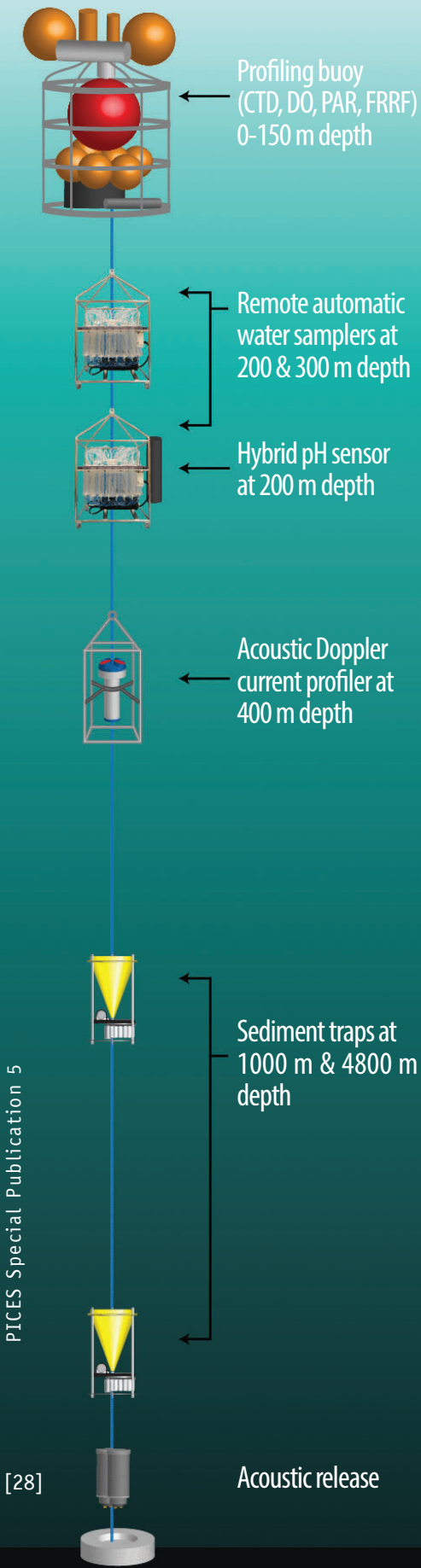
Line P oxygen data constitute possibly the longest open ocean biogeochemical time series available anywhere in the world ocean, reaching back to the 1950s (Whitney et al., 2007). These data show unequivocal evidence of a long-term downward trend (Figure 2-13). A long-term record of oxygen back to the 1950s is also available in the Oyashio region off northern Japan (Sasano et al., 2018). These data show a long-term downward trend with bidecadal oscillations (see Box on p. 62) on various density horizons (Figure 2-14).

[25]

[Figure 2-8] Time-series of pH (red) and apparent oxygen utilization (AOU) (blue) on the 1026.9 kg m^{-3} density surface (about 200 m depth) in the western subarctic region. This figure updates results from Wakita et al. (2013) by adding data from 2012 to 2015. Linear trends are statistically significant (p < 0.001) in both cases. AOU is the estimated cumulative loss of oxygen due to respiration since the water mass was last in contact with the atmosphere.

[Figure 2-9] Map of sampling stations along the A-Line in the northwestern North Pacific. A-Line is maintained by the Japan Fisheries Research and Education Agency, Tohoku National Fisheries Research Institute, Hokkaido National Fisheries Research Institute, and National Research Institute of Fisheries Science. Observations have been made along the A-Line since 1987.

Profiling buoy
(CTD, DO, PAR, FRRF)
0-150 m depth

Remote automatic
water samplers at
200 & 300 m depth

Hybrid pH sensor
at 200 m depth

Acoustic Doppler
current profiler at
400 m depth

Sediment traps at
1000 m & 4800 m
depth

Acoustic release

Illustration: Lori Waters
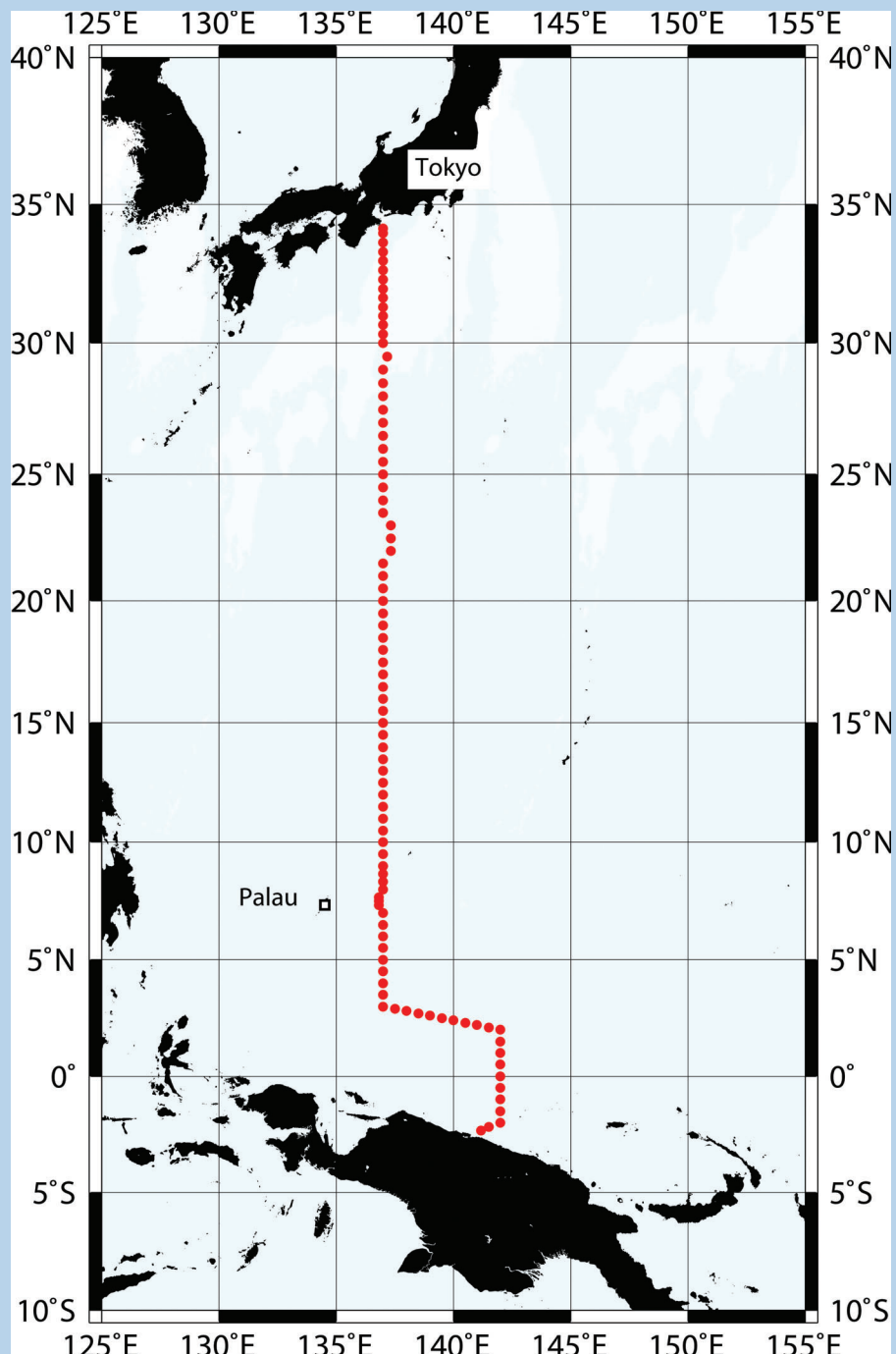
An in situ automated profiling system for ocean acidification research in the western subarctic gyre

As part of its program of ocean acidification research in the subarctic North Pacific, JAMSTEC has been conducting research at time-series station K2 in the subarctic western North Pacific.
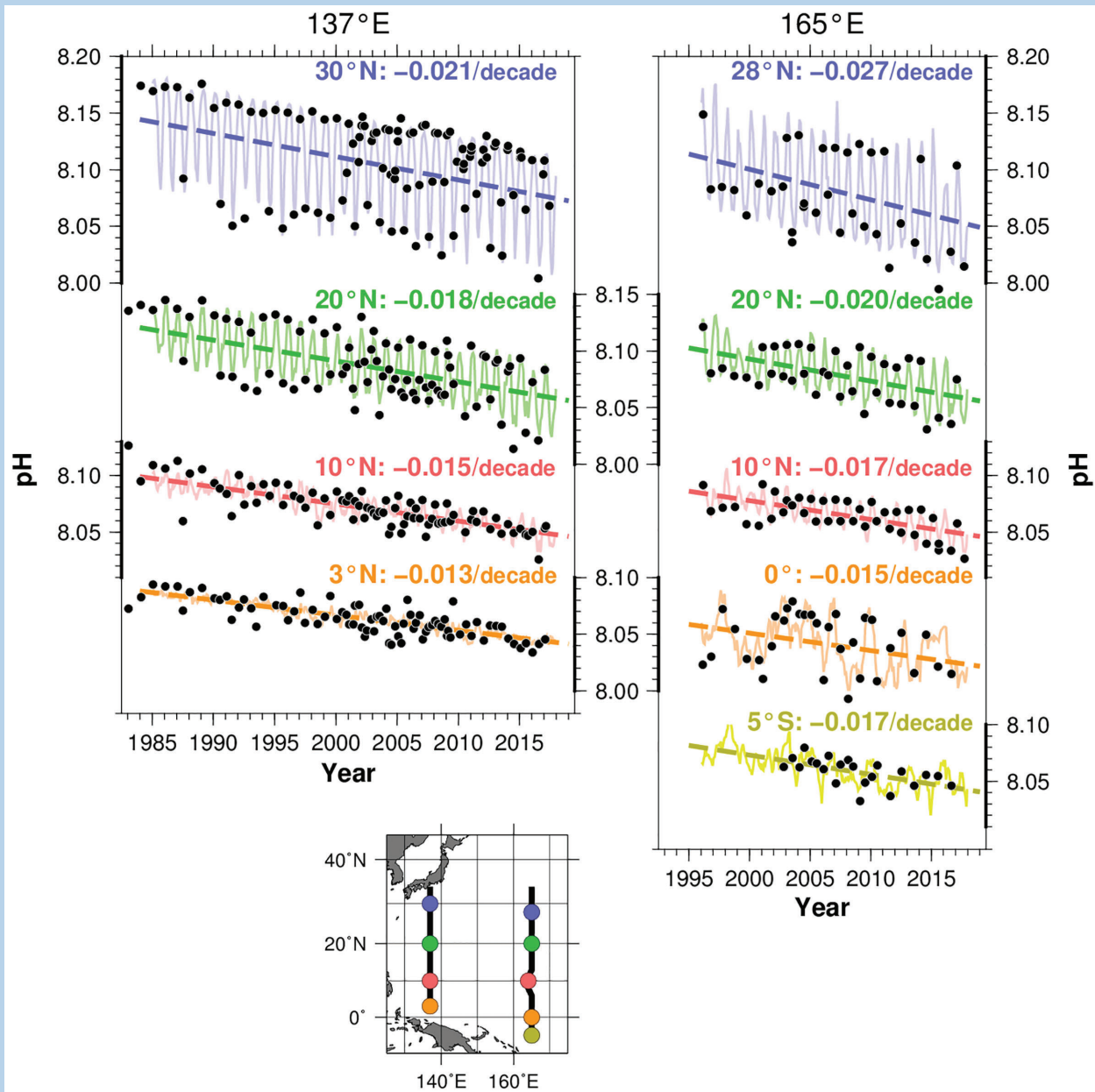
In conjunction with ship-based studies, a moored profiling buoy system has been deployed at K2 since 2015. The profiler measures temperature, salinity, oxygen, solar irradiance and Fast Repetition Rate Fluorometry (a measure of phytoplankton physiological state).

Additional instrumentation deployed at fixed depths on the mooring includes a remote automatic water sampler, a pH sensor, an acoustic Doppler current profiler, and sediment traps. Focal areas for this research include:
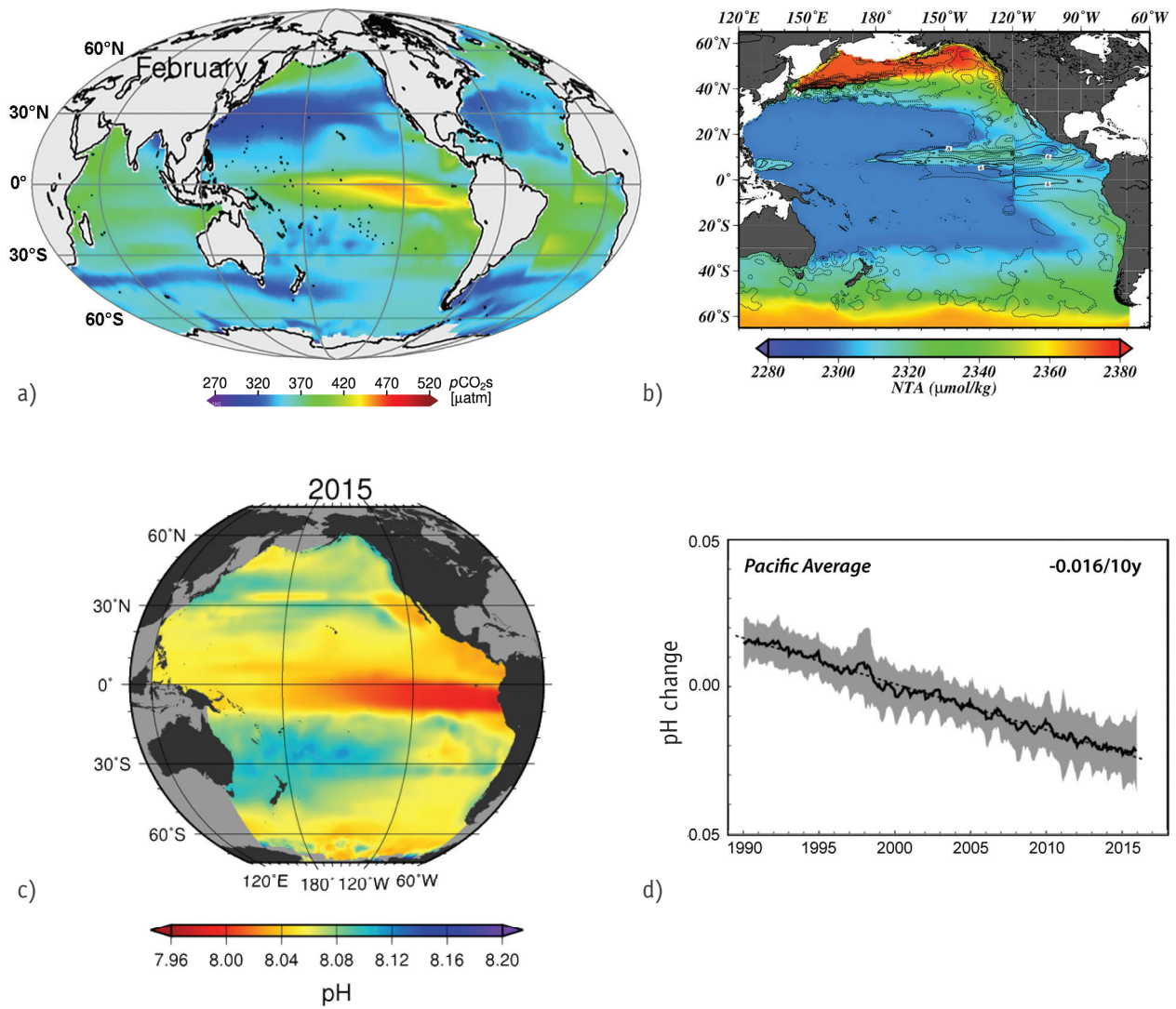
- The relationship between the plankton community and ocean acidification
- Measurements of carbonate shell density of planktonic foraminiferans and pteropods by Micro-focus X-ray Computed Tomography
- Assessment of impacts of ocean acidification on marine organisms based on dissolved chemical constituents
- Physical factors related to the progress of ocean acidification
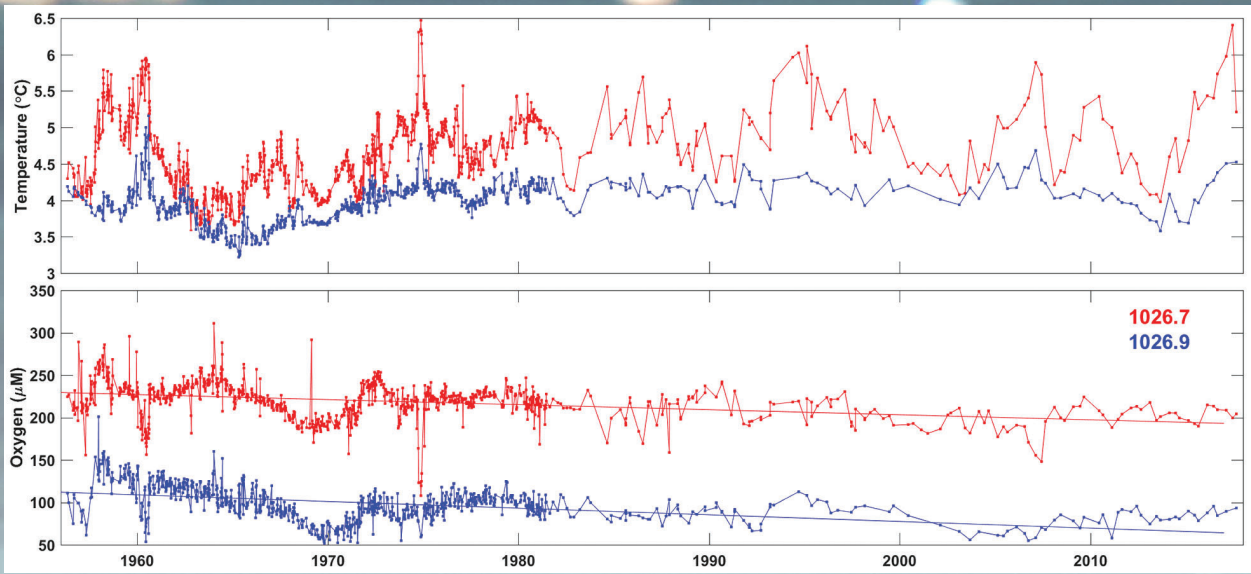
[Figure 2-10] Map of sampling stations along the 137°E line in the western North Pacific. The 137°E line is maintained by the Japan Meteorological Agency and is one of the longest continuous oceanographic time series in the world. Measurements of surface ocean CO_2 concentration have been made along 137°E since 1983. Time-latitude distributions of hydrographic stations occupied in winter and summer along 137°E are available in Oka et al., 2018.
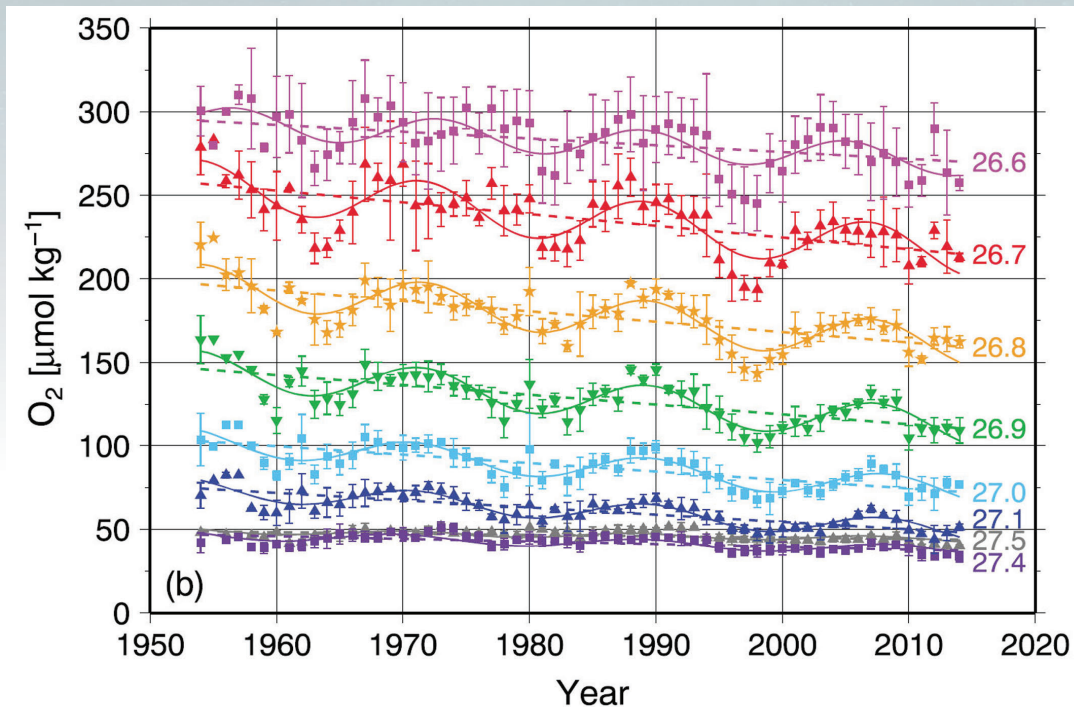
[Figure 2-11] Surface pH trends at 137°E and 165°E. pH at in situ temperature (solid black circles) was calculated from measurements of pCO$_2$, temperature and salinity at nTA=2299 µmol kg^{-1} (Takatani et al., 2014). Solid coloured lines and dashed lines represent reconstructed monthly pH and long-term linear trends, respectively (Ishii et al., 2011). Data from Japan Meteorological Agency.
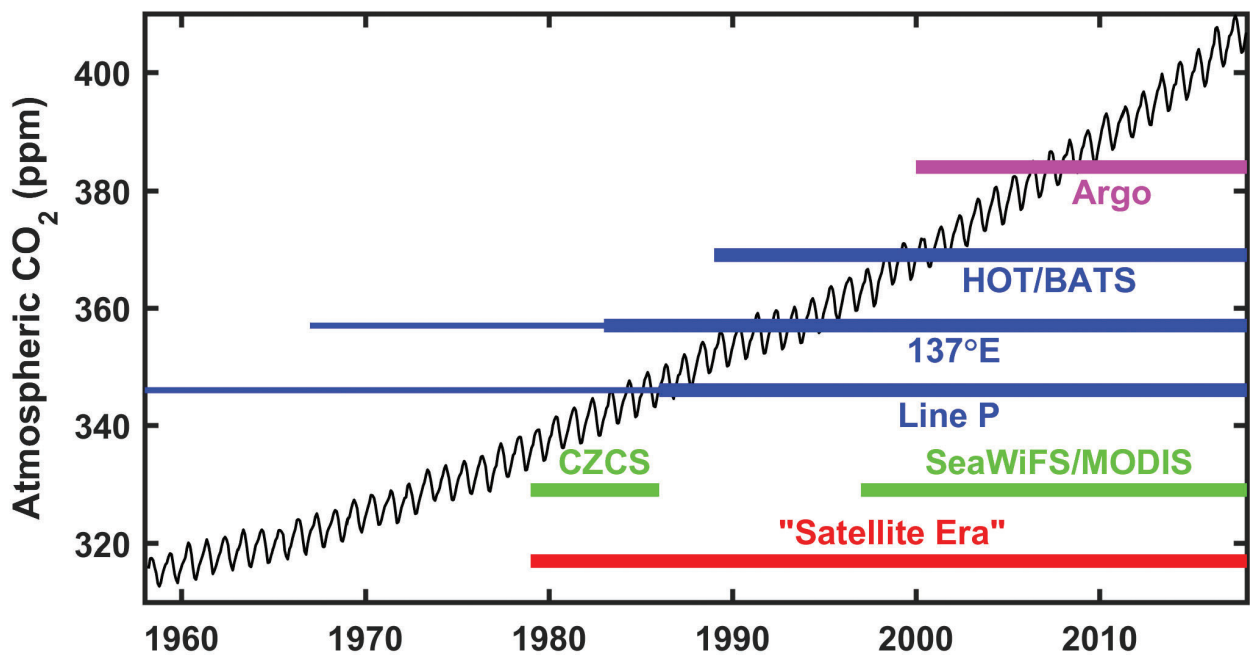
[Figure 2-12] (a) Global pCO$_2$ estimates from Iida et al. (2015), (b) Pacific nTA estimates from Takatani et al. (2014) (c) Pacific annual mean pH estimate, (d) change in average pH over time. Similar to 137°E, the basin-scale pH trend can be estimated using basin-scale pCO$_2$ data (SOCAT). Iida et al. (2015) constructed equations for global-scale estimation of surface pCO$_2$ using SOCAT data. Surface alkalinity in the Pacific Ocean can be estimated using the method of Takatani et al. (2014), which is based on alkalinity data in the PACIFICA database (Suzuki et al., 2013). JMA has reconstructed monthly averaged pH of Pacific surface water since the 1990s, which shows the basin-scale progress of acidification, with a pH trend of -0.016 per decade.

[Figure 2-13] Long-term trends in temperature and dissolved oxygen concentration at Ocean Station PAPA (50°N, 145°W) (individual profile concentrations plus linear trend calculated over 1956-2017). Colours represent different depths represented by water densities of 1026.7 (red) and 1026.9 (blue) kg m^{-3}. The long-term trends are between 0. 5 and 1.0 µmol L^{-1} y^{-1}. Data from Fisheries and Oceans Canada.

[Figure 2-14] Time series of annual mean dissolved oxygen in the Oyashio region at densities of 1026.6 to 1027.4 kg m^{-3}. Dashed and solid lines indicate long-term linear trends and the 18.6 year nodal tide cycle (see Chapter 4b), respectively. Error bars indicate standard deviation within each year.
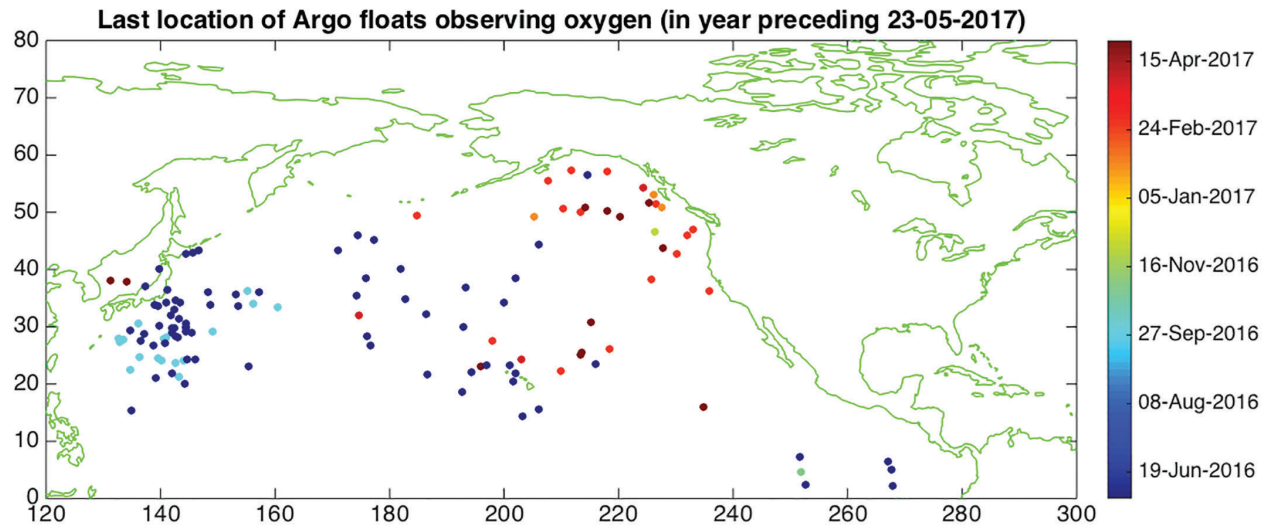
[Figure 2-15] Timeline of introduction of some ocean observing systems, shown relative to the trajectory of atmospheric CO_2 growth (thin black line); vertical positions of the lines are arbitrary. Thick blue lines indicate introduction of carbon system observations on 137°E and Line P. CZCS and SeaWiFS/MODIS are satellite ocean colour sensors. The "Satellite Era" indicates the period over which continuous global measurements have been made, e.g., of sea surface temperature and sea ice cover. Ocean colour is only continous since 1997. HOT and BATS are US time-series stations in the subtropical Pacific and subtropical Atlantic, respectively. Argo is a global network of autonomous profiling floats that measure temperature, salinity, and in some cases other chemical parameters such as oxygen.

Observing networks

Figure 2-15 shows the time line of introduction of an array of modern ocean observing systems against a backdrop of atmospheric CO_2 concentration (the vertical axis is arbitrary with respect to the horizontal lines). For 137°E and Line P, the thin lines represent the beginning of hydrographic observations, and the thick lines represent the beginning of carbon system measurements with modern methods. HOT used modern methods from its inception in 1988. The "satellite era" refers to the era (post-1979), during which observations of, e.g., sea surface temperature and sea ice cover have been made continuously and globally. Continuous coverage of ocean colour dates from 1996-1997. Global precipitation data products like GPCP and CMAP also begin in 1979. An important point to consider here is that all of these systems were introduced after the anthropogenic perturbation had already begun, so sampling of the 'baseline' state is not possible.

[33]
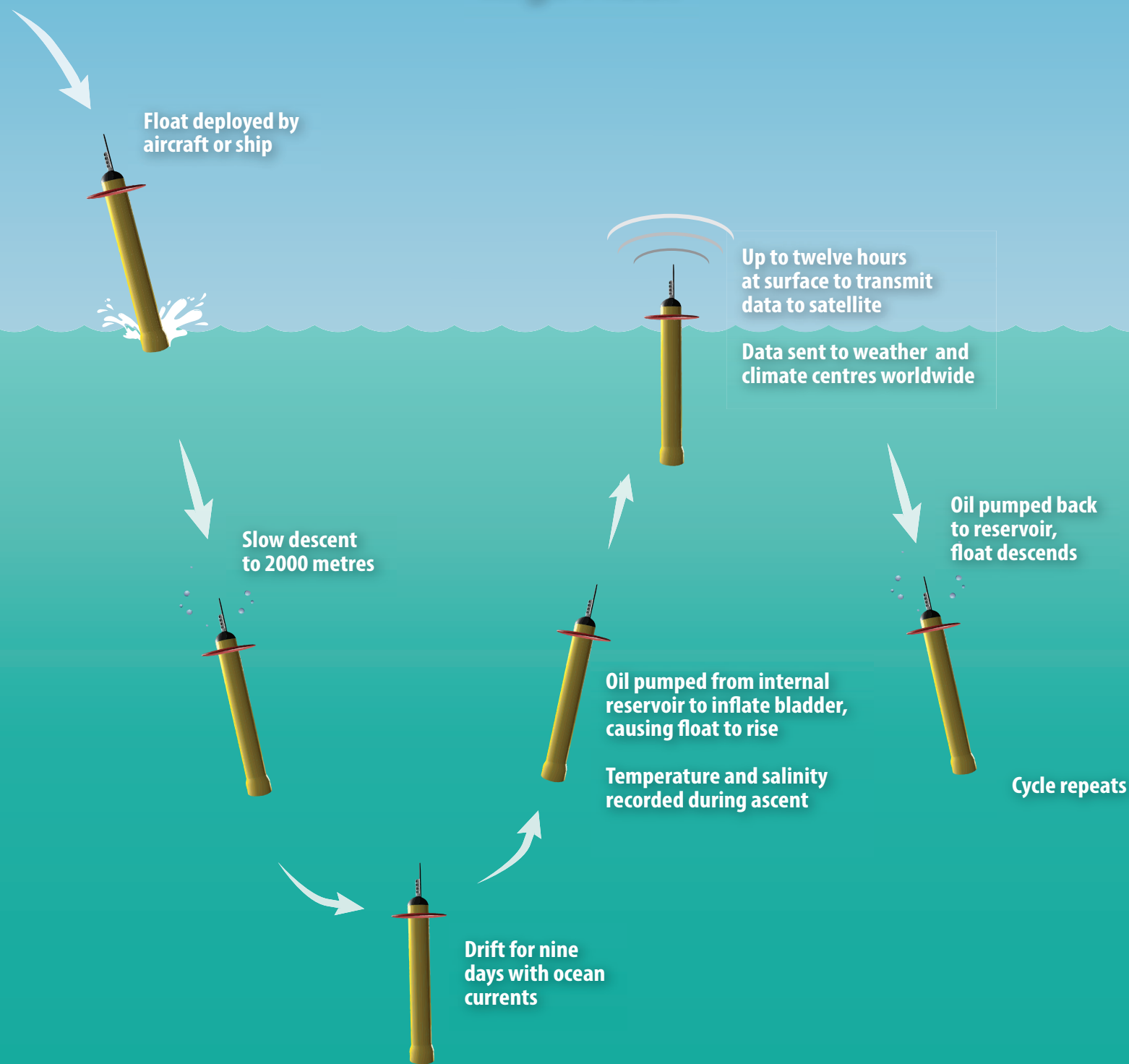
[Figure 2-16] Last known position of all of the Argo floats equipped with oxygen sensors that have been operational in the North Pacific. The colour scale indicates the date the float last transmitted data.

In many cases, the more advanced the technology, the more limited in time the data coverage is, (e.g., Argo floats were not introduced until around 2000 and biogeochemical sensors were not deployed aboard them until even later). There are currently more than 100 Argo floats with oxygen sensors deployed in the North Pacific. Other biogeochemical sensors are much less common.

Current open ocean observing systems include dedicated scientific research vessels (very high quality data, full depth profiles, but sparse sampling in space and time), ships of opportunity (surface only: pCO$_2$, DIC, alkalinity, nutrients), Argo floats, moorings, and satellites. Gliders are an emerging technology that have up to now mostly been deployed in coastal waters, but are now being deployed in the open ocean, e.g., along Line P. As shown in the table on page 36, all of these methods have advantages and disadvantages. Ship-based observations have given us our core understanding of the space-time distribution of DIC, alkalinity, pH and Ω (e.g., Feely et al., 2004). These cruises gather extremely high quality data and sample the full ocean depth, but they are very expensive to mount and so offer very limited space-time coverage. Similarly, time-series stations collect high quality data and full-depth (in some cases) profiles, and have greatly increased our understanding of climate variability and change, but spatial coverage is highly localized.

Argo Float

Float deployed by aircraft or ship

Slow descent to 2000 metres

Drift for nine days with ocean currents

Oil pumped from internal reservoir to inflate bladder, causing float to rise

Temperature and salinity recorded during ascent

Up to twelve hours at surface to transmit data to satellite

Data sent to weather and climate centres worldwide

Oil pumped back to reservoir, float descends

Cycle repeats

Platform	Advantages	Disadvantages
Time series stations	high quality data, full depth profiles	localized
Longline cruises	high quality data, full depth profiles	sparse sampling in space and time
Underway pCO$_2$	generally high quality data, global QA/QC effort well established	surface only
Ships of opportunity	high space/time data density, long time series in some cases	surface only, limited suite of parameters, variable data quality
Moorings	depth profiles, high frequency sampling	localized in space, data quality issues, data gaps
Argo	depth profiles, high frequency sampling, broad spatial coverage	CO$_2$ system measurements not generally available to date
Satellites	global, synoptic, real-time	surface T+S only

To fill the gaps, we have ships of opportunity, moorings, and Argo floats. The data obtained this way may not be of the same quality as the more labour-intensive measurement methods available on dedicated science vessels, but can be far more spatially extensive. These platforms contribute to making data coverage more complete, and autonomous sensor technology is improving with time. The US National Science Foundation recently funded a program to deploy large numbers of Argo floats in the Southern Ocean, some of which have pH sensors (Johnson et al., 2017). Moored observations of DIC have also been made (Fassbender et al., 2015), although this technology is still somewhat experimental and not yet available commercially.
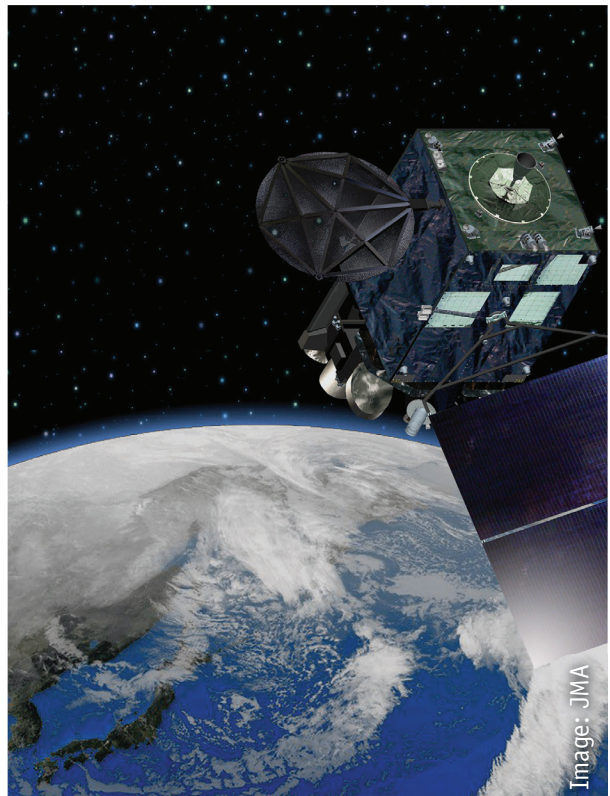
Credit: DFO Canada

[Figure 2-17] Map of the world ocean indicating the number of published empirical algorithms available for estimating carbon system variables from proxy data such as salinity, temperature, and oxygen. The North Pacific has more than any other region, but the East Asian marginal seas are impoverished in this respect. Reproduced with permission from Land et al. (2015).

Satellites have been measuring sea surface temperature for decades, but technologies for estimating sea surface salinity have only become available very recently (Land et al., 2015). This offers the possibility of calculating the full carbon system over the entire ocean, continuously and in real time, if some proxy can be found for two of the four key carbon system variables (see Chapter 1). Such proxies are unlikely to produce very precise estimates in the near future. Nonetheless, empirical algorithms for CO_2-system variables are more advanced in the North Pacific than in other regions. Atmospheric CO_2 concentration and wind speed at the ocean surface (required for calculating air-sea CO_2 flux) are also available from satellite observations.

Image: JMA

[37]
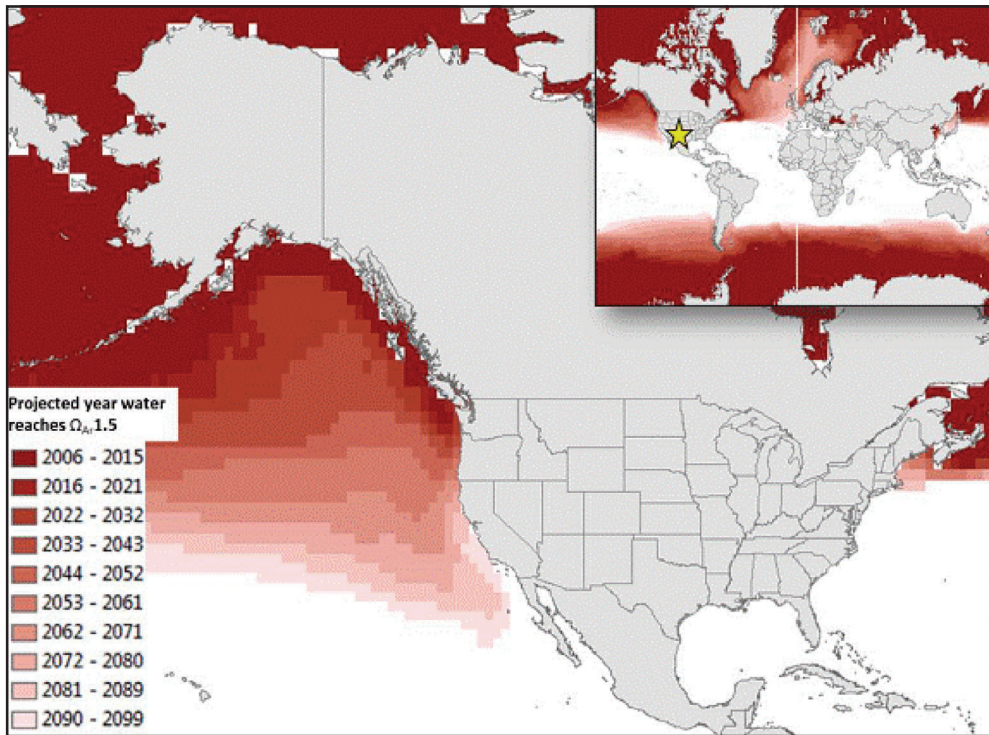
[3] Biological Impacts

To examine the scientific evidence for the effect of ocean acidification and hypoxia (singly or in combination with other factors) on marine organisms, 140 biological studies published on North Pacific native or cultured species (or closely related species) from 1990 to 2018 were collated, and key points are summarized here. These results include experimental studies conducted in controlled laboratory conditions, field observations, and large meta-population analyses.

Ocean acidification can affect organisms in different ways: some negative, some positive and some unchanged. Biological responses are complex, and can depend on the organism, the organism life stage, and local conditions. In addition to the known global decline in pH since preindustrial times, pH can vary locally due to river inputs, sea ice melt, currents, and algal blooms. Oxygen depletion can occur due to both natural and human drivers, and can affect organism behaviour, physiology, and survival. Different species may be more tolerant of, or more sensitive to, low oxygen levels, and lower oxygen may result in ecosystems with lower biodiversity.

[Figure 3-1] Projected year at which surface water reaches Ω_A=1.5 under emission scenario RCP8.5. RCP8.5 has the highest emissions of the RCP family of scenarios, with atmospheric CO_2 continuing to increase through 2100. Reproduced with permission from Ekstrom et al. (2015).

What does ocean acidification mean to marine organisms?

Of the stressor studies examined, 64% showed negative impacts of ocean acidification, 6% had a potential or projected negative impact, 10% had no effect, and 13% showed an unclear or mixed impact. Only 7% of studies showed a positive effect; these are mainly macroalgae species such as sea lettuce (*Ulva lactuca*), giant kelp (*Macrocystis pyrifera*), and red algae such as *Gracilaria lemaneiformis*. Of the 128 ocean acidification studies examined, the majority (67) were on molluscs. The juvenile (larval) stages of shellfish have been shown to be particularly sensitive to ocean acidification (Barton et al., 2012; Gazeau et al., 2013; Waldbusser et al.,

2015). For marine shellfish such as mussels, oysters and clams, the reduction of carbonate ion concentration resulting from ocean acidification (see Chapter 1) means that these animals do not have access to the biological building blocks that they need to form their shells. A previous analysis indicated that shellfish were likely to be the most sensitive to ocean acidification in the Pacific (Haigh et al., 2015). A study in the North Pacific (Ekstrom et al., 2015) indicates that large sections of the British Columbia coast already have surface seawater aragonite saturation below 1.5, which would be considered chronically stressful for marine molluscs (see Figure 3-1).

[39]
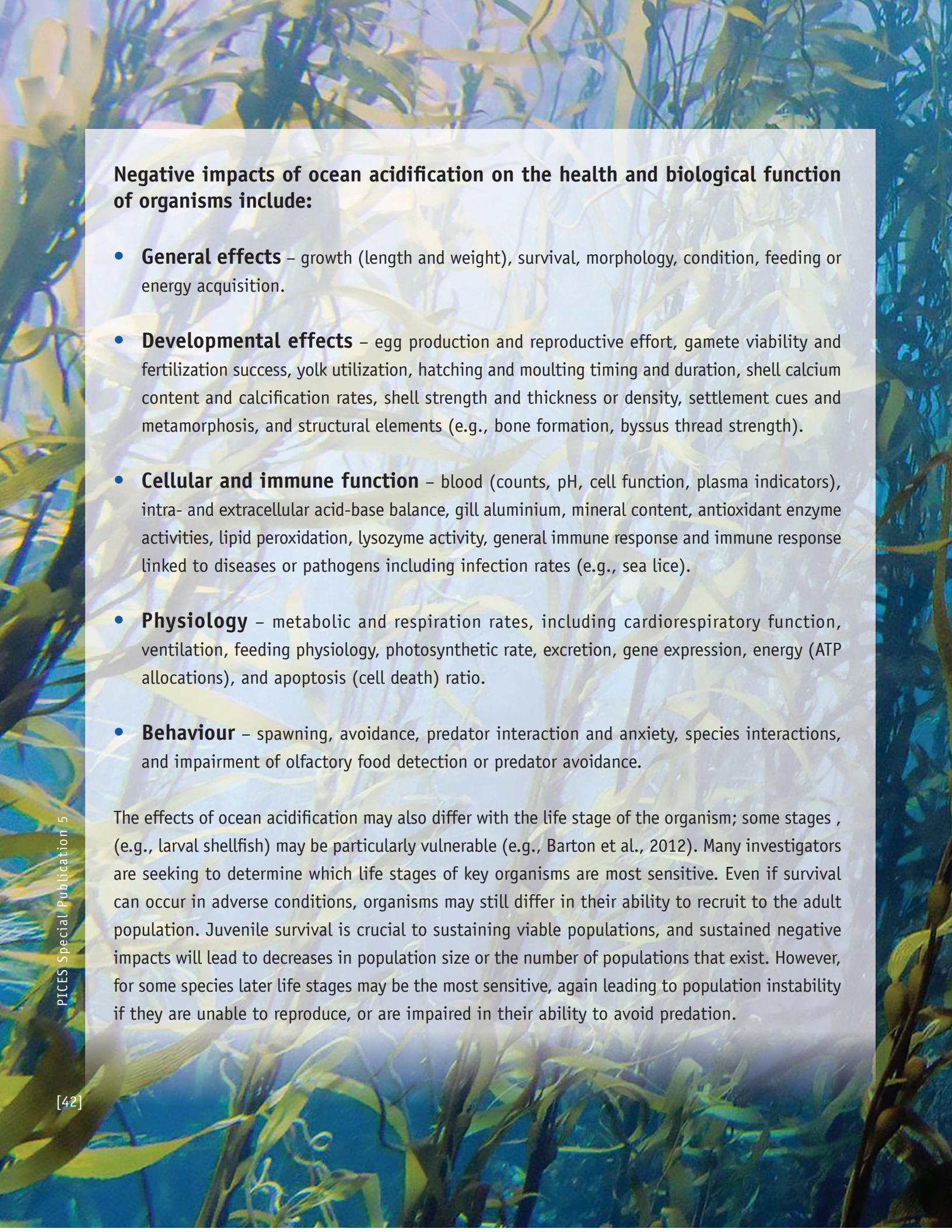
In our review of 128 published studies, key commercial, cultural or recreational species negatively affected by ocean acidification include: salmon (Pink salmon *Oncorhynchus gorbuscha*, Sockeye salmon *Oncorhynchus nerka* and Atlantic salmon *Salmo salar*), Yellowfin tuna (*Thunnus albacares*), crab (Tanner crab *Chinoecetes bairdi*, Dungeness crab *Metacarcinus magister*, and Red king crab *Paralithodes camtschaticus*), prawns (*Palaemon pacificus*, *P. borealis*), sea urchins (*Stronglyocentrotus purpuratus*, *S. fransciscanus*), oysters (*Crassostrea* or *Magallana gigas*, *Ostrea lurida*), mussels (*Mytilus edulis*, *M. galloprovincialis*), clams (*Venerupis philippinarum*, *Panopea generosa*), abalone (*Haliotis kamtschatkana*, *H. rufescens*), and coralline algae (*Lithothamnion phymatodeum*, *L. glaciale*). In addition, there are organisms which are important in food webs and as prey for commercial fish species that are negatively impacted by ocean acidification, including krill (*Euphausia pacifica*), pteropods (*Limacina helicina*) and coccolithophores (*Emiliania huxleyi*, *Gephyrocapsa oceanica*). Other non-commercial keystone species negatively impacted by ocean acidification include starfish (*Pisaster ochraceus*) and mussels (*Mytilus californianus*, *M. trossulus*).

Pteropods are pelagic snails that have evolved so that the 'foot' of their terrestrial cousins has become 'wings' or 'paddles'. They are sometimes colloquially referred to as the 'sea butterflies' or 'sea angels'. They live their whole lives in the open ocean. They are sometimes considered as 'sentinels' for ocean acidification impacts because their aragonite shells are considered particularly vulnerable to dissolution in a more acidic ocean (e.g., Feely et al., 2008; Bednaršek et al., 2012; 2014). Some species that migrate vertically into deeper waters with naturally low Ω seem to have a certain acclimation potential compared to non-migrators (Maas et al., 2012). Pteropods may experience shell dissolution even in waters with aragonite saturation very near or even slightly exceeding the chemical point of supersaturation (Ω_A=1) (Bednaršek et al., 2012; 2014; 2017).

Pteropods are most abundant in the subarctic and polar region, but species diversity is greatest in the subtropics (Pierrot-Bults and Peijnenburg, 2015). Because of their size and lipid content, they are believed to be important prey for juvenile salmon in the subarctic North Pacific, as well as for other fish and whales (Aydin et al., 2005). Pteropod shells in the sediments can be an important indicator of past ocean $CaCO_3$ saturation state in locations where they are preserved (e.g., Wall-Palmer et al., 2012). In the North Pacific, preservation of these shells is generally confined to depths less than 200 m (Fabry, 1989; Feely et al., 2004; Sabine et al., 2004).
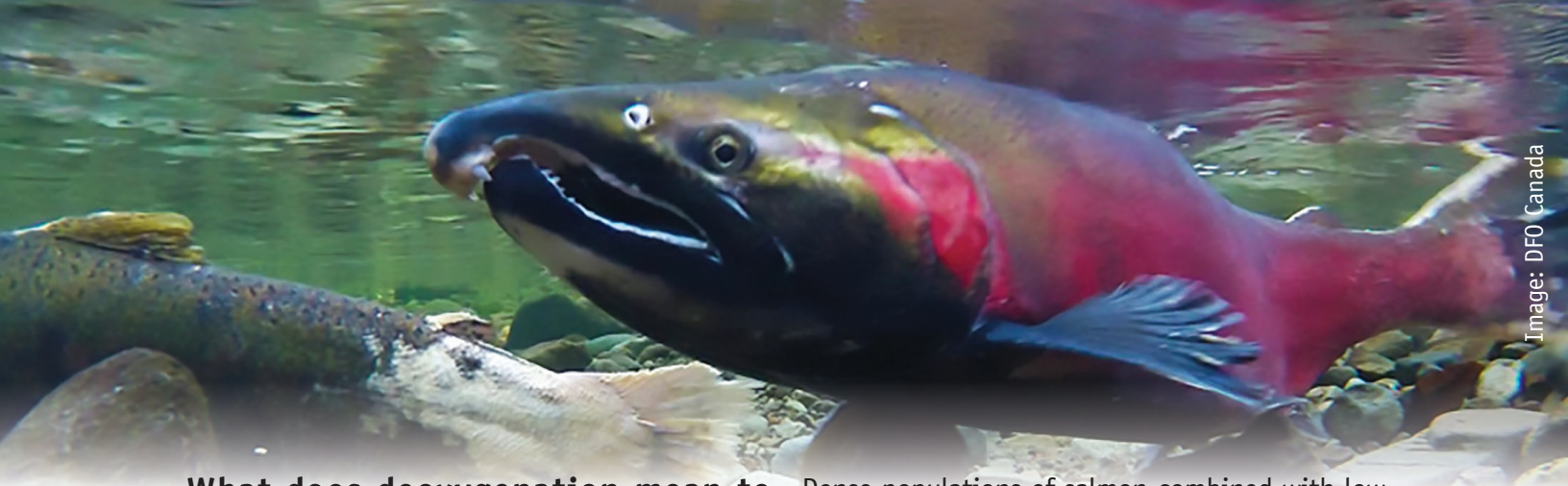
Images: DFO Canada

Negative impacts of ocean acidification on the health and biological function of organisms include:

- **General effects** – growth (length and weight), survival, morphology, condition, feeding or energy acquisition.

- **Developmental effects** – egg production and reproductive effort, gamete viability and fertilization success, yolk utilization, hatching and moulting timing and duration, shell calcium content and calcification rates, shell strength and thickness or density, settlement cues and metamorphosis, and structural elements (e.g., bone formation, byssus thread strength).

- **Cellular and immune function** – blood (counts, pH, cell function, plasma indicators), intra- and extracellular acid-base balance, gill aluminium, mineral content, antioxidant enzyme activities, lipid peroxidation, lysozyme activity, general immune response and immune response linked to diseases or pathogens including infection rates (e.g., sea lice).

- **Physiology** – metabolic and respiration rates, including cardiorespiratory function, ventilation, feeding physiology, photosynthetic rate, excretion, gene expression, energy (ATP allocations), and apoptosis (cell death) ratio.

- **Behaviour** – spawning, avoidance, predator interaction and anxiety, species interactions, and impairment of olfactory food detection or predator avoidance.

The effects of ocean acidification may also differ with the life stage of the organism; some stages , (e.g., larval shellfish) may be particularly vulnerable (e.g., Barton et al., 2012). Many investigators are seeking to determine which life stages of key organisms are most sensitive. Even if survival can occur in adverse conditions, organisms may still differ in their ability to recruit to the adult population. Juvenile survival is crucial to sustaining viable populations, and sustained negative impacts will lead to decreases in population size or the number of populations that exist. However, for some species later life stages may be the most sensitive, again leading to population instability if they are unable to reproduce, or are impaired in their ability to avoid predation.

[43]
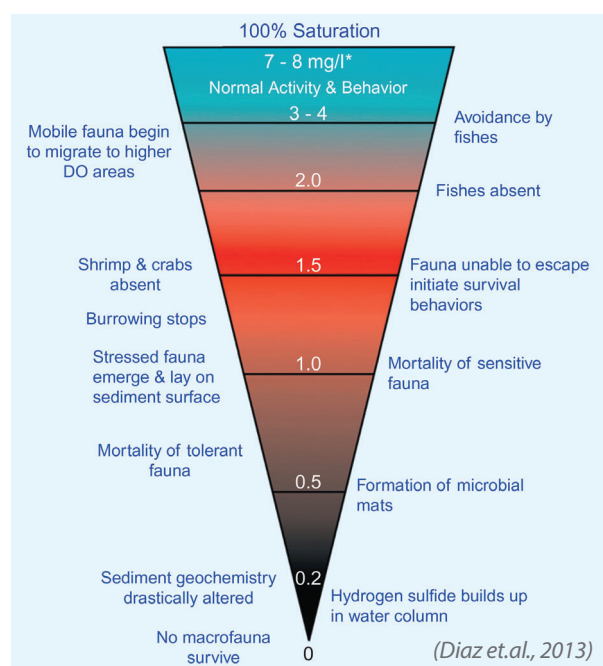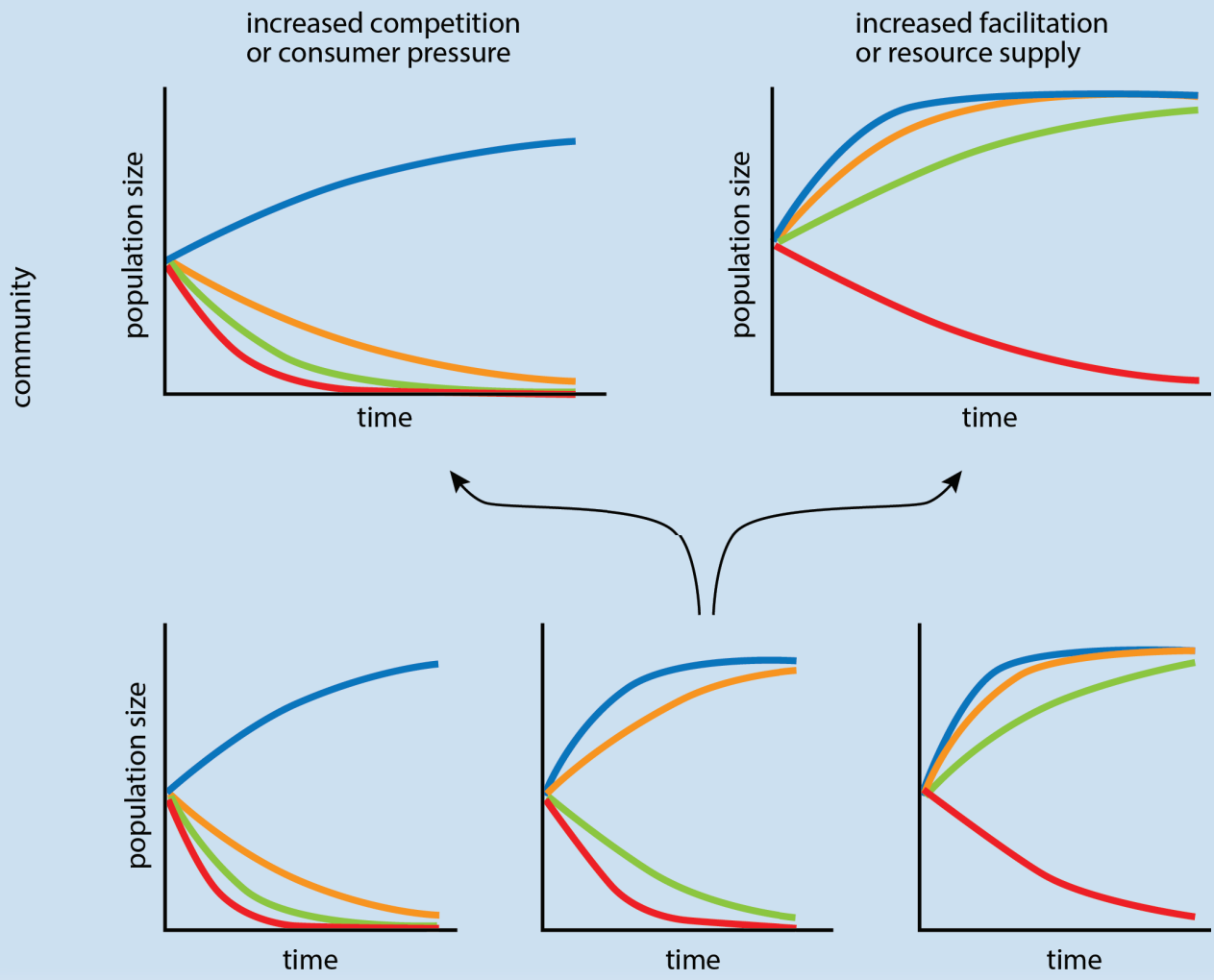
What does deoxygenation mean to marine organisms?

While increases in carbon dioxide in the atmosphere are leading to ocean acidification, carbon dioxide is also a greenhouse gas and will therefore contribute to declining ocean oxygen concentrations due to surface warming and stratification (see Chapter 1). While some organisms have a higher tolerance to low oxygen levels (e.g., comb jellies and some species of squid), others show less tolerance (fishes in general). Some organisms are able to avoid low oxygen zones by shifting their depth distribution, but this can shrink the vertical extent of potential habitat (e.g., Koslow et al., 2011). Low oxygen levels have already caused mass deaths of fish and crustacean species in the North Pacific (Grantham et al., 2004; Gewin, 2010). Low, but non-lethal, oxygen concentrations may also affect tolerance to other stressors such as parasites, diseases, and pollutants. Studies of hypoxia with Pacific species were more limited in our search (13 studies), but of those examined, 54% showed a negative impact, 38% a mixed effect, and 8% no effect. Pacific species showing negative effects include Steelhead or Rainbow trout (*Oncorhynchus mykiss*), Atlantic salmon (*Salmo salar*), Sockeye salmon (*Oncorhynchus nerka*), Slender sole (*Lyopsetta exilis*), Spot prawn (*Pandalus platyceros*), Pacific oyster (*Crassostrea gigas*), and the Manila clam (*Venerupis philippinarum*).

Dense populations of salmon combined with low river discharge can actually trigger hypoxic events (Sergeant et al., 2017). Hypoxia can affect the physiology of animals, including mitochondrial function, dissolved oxygen consumption, heart rate, cardiorespiratory function, metabolic rate, reduced survival, increased pre-spawning mortality, and tissue damage. Changes in animal behaviour due to hypoxia include avoiding low dissolved oxygen waters, swimming capacity, feeding, and predator evasion. Some studies have suggested that hypoxic acclimation may occur and improve tissue oxygen utilization in fish, leading to cardiorespiratory changes, and that pre-conditioning may benefit some species in future oxygen limited conditions.

PICES Special Publication 5

100% Saturation
7 - 8 mg/l*
Normal Activity & Behavior
3 - 4
Mobile fauna begin to migrate to higher DO areas
Avoidance by fishes
2.0
Fishes absent
Shrimp & crabs absent
1.5
Fauna unable to escape initiate survival behaviors
Burrowing stops
Stressed fauna emerge & lay on sediment surface
1.0
Mortality of sensitive fauna
Mortality of tolerant fauna
0.5
Formation of microbial mats
Sediment geochemistry drastically altered
0.2
Hydrogen sulfide builds up in water column
No macrofauna survive
0
(Diaz et.al., 2013)

[Figure 3-2] Conceptual outline of how non-additive effects of environmental change drivers can arise within an organism, population or community despite a lack of non-additivity at lower levels of organization. Blue represents the current 'control' conditions, green represents acidification or low oxygen, orange represents warming, and red represents the simultaneous application of both stressors. In the best case (top panel right), increased resource supply can overcome one stressor but not both. In the worst case (top panel left), other biotic interactions can make the population nonviable given either stressor, or both. Excerpted with permission from Kroeker et al. (2017).

Multiple stressors and other marine ecosystem considerations

Ocean acidification and hypoxia will not occur as single stressors to marine ecosystems, but rather will coexist with each other and with other stressors, such as increasing temperature. Initially, biological research in the area of ocean acidification concentrated on pH (or pCO_2) only (80% of the studies examined), and focused on short-term responses in single species. Such studies are informative but of limited utility in terms of predicting actual biological responses in a natural environment of populations encountering multiple stressors. More recently (since 2010) research is incorporating combinations of multiple stressors (e.g., ocean acidification, warming, hypoxia, reduced food availability) in warming climate scenarios. Multiple stressors may create interactions producing antagonistic, additive or synergistic responses in individuals and non-linear responses at the population level (Kroeker et al., 2017, see Figure 3-2).

Sex-linked physiological impacts may also occur within populations, where either males or females (depending on species) may respond differently to ocean acidification and may either skew gender distributions through differential early survival, or population size by altering reproductive capacity (Ellis et al., 2017). Early studies of ocean acidification impacts provided responses that were either positive, negative or unchanged for the same species under similar stressor conditions, and later studies suggested this may have been attributable to food supply. In situations where abundant food was available, organisms were able to buffer the stress of higher metabolic demand. Biological impacts in the marine environment may be affected by ocean acidification indirectly through the creation of new predator-prey relationships, and such changes in food web interactions may be driven by the availability of planktonic organisms at the base of the food chain. Global changes may alter the timing of events in the natural

[Figure 3-3] The press-pulse framework, showing the components of climate change and climate variability experienced by biological systems. Many organisms have adapted to cope with climate variability (a) and weather (b), but as climate moves further from preindustrial (c) extreme events beyond the species' tolerance occur more often. Extreme weather events more often cross into the yellow zone where large population losses occur, or even into the pink zone of local extinction (d, e). Reproduced with permission from Harris et al. (2018).

life cycle of marine organisms (phenology), as well as creating a timing mismatch between predator and prey interactions. This has the potential to affect important fisheries resources in the North Pacific (Holsman et al., 2018).

While ongoing climate change can lead to long-term changes in biological systems, extreme events can further intensify impacts on biota (Harris et al., 2018, see Figure 3-3). The scale of the biological effect can be influenced by the timing, severity and duration of the extreme event and can lead to major declines in population productivity and biodiversity. Localized extreme events may create regional declines and, if spread over a wider distributional range, may have longer lasting or irreversible effects as surrounding populations will not be able to recolonize the damaged areas. Extreme events can also either directly or indirectly affect socio-economically valuable fisheries. One such extreme event in the North Pacific was a persistent large warm water

anomaly (marine heatwave) which developed in the northeastern Pacific in the winter of 2013-2014 (Bond et al., 2015). Such warm water events can lead to changes in fisheries productivity by impacting food quality and fish condition, resulting in necessary reductions in catch quotas (Holsman et al., 2018). Therefore, assessment of single or multi-stressor impacts on marine ecosystems must also consider potential peaks of disruption caused by extreme events. Longer-term biological research involving multiple species and multiple stressors that cover the variability of climate and extreme event disturbances will help provide a more realistic picture of biological tolerances of organisms to future climate, which will permit better planning for resource management. While some levels of global change may be difficult to manage for (e.g., ocean acidification and global warming), local initiatives such as reducing nutrient loading and water usage can mitigate impacts on a regional scale by preventing eutrophication.
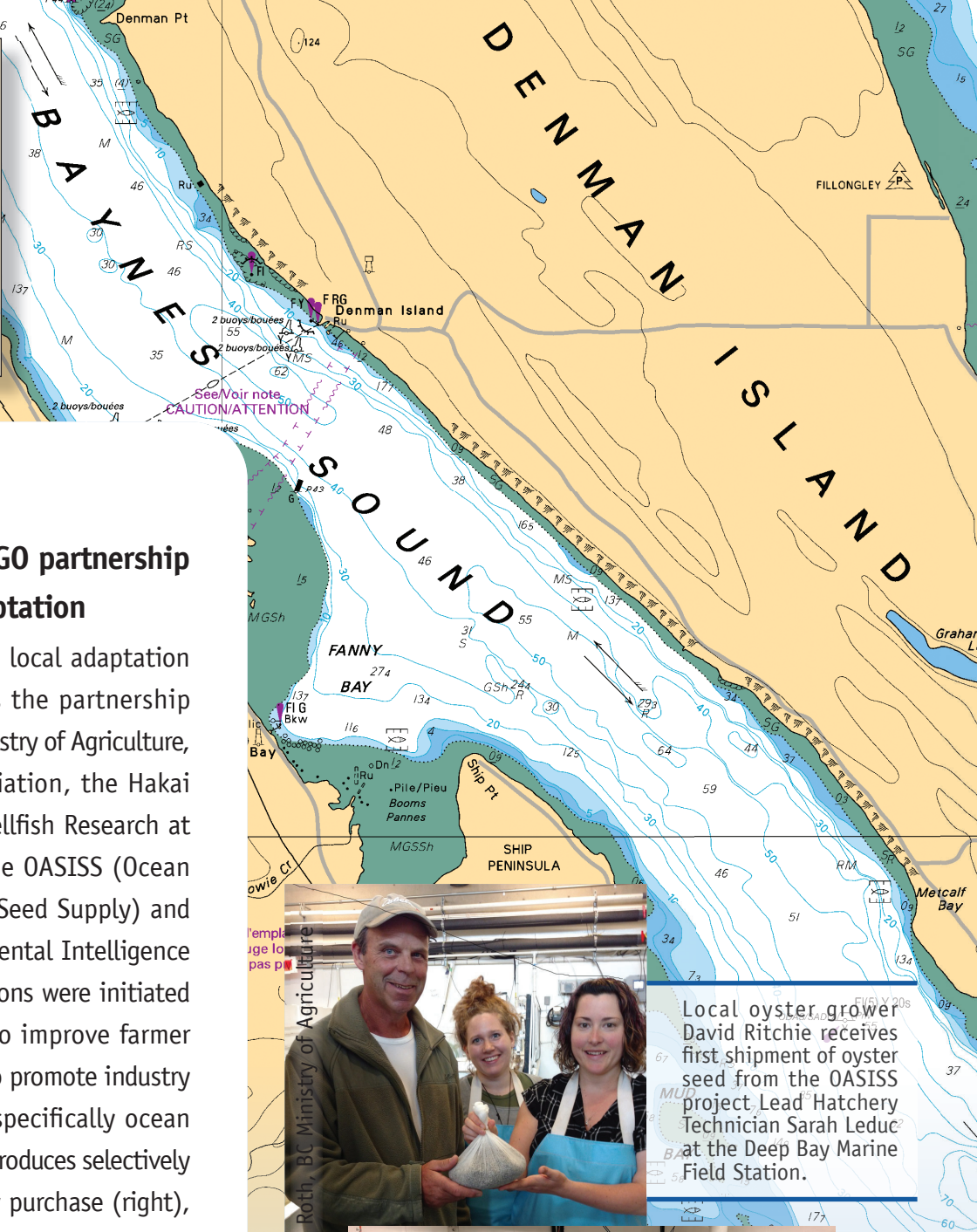
Acclimation and adaptation potential

In order to determine the long-term effects of ocean acidification and deoxygenation on marine ecosystems (evolutionary responses), we must consider the acclimation and adaptation potential of the organisms. Within a population, organisms may behave, look or function differently with different environmental conditions; this is known as *phenotypic plasticity*. Some individuals may respond better than others to stressors such as ocean acidification. These responses help to maintain organism function in a new environment, and may or may not be reversible or inherited by the next generation (Sunday et al., 2014). The capacity of a population to adapt to change may also depend on the variability that the organisms normally encounter, and the strength and rapidity of the change they experience. Some studies have found that acclimating adults to projected future conditions confers an advantage on their offspring, whereas others have not observed any benefits, especially when multiple stressors are applied.

Acclimation can allow for longer-term (evolutionary) adaptation to occur, such that the selection of traits that make the organism better adapted to the new environment (e.g., lower pH) are passed on to future generations. Adaptation can be studied using quantitative genetics, to examine if changes are related to heritable genotypes or environments, or through long-term multiple generation biological experimentation. Strong environmental drivers, such as ocean acidification, may generate populations adapted to an acidified world but restrict the genetic variation that may permit adaptation to a new stressor such as a new disease or virus. Aquaculture can use selective breeding practices (both phenotypic and genetic) to develop populations that are better adapted to their changing environmental conditions, and use genetic 'banking' facilities to maintain genetic diversity. Within a species, there may be differences in adaptive capacity due to the variability and strength of an environmental driver, and how that population has been genetically altered by selection over previous generations. Therefore, biological adaptation potential can not be extrapolated from one species in one location to all populations of that species globally. To date, the majority of biological studies have concentrated on single species over short time scales that do not capture the potential for evolutionary adaptation.

Baynes Sound

An industry-government-NGO partnership for OA monitoring and adaptation

One direct example of providing local adaptation tools for ocean acidification is the partnership between the British Columbia Ministry of Agriculture, the BC Shellfish Growers Association, the Hakai Institute, and the Centre for Shellfish Research at Vancouver Island University. The OASISS (Ocean Acidification Shellfish Industry Seed Supply) and BaSEIC (Baynes Sound Environmental Intelligence Collaboration) project collaborations were initiated by the Ministry of Agriculture to improve farmer access to juvenile shellfish and to promote industry adaptation to climate change, specifically ocean acidification. The OASISS project produces selectively bred juvenile oysters for industry purchase (right), while the BaSEIC project, led by the Hakai Institute, provides high resolution seawater monitoring data (alkalinity, pCO_2, aragonite saturation, pH, salinity, and temperature) (bottom right). Baynes Sound is a highly productive shellfish culture area. All BaSEIC data are available at http://www.ipacoa.org/Explorer. This real-time monitoring capacity provides ocean acidification data on a local scale, which can be used by shellfish farmers to monitor site conditions and make informed management decisions.

Myron Roth, BC Ministry of Agriculture

Local oyster grower David Ritchie receives first shipment of oyster seed from the OASISS project. Lead Hatchery Technician Sarah Leduc at the Deep Bay Marine Field Station.

Wiley Evans, Hakai Institute

Coastal ocean acidification seawater monitoring using a combined pCO_2 / TCO_2 analyzer at Fanny Bay Oysters in Baynes Sound.

Summary

Overall, the expected impacts of ocean acidification and deoxygenation will be negative for the majority of Pacific wild and cultured species considered here. Biological responses will vary according to species, life stage, sex, food availability, and the combination of stressors applied, which may lead to different responses on an individual or population scale. Extreme events will further pressure marine ecosystems and affect population productivity and biodiversity. Population plasticity may allow some organisms to acclimate in the short term, but the potential for longer-term population adaptation will be a function of the local variability experienced and the strength of the selective pressure applied. There are a number of scientific initiatives on the local, national, and international scale aiming to increase our scientific understanding of the variability of coastal environmental conditions and their likely future evolution and impacts.

[51]
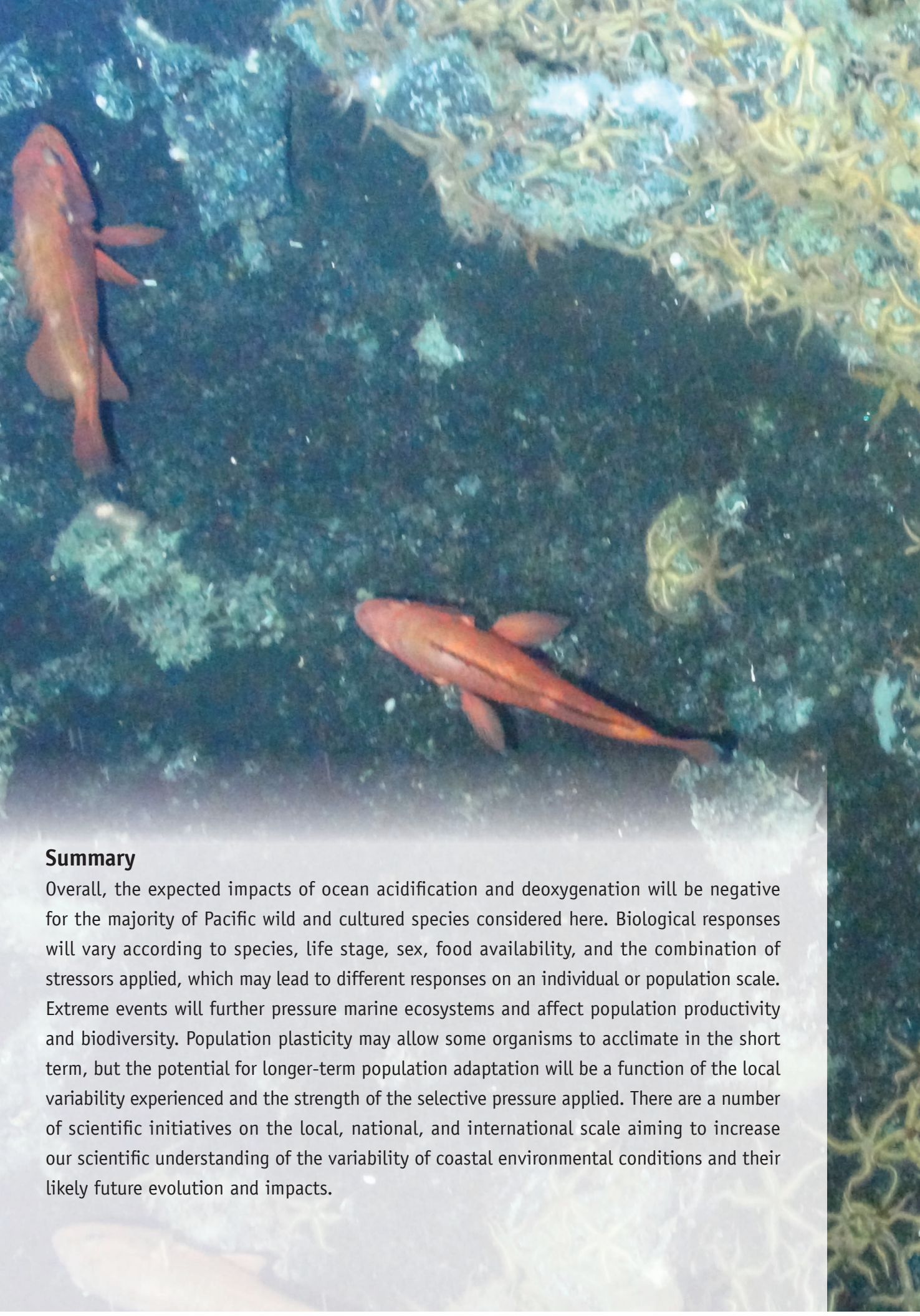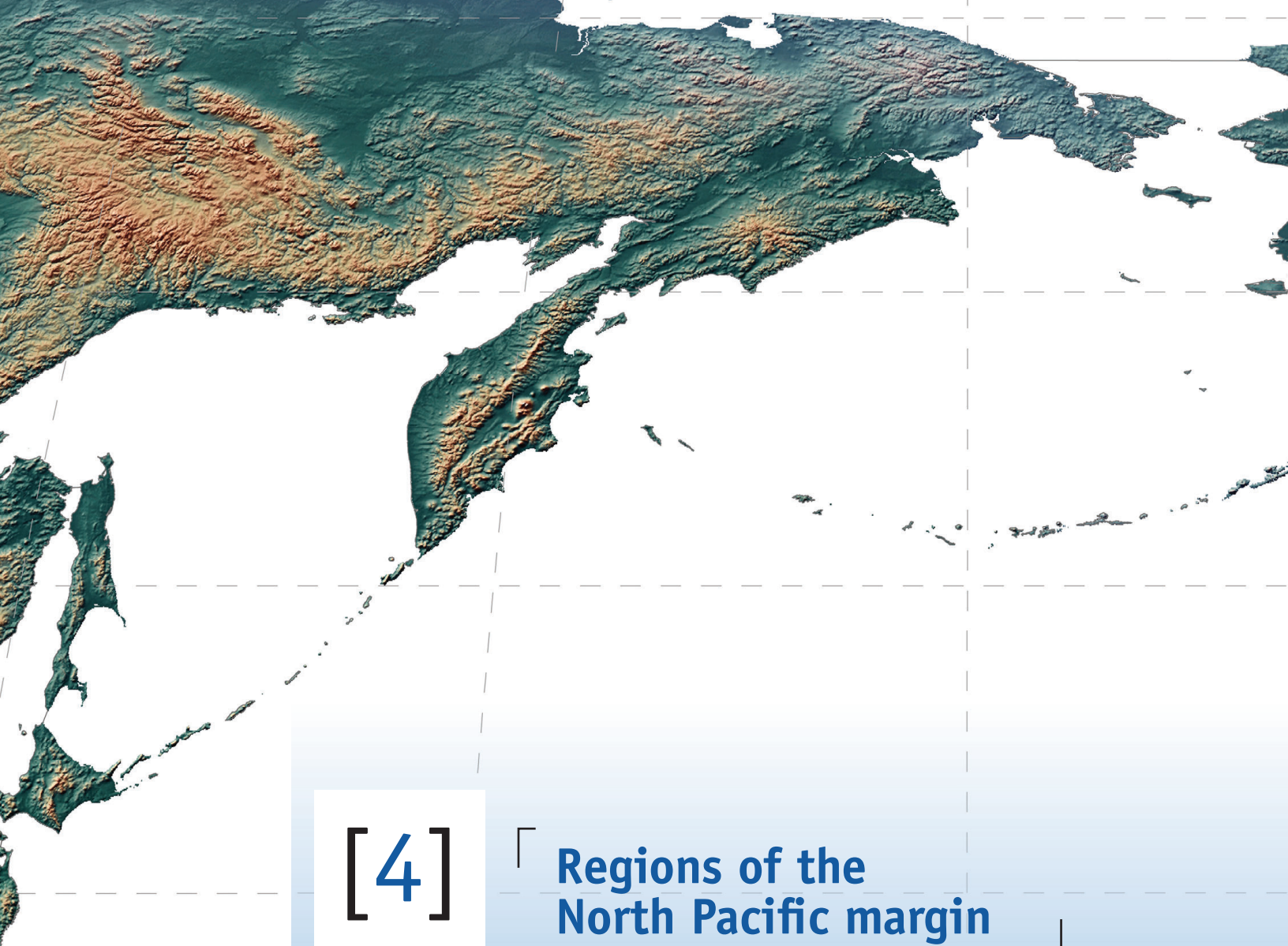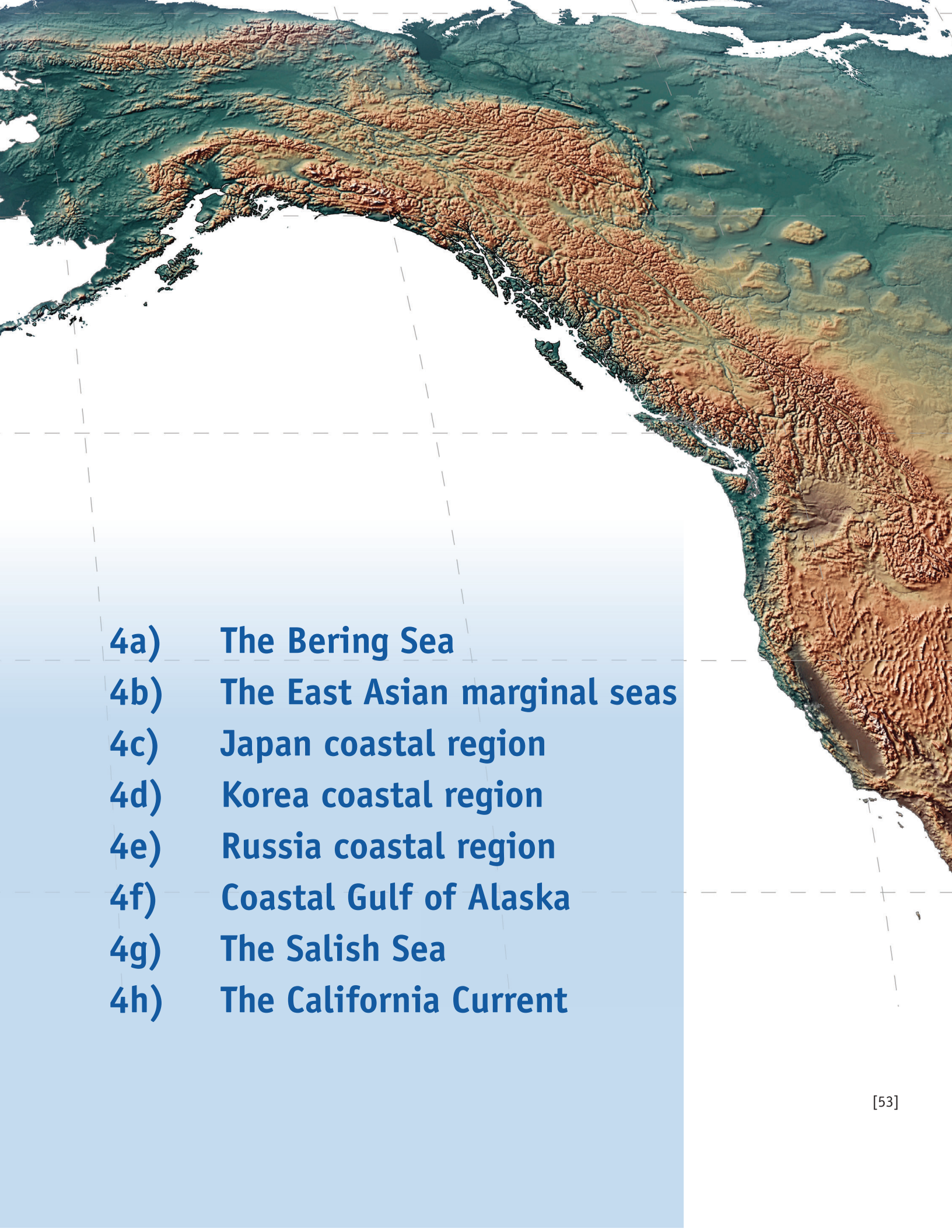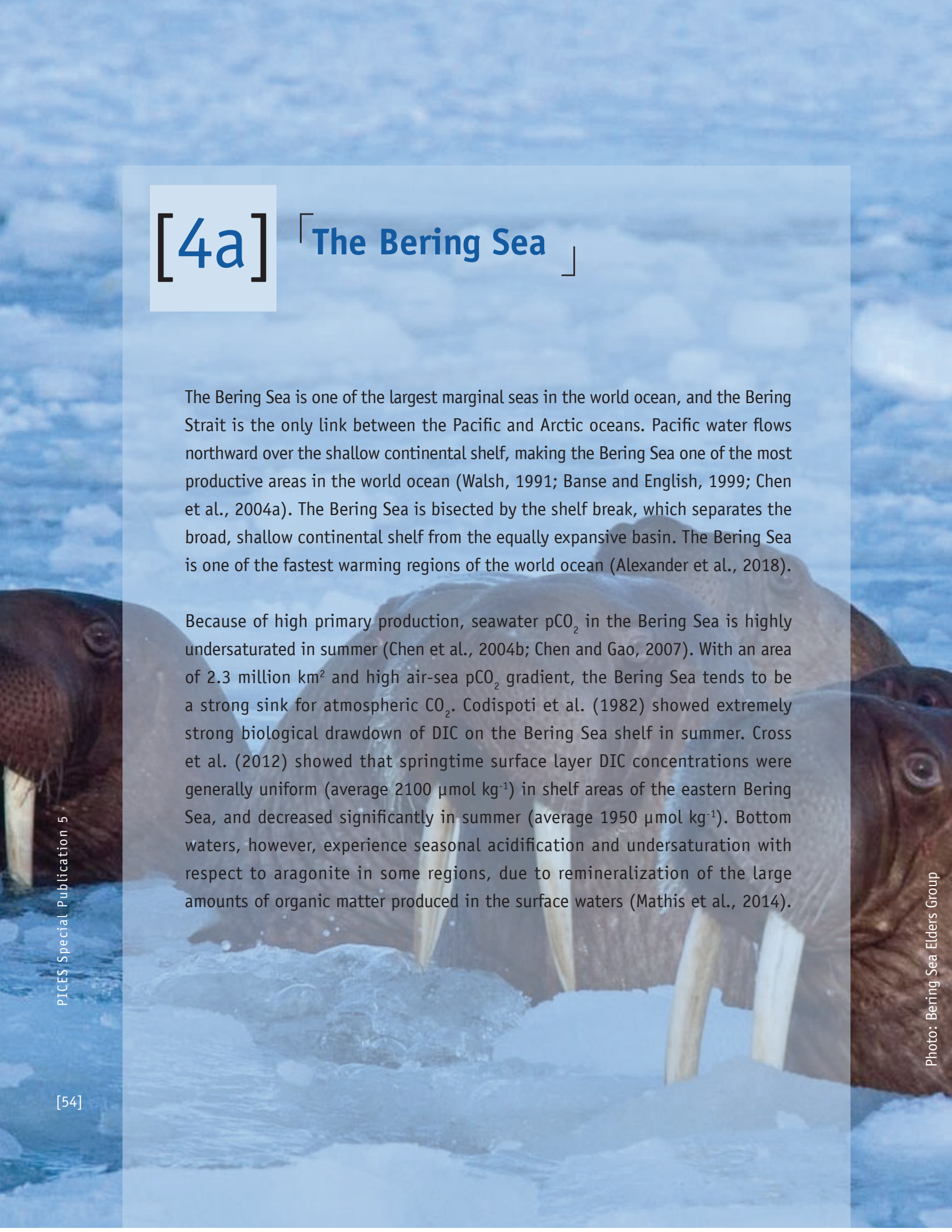
[4] Regions of the North Pacific margin
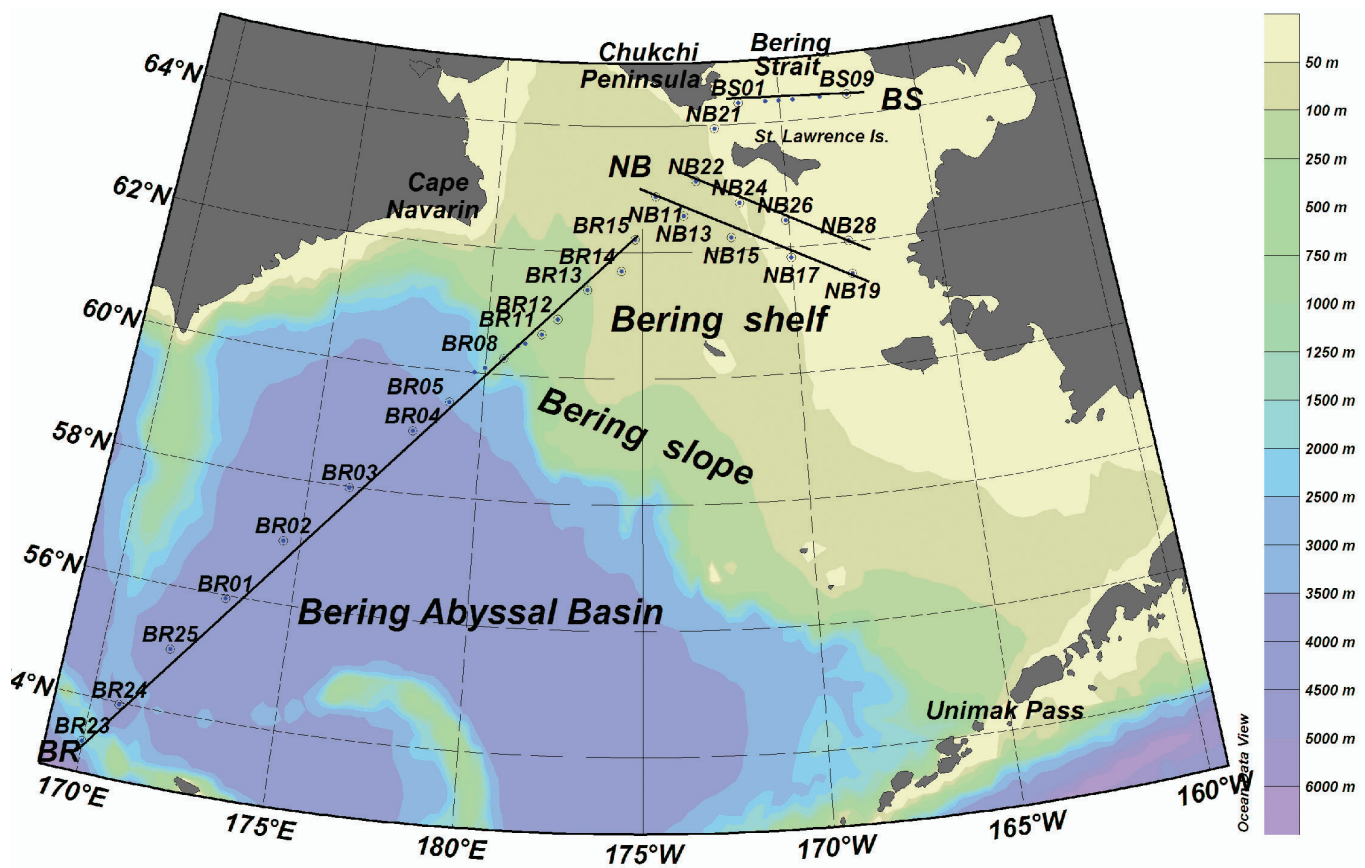
[4a] 「The Bering Sea 」

The Bering Sea is one of the largest marginal seas in the world ocean, and the Bering Strait is the only link between the Pacific and Arctic oceans. Pacific water flows northward over the shallow continental shelf, making the Bering Sea one of the most productive areas in the world ocean (Walsh, 1991; Banse and English, 1999; Chen et al., 2004a). The Bering Sea is bisected by the shelf break, which separates the broad, shallow continental shelf from the equally expansive basin. The Bering Sea is one of the fastest warming regions of the world ocean (Alexander et al., 2018).

Because of high primary production, seawater pCO_2 in the Bering Sea is highly undersaturated in summer (Chen et al., 2004b; Chen and Gao, 2007). With an area of 2.3 million km² and high air-sea pCO_2 gradient, the Bering Sea tends to be a strong sink for atmospheric CO_2. Codispoti et al. (1982) showed extremely strong biological drawdown of DIC on the Bering Sea shelf in summer. Cross et al. (2012) showed that springtime surface layer DIC concentrations were generally uniform (average 2100 µmol kg^{-1}) in shelf areas of the eastern Bering Sea, and decreased significantly in summer (average 1950 µmol kg^{-1}). Bottom waters, however, experience seasonal acidification and undersaturation with respect to aragonite in some regions, due to remineralization of the large amounts of organic matter produced in the surface waters (Mathis et al., 2014).
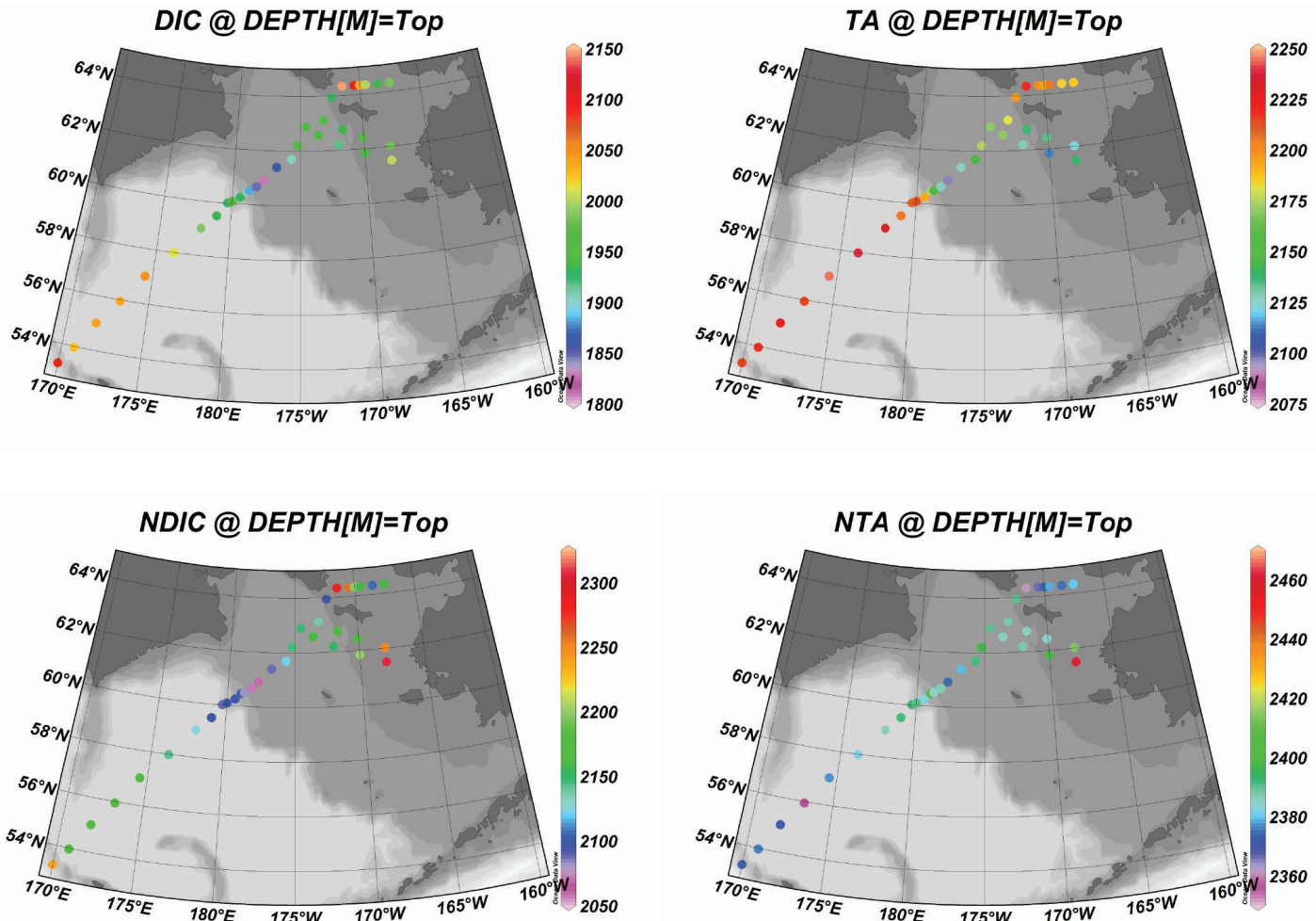
[Figure 4a-1] Map of sampling locations in the Bering Sea during CHINARE-Arctic III aboard the R/V *Xuelong* (summer 2008). Overlapping transect lines have been offset slightly for illustrative purposes.

Surface water pCO$_2$ distribution

During July 2008, the CHINARE-Arctic III expedition aboard the R/V *Xuelong* sampled the Bering Sea basin and the Bering shelf and slope area (Figure 4a-1). The ship measured sea surface temperature, salinity, and pCO$_2$ along the cruise track. There were very strong gradients in seawater pCO$_2$ along the transect, associated with the transition between the shelf and the deep basin. South of 57°N, surface pCO$_2$ in the deep western basin of the Bering Abyssal Basin was high with a typical value of 348±10 ppm. However, pCO$_2$ began to decline abruptly between 59.5°N and 61.5°N, with a minimum 148 ppm at about 61°N, and increased abruptly again to 225 ppm at 62°N. In contrast to the deep basin, low pCO$_2$ was observed over the shelf, typically ranging from about 150 to 240 ppm.

[55]

DIC @ DEPTH[M]=Top

TA @ DEPTH[M]=Top

NDIC @ DEPTH[M]=Top

NTA @ DEPTH[M]=Top

[Figure 4a-2] Distributions of DIC and total alkalinity (TA) in the Bering Sea in summer 2008. nDIC, nTA indicate concentrations normalized to a salinity of 35 to remove the effect of dilution by freshwater (see Chapter 1).
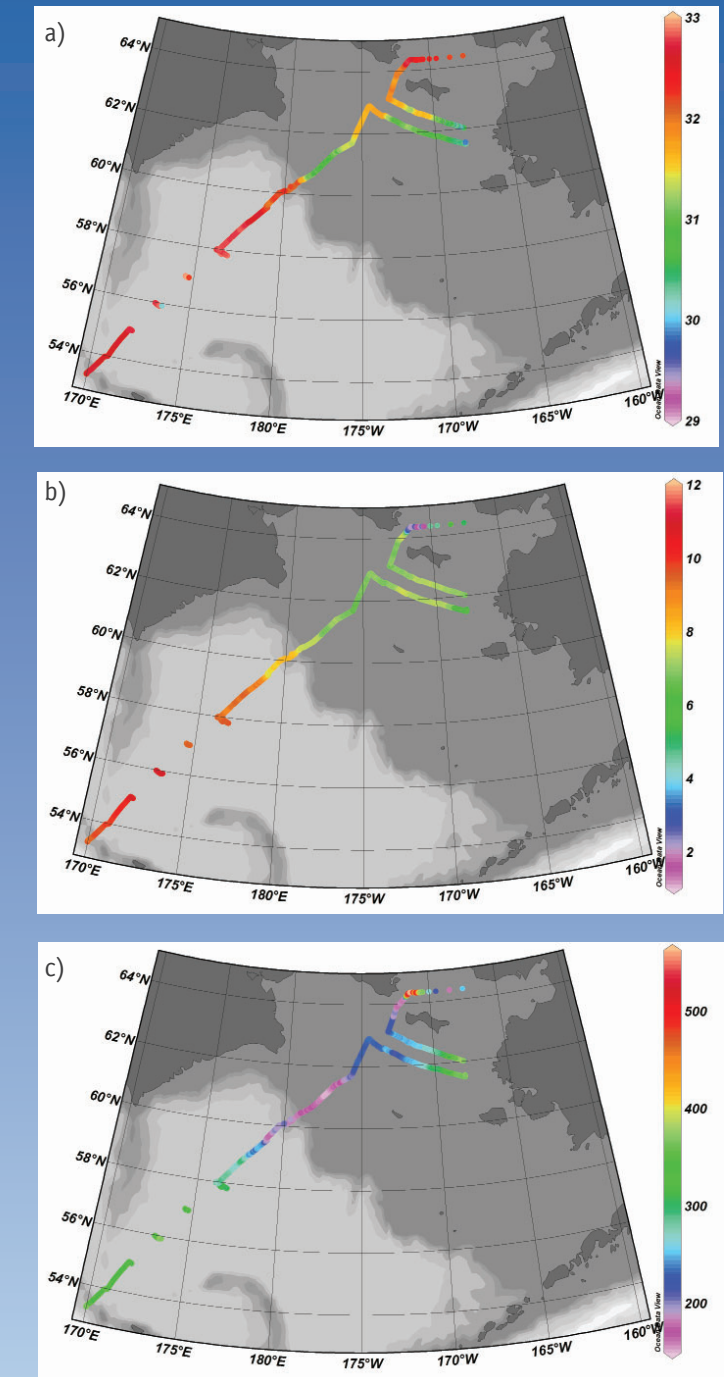
Surface seawater pCO_2 along transect NB increased gradually eastward accompanied by decreased sea surface salinity. It is worth noting that the maximum pCO_2 observed along transect NB approached the atmospheric concentration (379 ppm), at the easternmost location. Surface seawater pCO_2 along transect BS rose sharply, and then dropped gradually eastward. The western Bering Strait, south of the Chukchi Peninsula, showed lower sea surface temperature and higher sea surface salinity than in other regions, and seawater pCO_2 was mostly supersaturated.

DIC and TA distributions

Summertime surface seawater DIC, nDIC, TA and nTA concentrations in the Bering Sea ranged from 1827-2145 µmol kg^{-1},

2070-2306 µmol kg^{-1}, 2097-2244 µmol kg^{-1}, and 2356-2461 µmol kg^{-1}, respectively (Figure 4a-2). (nDIC and nTA are normalized to a constant salinity of 35 to remove the influence of fresh water dilution: see Chapter 1). The minimum surface DIC was observed at station BR12, and the maximum DIC at station BS01, coincident with the minimum and maximum pCO$_2$. Surface salinity and TA at the easternmost stations NB19 and NB28 were lower than at other stations on transect NB, while the highest normalized TA was observed at NB19 and NB28. The eastward decreasing trend of TA and salinity suggests that the transect NB area may be affected by river runoff. Many boreal rivers, such as the Yukon, contain very high nTA (i.e., while the alkalinity in river water is lower than seawater values, salinity is near zero so that river inputs cause a strong positive anomaly in nTA concentrations observed in the ocean). Data from the CHINARE-Arctic III expedition show little variation in nTA, suggesting that CaCO$_3$ production and dissolution may be a minor effect in this area (Gao et al., 2012). However, intense blooms of calcifying phytoplankton (coccolithophores) have been observed in the Bering Sea (Figure 4a-4).

[Figure 4a-3] Distributions of (a) sea surface salinity (SSS), (b) sea surface temperature (SST, °C), and (c) partial pressure of CO$_2$ (pCO$_2$, ppm) along the sampling lines shown in Figure 4a-1, during summer 2008.
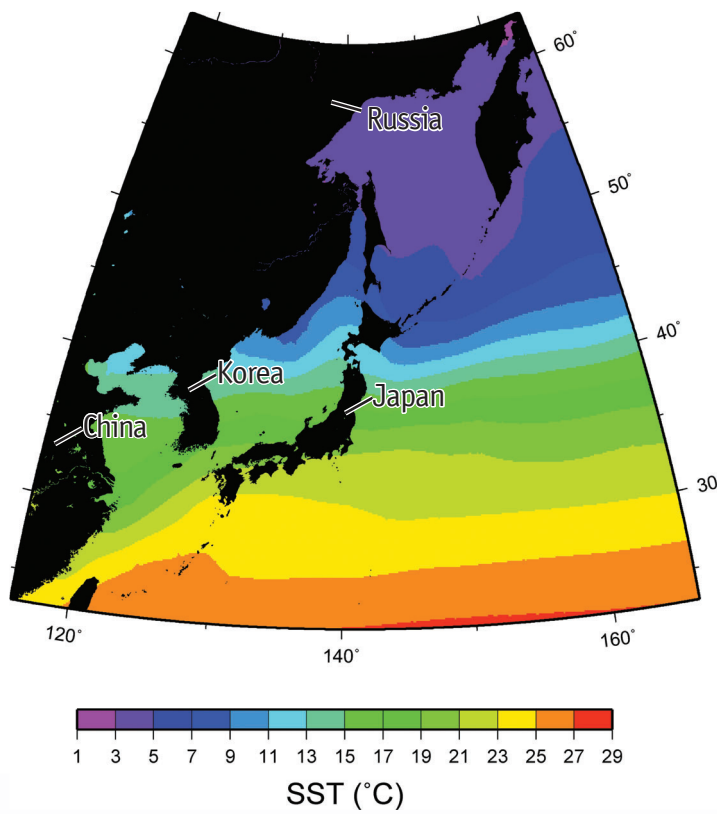
[Figure 4a-4] Satellite image of a coccolithophore (calcifying phytoplankton) bloom in the Bering Sea in summer 1998. Highest concentrations turn the water white like tiny particles of chalk (pure white in the southwest corner is cloud). Inset image shows an electron micrograph of the coccolithophore *Emiliana huxleyi*. The cell is about 10 µm in diameter and the individual $CaCO_3$ 'plates' (coccoliths) are 1-2 µm.

Ventilation of the deep Bering Sea

In contrast to the broad, productive shelf in the east, the western Bering Sea is a deep (>3000 m) basin that shares many characteristics with the adjacent waters of the open subarctic Pacific. The deep waters are very old (Figure 1-4), and like the waters of the oxygen minimum zone at lower latitudes, they are depleted in O_2 and enriched in DIC (acidic). Bottom waters experience episodic renewal with dense water that forms on the shelf (Warner and Roden, 1995), but the main mass of deep water, (e.g., 1000-3000 m) has experienced no recent ventilation. The aragonite saturation horizon is mostly shallow (100-200 m), except in a few areas near the Russian coast that experience deep convective mixing.
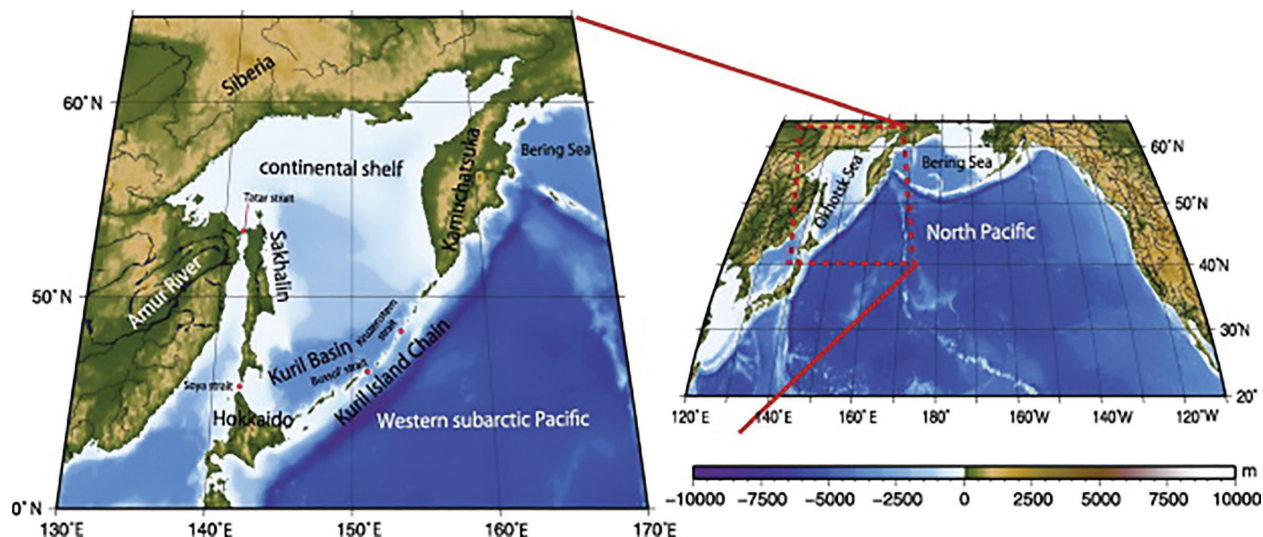
[59]

[Figure 4b-1] Map of the northwestern Pacific Ocean showing the position of the East Asian marginal seas relative to the four western Pacific PICES member countries. The colour contours are annual mean sea surface temperature (SST).

[4b] 「The East Asian marginal seas」

Along the east coast of Asia are a series of marginal seas enclosed by the Kamchatka Peninsula and island chains stretching from the Kuril Islands in the north through Japan and Okinawa to the Philippines in the south. This chain of enclosed seas, containing both broad continental shelves and basins thousands of metres deep, is an oceanographically unique environment with no equivalent anywhere else on Earth. People have harvested fish and other sea life from these seas for thousands of years.

[Figure 4b-2] Geography and bathymetry of the Sea of Okhotsk. Reproduced with permission from Nishioka et al. (2014).
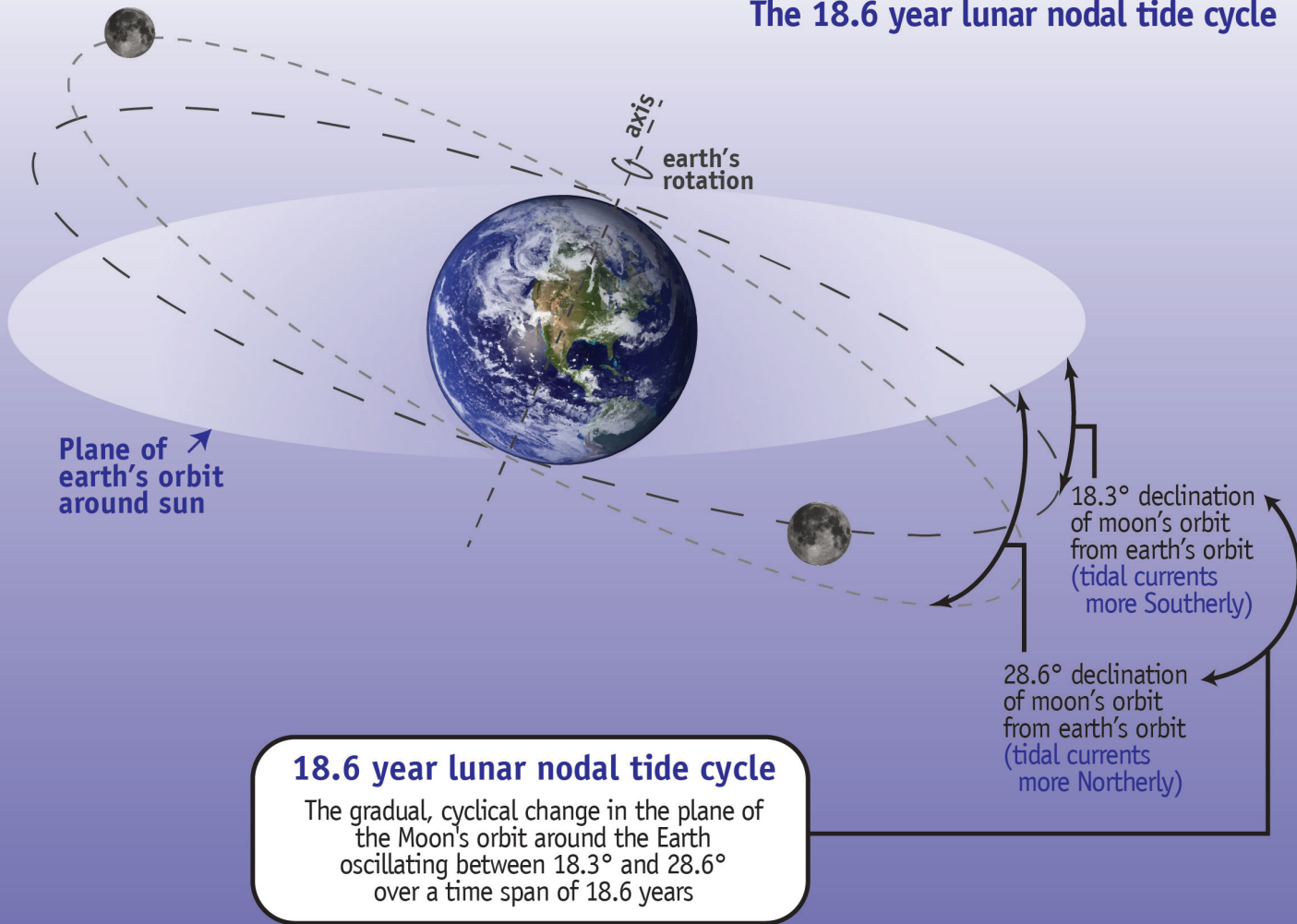
At the northern end of this chain of marginal seas is the Sea of Okhotsk (Figure 4b-2). Its land boundaries are mainland Russia, the Kamchatka Peninsula, Sakhalin Island, Hokkaido Island, and the Kuril Islands. The Sea has a broad continental shelf covering its entire northern half, with a limited area of deep (>3000 m) water at the southern end (the Kuril Basin). A second deep basin in the central Sea (the Deryugin Basin) is only about half as deep as the Kuril Basin.

The Amur River is one of the longest rivers in the world, with a total drainage area of more than two million square kilometres. The annual discharge exceeds 300 billion cubic metres, which forms the largest part of the freshwater inflow into the Sea of Okhotsk. The Sea is connected to the open Pacific by the Kuril Straits; the deepest passage among these is the Bussol Strait (~2300 m). Sea ice forms on the northwestern shelf in winter, and spreads southward across the Sea. Sea ice area has declined substantially in recent decades (Ohshima et al., 2014).

Sea ice formation generates Dense Shelf Water (DSW), which plays an important role in ventilation of the interior of the Sea and of the open Pacific (via Kuril Straits mixing).

Formation of DSW on the northwestern shelf and mixing in the Kuril Straits is a major source of oxygen to the subsurface layers of the North Pacific. North Pacific Intermediate Water (NPIW), which forms downstream of the Oyashio by mixing with Kuroshio Water, is the deepest layer of recently ventilated water in the North Pacific, reaching depths of 500-600 m in subtropical latitudes (see Chapter 2). The 18.6 year nodal tide cycle (see page 62) is detectable in ocean biogeochemical data from the open Pacific, and these signals are attributed to tidally induced mixing in the Kuril Straits (Ono et al., 2001; Andreev and Baturina, 2006; Sasano et al., 2018). It is important to note that ventilation by Kuril Straits mixing affects water properties at depths up to 2000 m, much greater than the depth of NPIW proper (Talley, 2001).

The 18.6 year lunar nodal tide cycle

axis

earth's rotation

Plane of earth's orbit around sun

18.3° declination of moon's orbit from earth's orbit (tidal currents more Southerly)

28.6° declination of moon's orbit from earth's orbit (tidal currents more Northerly)

18.6 year lunar nodal tide cycle

The gradual, cyclical change in the plane of the Moon's orbit around the Earth oscillating between 18.3° and 28.6° over a time span of 18.6 years
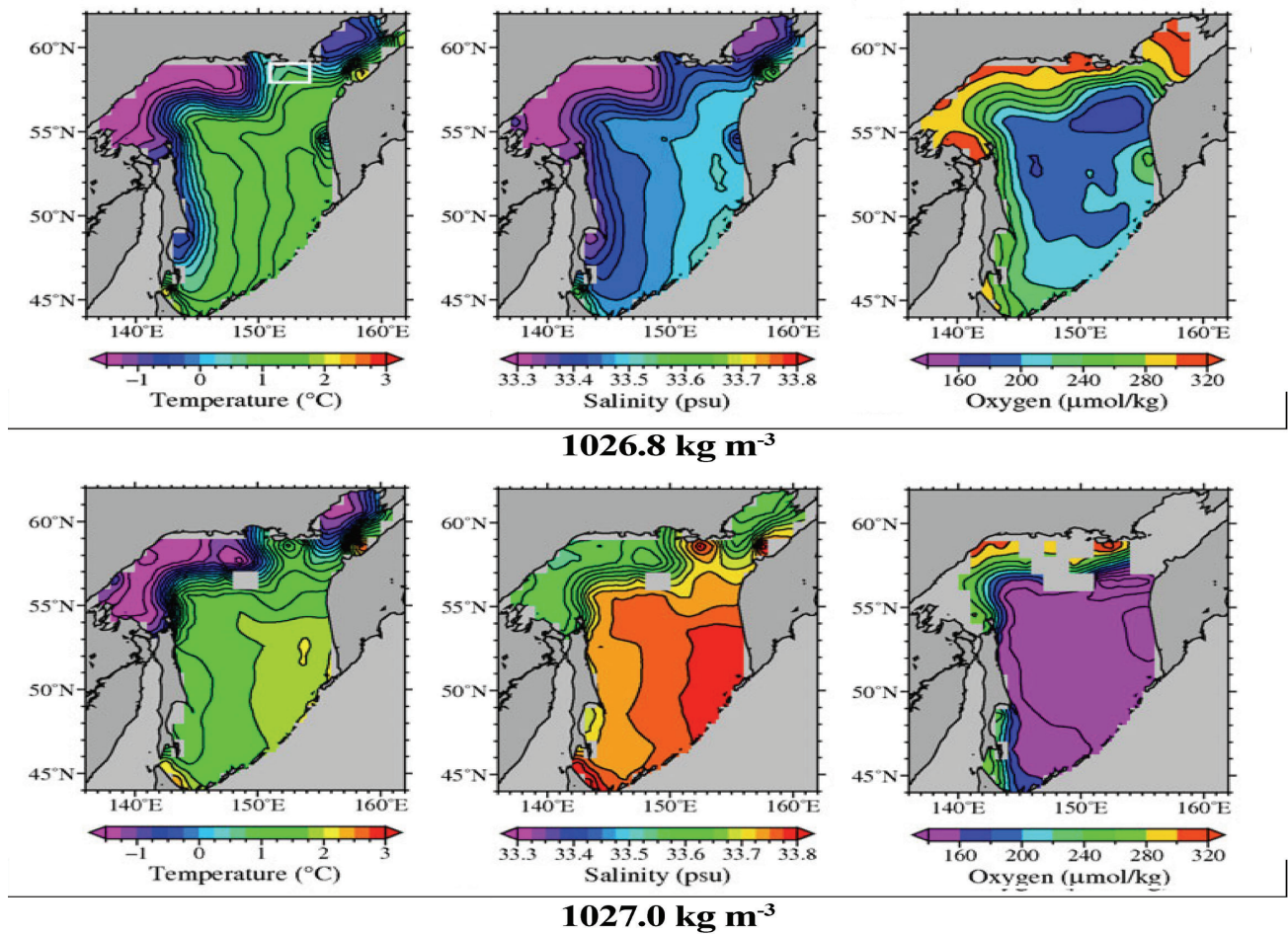
The 18.6 year lunar nodal tide cycle is a gradual, cyclical change in the plane of the Moon's orbit around the Earth. The lunar nodal tide cycle affects the strength and direction of tidal currents. When the angle of the orbital plane to the Earth's equatorial plane is greatest (the range is from 18.3 to 28.6°), the current is more northward (in the Northern Hemisphere).

Tidal currents and the mixing they generate as they flow over rough topography affect the temperature, salinity, and chemical composition of the ocean. As a result, the 18.6 year cycle is detectable in many data records. It has been detected in sea surface temperatures, coastal air temperatures, and oxygen and nutrient concentrations in the subsurface ocean.

Tidal mixing along the Aleutian and Kuril island chains plays a large role in the ventilation of the interior of the North Pacific Ocean. Even in the Gulf of Alaska, 10,000 km away, mixing in the Kuril Straits is an important determinant of the subsurface oxygen concentration.

1026.8 kg m⁻³

1027.0 kg m⁻³

[Figure 4b-3] Temperature, salinity and oxygen concentration in the Sea of Okhotsk at densities of 1026.8 and 1027.0 kg m^{-3}. Excerpted with permission from Uehara et al. (2012).

There was, until very recently, a very limited amount of oceanographic data from the Sea of Okhotsk. Oceanographers took an interest in the Sea because of its role in the formation of NPIW (e.g., Talley, 1991). The Far Eastern Regional Hydrometeorological Research Institute (FERHRI) has a data archive of ship-based observations of temperature, salinity, and oxygen (Uehara et al., 2012). There are about four times as many Sea of Okhotsk data in the FERHRI data base as in international repositories such as the Japan Ocean Data Center and the US National Ocean Data Center, and many of the data in the international repositories are old. The FERHRI data base has a preponderance of data collected after 1980 (Uehara et al., 2012). The available data have a distinct summertime bias, with minimal sampling in January and February. A climatology of the FERHRI data shows that the Sea is relatively well ventilated at water densities of 26.8 (equivalent to NPIW) and 27.0, but that O_2 concentration declines sharply over this depth range (Figure 4b-3).

FERHRI Research vessel *"Pavel Gordienko"*

Lyakhin (1970) mapped the saturation state of $CaCO_3$ in the Sea using data from research cruises conducted during 1949, 1951, and 1964. This is a remarkable achievement when one considers that (a) even decades later, only a few groups had the capacity to make measurements of sufficient precision and accuracy to make such calculations, and (b) the calculations (which involve the solution of a system of nonlinear equations) had to be made without the aid of digital computers. The seasonal and vertical distribution of saturation is as one would expect, with highest saturation states in the surface waters in summer (see Chapters 4a and 4g). The saturation state dropped as low as 150% in surface waters in winter, and waters below about 200 m are undersaturated. Minimum values (about 70%) were observed at depths of 800-1500 m in the Kuril Basin. Lyakhin noted that the deep waters are contiguous with those of the open North Pacific and have similar chemical composition, as also indicated by the oxygen distribution in the FERHRI climatology.
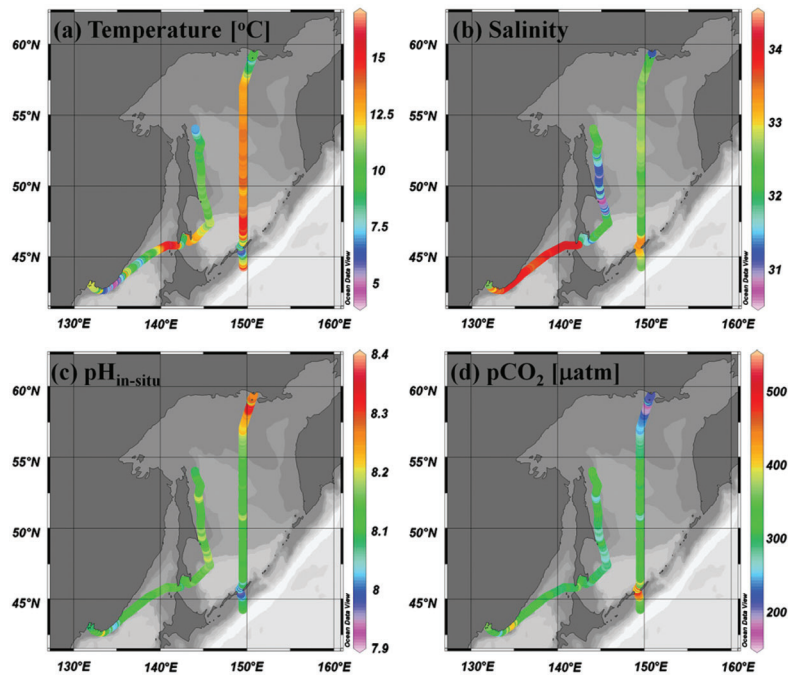
In the summer of 1993, Canadian and Russian oceanographers undertook WOCE section P1W, which sampled water properties over the full water column at intervals of 30 nautical miles (~56 km) along a section running from northwest to southeast across the Sea (Freeland et al., 1998). While Freeland mentions having sampled carbon system properties (DIC, alkalinity, and pH), none of the data are presented. Oxygen was also sampled, and both oxygen and other ventilation tracers such as chlorofluorocarbon indicate that the Kuril basin is fairly well ventilated. However, there are limited areas where bottom waters are poor (< 100 µM) in oxygen. Recent data suggest that formation of DSW and, therefore, ventilation of the deep basins has weakened over the past half century (Kashiwase et al., 2014; Ohshima et al., 2014). Hill et al. (2003) compared the P1W data to FERHRI data collected a half century earlier and concluded that the waters had become warmer and saltier.

There have been several journal special issues devoted to the oceanography of the Sea of Okhotsk, including the *Journal of the Remote Sensing Society of Japan* (1996), the *Journal of Geophysical Research* (2004), and *Progress in Oceanography* (2014), as well as several PICES Scientific Reports (No. 2, 1995; No. 6, 1996; No. 8, 1998; No. 12, 1999; No. 26, 2004; No. 36, 2009). Unfortunately, none of the papers in these volumes deal directly with carbon chemistry data. Pavlova et al. (2008) measured alkalinity and dissolved calcium
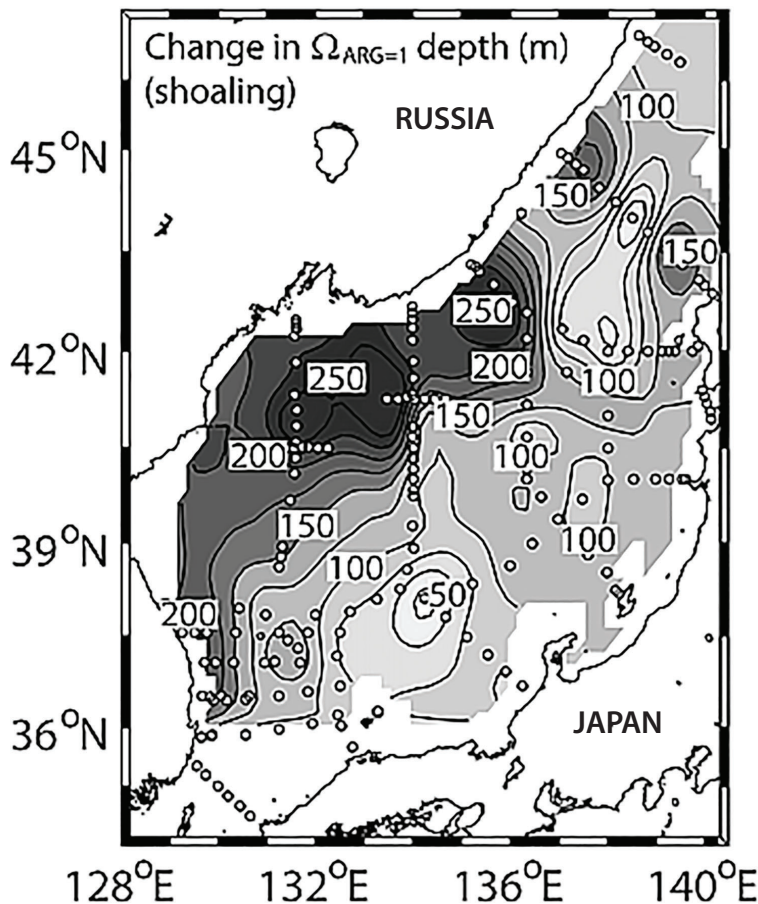
[Figure 4b-4] Continuous underway measurements of sea surface temperature, salinity, pH, and pCO$_2$ in September 2007. Reproduced with permission from Tishchenko et al. (2011a).

concentration at 41 locations in the Sea of Okhotsk. Tishchenko et al. (2011a) collected surface water pH and pCO$_2$ over the length of the Sea in late summer 2007 (Figure 4b-4). Broerse et al. (2000) measured CaCO$_3$ flux with sediment traps at 258 and 1061 m depth and estimated the degree to which intermediate waters are corrosive to the calcite particles. Other papers have measured the abundance and diversity of calcareous microfauna such as foraminifera and radiolaria (e.g., Nimmergut and Abelmann, 2002; Bubenshchikova et al., 2008). But on the whole it is probably safe to say that the baseline state for the progress of ocean acidification in the Sea of Okhotsk is not well observed. Several papers have addressed primary production in the Sea of Okhotsk, which is said to be extremely high, particularly over the continental shelf (Saitoh et al., 1996; Sorokin and Sorokin, 1999). While observations of carbon system

variables were not reported, it is likely that the CaCO$_3$ saturation state is high over the continental shelf in summer (Lyakhin, 1970), as it is on the Bering Sea shelf (Chapter 4a) and in parts of the Salish Sea (Chapter 4g). High productivity also leads to low oxygen concentrations in bottom waters, depending on the topography and circulation. As noted above, oxygen is low in bottom waters of the Deryugin and Kuril basins (depths >1000 m), but not over the continental shelf (Freeland et al., 1998).
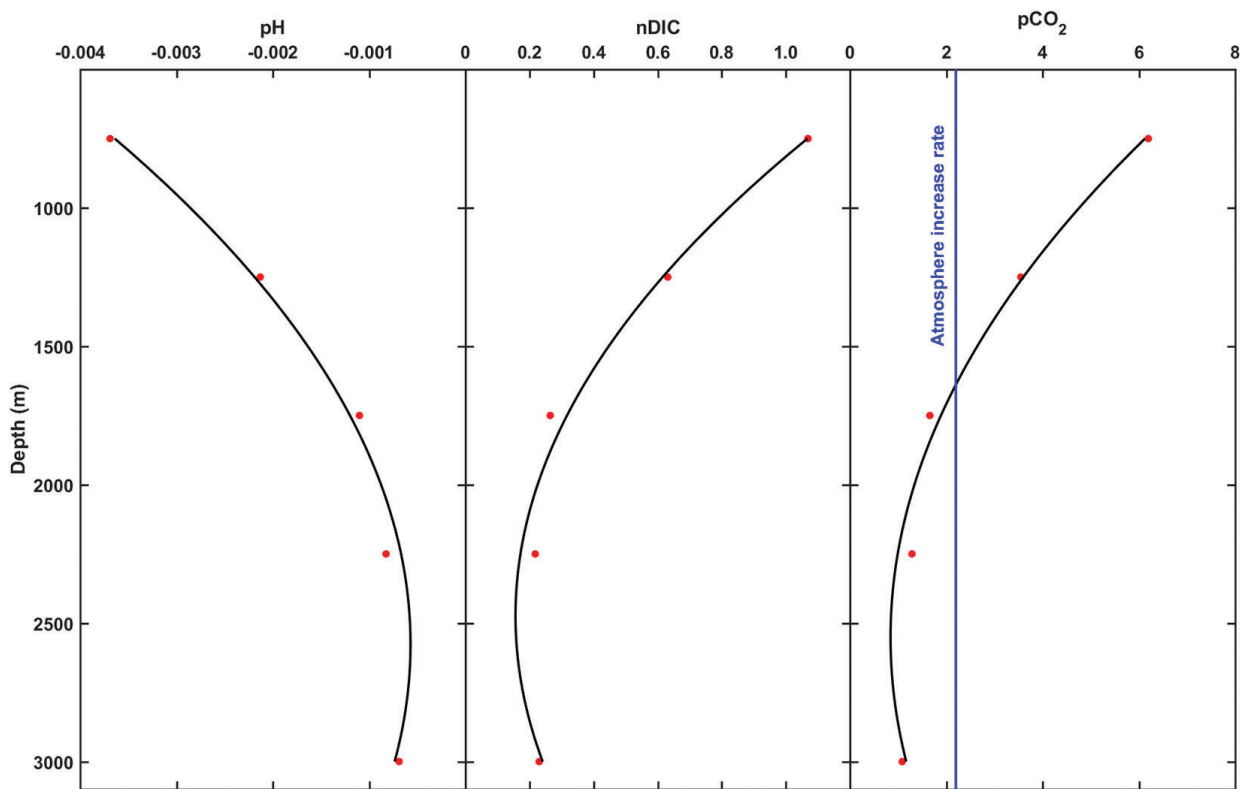
In the East Asian marginal seas, particularly in the area between Japan and the Asian mainland, there is a deep convection system and subpolar front independent of the analogous features in the open North Pacific. Chen et al. (2017) suggest that this region may therefore serve as an analogue for the world ocean as a whole under anthropogenic warming.

[65]

[Figure 4b-5] Historical shoaling of the aragonite saturation depth (Ω_A=1) due to anthropogenic CO_2. Open circles indicate sampling locations during the summer 1999 survey. Contour lines indicate intervals of 25 m. Modified with permission from Kim et al. (2010).

Gamo et al. (1986) were the first to detect a decline in oxygen concentration with time in the region. It has since been demonstrated that interior ocean waters off Japan and Korea have undergone drastic changes over the last 60 years, including continuous warming and a significant decrease in dissolved oxygen concentrations in the deep waters (Kim and Kim, 1996; Kim et al., 1999; 2004; Chen et al., 1999; Gamo, 1999; Kim et al., 2001; Ponomarev and Salyuk, 2001; Kang et al., 2004). There is strong experimental evidence of acidification associated with

this oxygen decline (Kim et al., 2010; 2014). Using TA, pH, and DIC data obtained in 1992, 1999, and 2007 for depths 50-1000 m, Kim et al. (2010) estimated the effect of anthropogenic CO_2 on the aragonite saturation horizon depth (Ω_A=1). Anthropogenic CO_2 accumulation has displaced the saturation depth upward by 50-250 m in various locations across the basin (Kim et al., 2010). More recent data suggest that acidification below 500 m in this region is primarily due to respiration of organic matter, rather than directly attributable to anthropogenic CO_2.
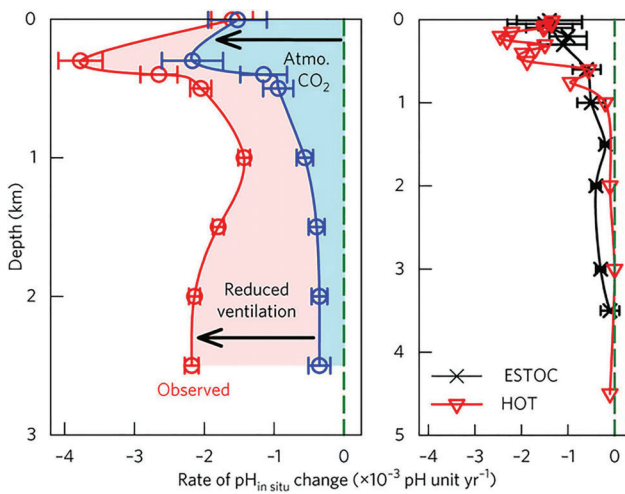
[Figure 4b-6] Rates of change of hydrochemical parameters at depths of 750-3000 m in the central region of the East Asian marginal seas. Rates of change for pH, nDIC, and pCO_2 are in pH units y^{-1}, mmol m^{-3} y^{-1}, and ppm y^{-1}, respectively. nDIC represents DIC normalized to a salinity of 35. Solid curves are second order polynomials fit to discrete depth data. Blue line shows the rate of change expected based on atmospheric CO_2 increase alone.

Since 1999, more than 20 hydrochemical surveys have been undertaken by the Pacific Oceanological Institute (Russia) and Seoul National University (Korea) under the auspices of the Circulation Research of the East Asian Marginal Seas (CREAMS) program (http://meetings.pices.int/members/advisory-panels/AP-CREAMS). Most stations were located to the north of 40°N; only four stations were located between 40°N and 38°N latitude. Two north-south sections along 132° 20'E and 134° 00'E were the most carefully sampled over the period 1999-2014. Seasonal variability of hydrochemical parameters in the northern region is very strong (Tishchenko et al., 2003).

These data sets indicate that pH and dissolved oxygen concentration in intermediate, deep, and bottom waters have decreased over time. The opposite trend was found for nutrients (phosphate, nitrate, silicate), nDIC and pCO_2. The decline of oxygen concentration is in agreement with previous published estimates (Gamo et al., 1986; Kim and Kim, 1996; Chen et al., 1999; Gamo, 1999; Kim et al., 1999; 2001; 2004; Ponomarev and Salyuk, 2001; Kang et al., 2004). The deoxygenation rate for depths 2000-3000 m was estimated as 10% per 30 years (0.67 µmol kg^{-1} y^{-1}) by Gamo et al. (2014); this is in very good agreement with more recent data.

Acidification and deoxygenation in this region occur in concert and are mainly caused by respiration of organic matter. Nutrient (nitrate, phosphate) concentrations also increase, indicating that excess DIC arises from respiration rather than uptake of anthropogenic CO_2. Chen et al. (2017) suggest that a weakening of deep convection over time is responsible for these trends, i.e., it is not so much that the rate of deep respiration has increased as that the products of respiration are accumulating at a greater rate due to enhanced stratification. Chen et al. (1999) earlier suggested that at abyssal depths, some regions in the East Asian marginal seas have been anoxic in the geologic past and could become so again.

The southern regions are strongly affected by river runoff and anthropogenic nutrient sources, as well as by inflows of open ocean water from the Kuroshio. Unlike the southernmost regions enclosed by the Philippine and Indonesian island groups, the East China Sea and the Yellow Sea are separated from the open Pacific only by the relatively sparse Ryukyu island chain. Lui et al. (2015) observed that there is a measurable acidification and deoxygenation signal associated with the inflow of Kuroshio Intermediate Water. The downward trend in the Kuroshio water was estimated to be about equally divided between the effect of anthropogenic CO_2 uptake and the effect of increased respiration, leading to rates of pH decline greater than the global average, even without any local

[Figure 4b-7] Rate of change of pH between 1965 and 2015 in the central region of the East Asian marginal seas. Blue indicates change due to increasing atmospheric CO_2, while the red indicates change due to respiration. Rates at the open ocean stations ESTOC (subtropical Atlantic) and HOT (subtropical Pacific) are shown for comparison. Reproduced with permission from Chen et al. (2017).

eutrophication effects. Chen et al. (2007) noted that, as in the Bering and Okhotsk seas, the continental East China Sea experiences seasonal oxygen depletion. This implies low pH and $CaCO_3$ saturation states as well (see Chapter 4a), although these authors did not measure carbon system parameters. The area experiencing low oxygen concentrations (90-135 µM) was estimated as 12,000 km^2. Ning et al. (2011) observed a long-term decline in summer bottom water oxygen in the East China Sea from 1975-1995. They estimated that warming (i.e., solubility) accounts for about 25% of the decline, with the rest associated with local anthropogenic sources and increases in stratification also with primarily local/terrestrial causes. Local impacts in coastal areas are discussed further in Chapters 4c-e.

How do we know ancient oceans were anoxic?

Ocean acidification and deoxygenation are associated with some of the great mass extinction events of the geologic past. When periods of exceptional volcanic activity pump billions of tons of CO_2 into the atmosphere over tens of thousands of years, the climate becomes much warmer, reducing the solubility of oxygen in seawater, and the oceans become more acidic due to uptake of CO_2 from the atmosphere. For most of Earth history, life existed only in the oceans, and some of the great mass extinction events have been primarily marine. CO_2 is a plausible mechanism for extinction of calcareous organisms like snails or clams (from which much of our fossil knowledge of these events derives), and we know from rock strata laid down at these times that periods of exceptional volcanic activity occurred. Cumulatively, the total quantity of CO_2 released during some major volcanic episodes was much larger than what humans are emitting today, but the rate was much less.

Evidence for anoxia in ancient oceans is derived from minerals in the sediments that contain redox sensitive elements like uranium. In the modern ocean, uranium is conservative, meaning its concentration changes only with precipitation and evaporation at the surface. In anoxic sediments, however, uranium forms solid minerals that are preserved in the sediments for millions of years. This also true of, e.g., zinc, silver, and cadmium, whereas other elements like iron and manganese are insoluble in oxygenated seawater and soluble under anoxic conditions. Total sulfur is another indicator of anoxic bottom water, as it is preserved in the form of sulfides, e.g., of zinc when hydrogen sulfide is present in the bottom water (Masuzawa and Kitano, 1984). Anoxic conditions are also indicated by the disappearance of bottom-living microfauna such as foraminifera and radiolaria, which can not tolerate anoxic conditions (e.g., Oba et al., 1991; Itaki et al., 2004).

Similarly, carbonate minerals in sediment cores give us evidence of ancient ocean acidification. Recall that the saturation depth is the depth below which calcium carbonate minerals dissolve and hence are not preserved in the sediments (Chapter 1). During the Paleocene-Eocene Thermal Maximum (about 55 million years ago), the fraction of $CaCO_3$ in some sediment cores declined from 80-90% to 0% in what would be considered, in geologic time, the blink of an eye (Zachos et al., 2005). At depths where $CaCO_3$ shells had previously been preserved intact, they were absent from new strata laid down after the event, and did not fully recover for about 100,000 years. This strongly suggests that the cause of the event was a rapid release of CO_2 into the atmosphere and ocean. In some deep basins of the East Asian marginal seas, there have been anoxic events where both the bottom-living calcareous microfauna and surface-living (planktonic) ones that rain down through the water column disappeared, while noncalcareous plankton did not (Oba et al., 1991). This implies that the bottom water was acidified and corrosive to $CaCO_3$.

[69]

[4C] Japan coastal region
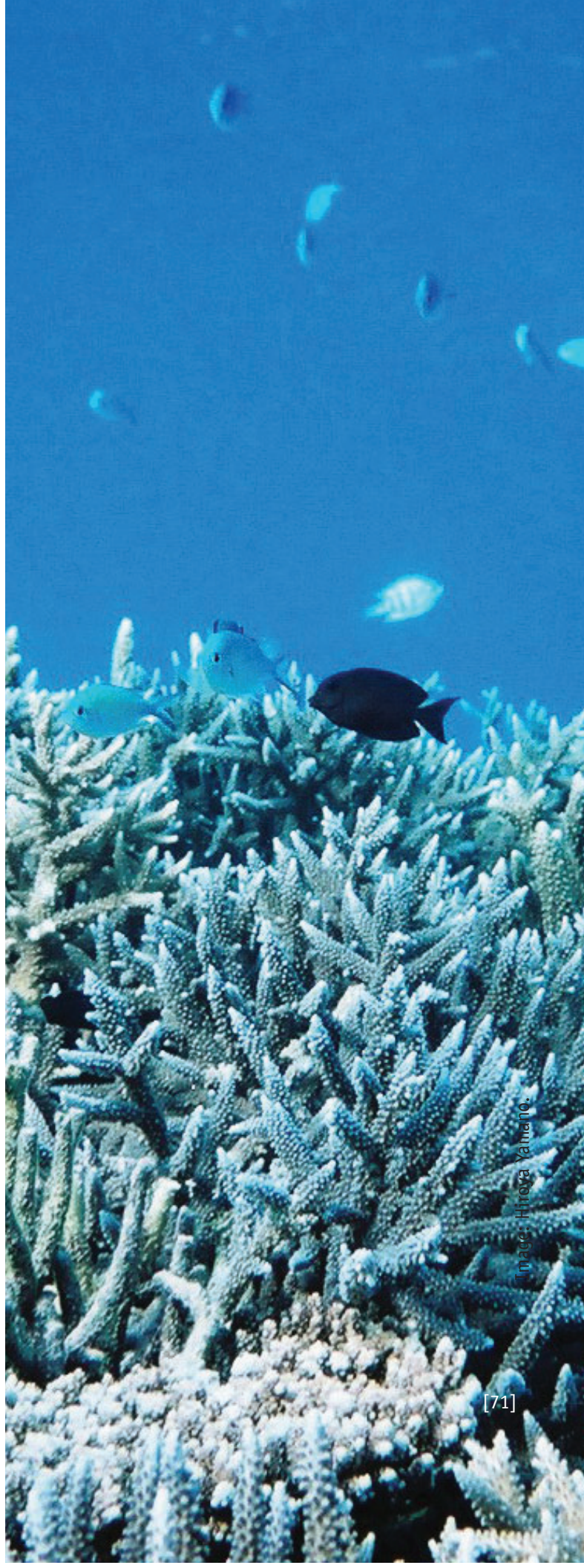
Japan has one of the longest coastlines of any country in the world, at nearly 30,000 km. Japan extends from the subarctic to the subtropical climatic zones, so coastal ecosystems are highly variable. Large submarine forests of Laminariaceae kelps are found along the northern part of the Japan coast, while coral reefs surround the coasts of the southernmost islands. In between is a mixed submarine forest of laminariaceae and sargassums, which covers wide areas of the Japanese coast. All of these environments provide habitat for benthos and groundfish, and they also function as nursery grounds for pelagic fishes such as Japanese sardine and chub mackerel. Protection of the Japanese coastal environment is thus highly important for North Pacific ecosystems and fisheries.

Japan is located at the subtropical-subarctic boundary, and its coastline is exposed to a significant latitudinal gradient of water temperature. Anthropogenic warming has already begun to shift isotherms northward along the coast, causing significant change of vegetation. Coral reefs in the Okinawa islands face frequent bleaching due to high summer water temperature, (e.g., Yara et al., 2014; Kayanne, 2017). In the temperate area, seaweed forests are changing rapidly from a mixture of laminariaceae and temperate sargassum species to tropical sargassum species, without laminariaceans (Tanaka et al., 2012). As the subtropical sargassum forest has far less productivity compared to the present temperate forest, such change significantly affects coastal fisheries. Model simulations suggest that these changes, due to increasing temperature, could cause existing coastal ecosystems to collapse within this century (Yara et al., 2012; 2016; Takao and Fujii, 2015).

Ocean acidification may cause additional problems for Japanese coastal ecosystems and hence hasten ecosystem collapse. The northward shift of coral reefs will be significantly obstructed by acidification of temperate coastal waters (Yara et al., 2012; 2016). Even in the temperate and subarctic coastal areas, calcifiers may be affected by ocean acidification within this century. A recent experimental study suggested that some calcifiers respond not to daily-averaged Ω but to the minimum encountered during the day or night (Onitsuka et al., 2018). It is therefore important to design coastal monitoring programs with high temporal resolution to resolve diurnal variation of pH and/or pCO_2, and to capture the daily minimum pH.

Japan has a richly indented coastline, and small fishing ports and villages have been constructed in such indentations throughout history. The present-day coastline is thus characterized by alternation of natural coast and fishing port/village over scales of a few kilometres. Seawater near these ports may have enhanced CO_2 concentration because of degradation of organic substances, and high-CO_2 water may be transported to the surrounding natural coastal areas. Ocean acidification monitoring thus requires high spatial as well as temporal resolution, so that the contribution of local human activities can be understood.

[71]

[Figure 4c-1] Sampling stations maintained by members of the Japan Ocean Acidification Network. See table on next page for details.

Coastal ocean acidification monitoring

The earliest coastal pH monitoring started in 1982 at Onjuku and in 1992 at Kashiwazaki, by the Marine Ecology Research Institute (MERI). These observations were originally made as part of MERI's regular monitoring of its rearing waters. pH measurement was made by glass electrode standardized against NBS standards. Data obtained at these two stations provide a unique long-term time series of coastal pH. After 2000, six additional monitoring stations using modern pH and pCO_2 sensors have been added.

Four monitoring stations (Akkeshi, Oshoro, Tateyama, and Sesoko) have operated under the JSPS project "Japan Coast Ocean Acidification Monitoring and its Effect on Fisheries" since 2015, but the other stations are operated by individual funds. There is no fund to cover coastal ocean acidification monitoring sites comprehensively, so investigators have voluntarily organized a Japan Ocean Acidification Network (JOAN) as a platform for information exchange and collaboration in measurement and analysis. Several stations have been incorporated into the Global Ocean Acidification Observing Network (GOA-ON), but most stations have not yet done so.

Continuous measurements of pCO_2 are collected at only two long-term stations, while pH is measured at most stations. At most stations pH is measured by sensors, but at some stations it is measured by regular water sampling, and pH readings are taken by glass electrodes. DIC and alkalinity are measured at most stations, which helps greatly in calibrating instrumental measurements and correcting offsets between stations.

| Site ID	Location	Institute	Duration	Frequency of pH or pCO₂ measurement	Detection of OA	Registration to GOA-ON	pCO₂	pH	DIC	TAlk	others	PI and contact address
M1	Akkeshi Bay	Akkeshi observatory, Hokkaido Univ.	2017~present			●		●	●	●		Masahiro Nakaoka (nakaoka@fsc.hokudai.ac.jp)
	Lake Akkeshi	Hokkaido Univ.				●		●	●	●		
M2	Oshoro	Hokkaido Univ.	2013~present	continuous				●	●	●	nutrients	Masahiko Fujii (mfujii@ees.hokudai.ac.jp)
M3	Tsugaru Strait / shoreline	JAMSTEC	2013~present	once / week		●			●	●	nutrients, DOC, TDN, ¹⁸O, phytoplankton	Masahide Wakita (mwakita@jamstec.go.jp)
	Tsugaru Strait / coastal water		2009~present	4 times / year					●	●	nutrients, Chl a, ¹⁸O, phytoplankton, zooplankton	
M4	Kashiwazaki	MERI	1992~present (pH)	once / day	●			●			T, S, DO	Jun Kita (kita@kaiseiken.or.jp)
			2015~present (pCO₂, TAlk)	continuous (pCO₂)			●			●		
M5	Onjuku	MERI	1982~present (pH)	once / day	●			●			T, S, DO	Jun Kita (kita@kaiseiken.or.jp)
M6	Tokyo Bay	TUMSAT	2011~present	once / month				●	●	●	nutrients, DO,Chl a	Michiyo Yamamoto-Kawai (michiyo@kaiyodai.ac.jp)
	Tateyama Bay		2015~present	continuous		●		●	●	●	nutrients	
M7	Shimoda Bay / inlet	Tsukuba Univ	2014~present	continuous				●	●	●	light intensity	Shigeki Wada (swadasbm@shimoda.tsukuba.ac.jp)
	Shimoda Bay / coastal water		2011~present	1-2 times / month					●	●	nutrients, Chl a, POC, light intensity	
M8	Sesoko Is.	Ryukyu Univ.	2000~present	continuous		●		●	●	●	DO, nutrients, Chl a, etc.	Haruko Kurihara (harukoku@sci.u-ryukyu.ac.jp)
M9	Arasaki	FRA	2009~2011				●					Tsuneo Ono (tono@fra.affrc.go.jp)
M10	Sadamisaki	Ehime Univ.	2002~2008				●				nutrients, Chl a, T, S, turbidity	Naoki Yoshie (yoshie.naoki.mm@ehime-u.ac.jp)
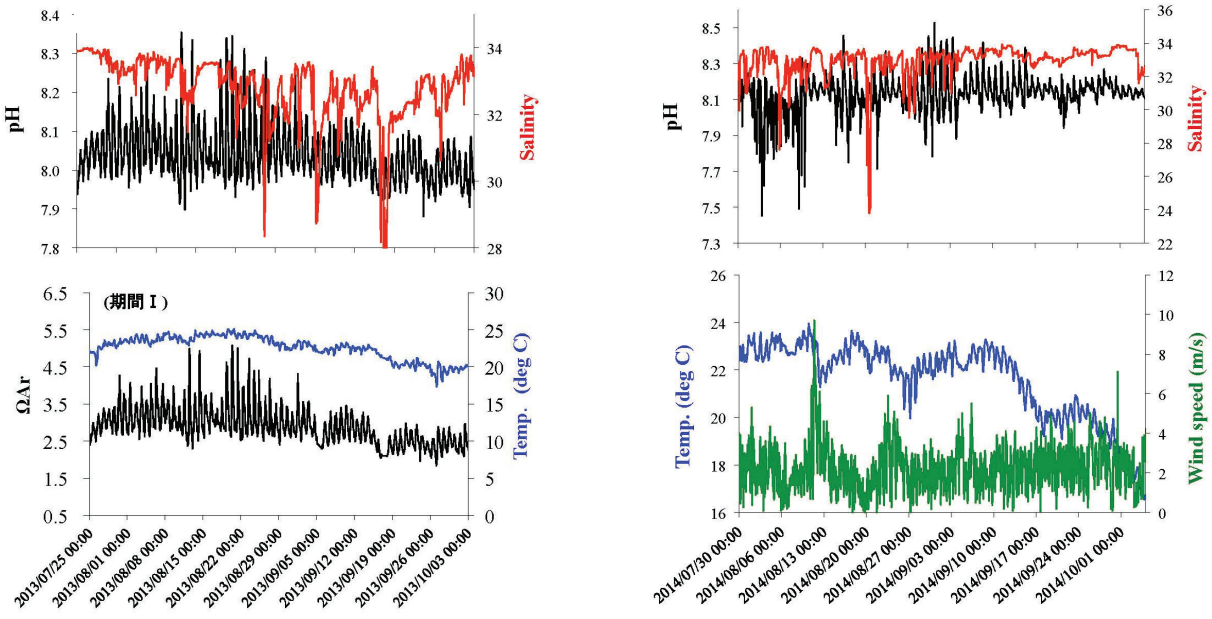
[Figure 4c-2] Location of Oshoro Bay station on Hokkaido Island (Station M2).

High-frequency variation at coastal sites

The Oshoro Marine Station of Hokkaido University is located at Oshoro Bay on the west coast of Hokkaido Island (Figure 4c-2). The bay is filled with seaweeds, which cause large diurnal and seasonal variations in pH and related water properties at this location. A glass electrode pH sensor (SP-11, Kimoto Electric) and temperature and salinity sensors (ACTW-USB, JFE Advantech) are placed at 2m depth at the end of a pier (about 50 m from shore). Water sampling for DIC, alkalinity, and nutrient concentrations is carried out periodically. Preliminary results show strong diurnal variation in pH as well as Ω_A in summer. The average amplitude of the diurnal pH variation was 0.18 and 0.28 in 2013 and 2014, respectively, but can be as large as 0.83. Nighttime values of Ω_A are sometimes less than 1. Investigators are now developing regional carbon cycle models to determine the combination of forcing factors that cause such a large diurnal change (Takao et al., 2015). High diurnal variation in pH is also observed in other subarctic seaweed-bed areas such as Akkeshi station, especially in summer. At stations in temperate coastal areas, such as Shimoda Bay, the amplitude of diurnal pH variation is only about 0.4. At Sesoko Station, a coral-reef station located adjacent to Okinawa Island, diurnal pH variation is around 0.2 year round.
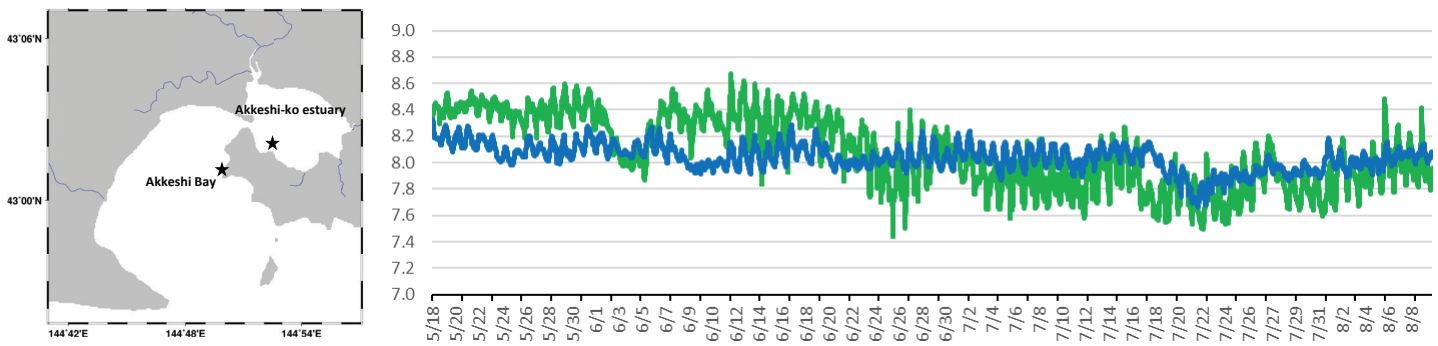
[Figure 4c-3] Time series of water temperature, salinity, pH, Ω_A, and wind speed observed at Oshoro station in summer/fall in 2013 (left panels) and 2014 (right panels). Reproduced with permission from Takao et al., 2015.

The Akkeshi Marine Station is also operated by Hokkaido University, but is located on the opposite coast, adjacent to the open Pacific (Figure 4c-1, 4c-4). Continuous pH monitoring in Akkeshi Bay (coastal) and in the eelgrass beds of the Akkeshi-ko estuary (brackish) has been carried out since May 2017, with similar instrumentation as described above. This location also shows substantial diurnal variation, especially in summer.

Meta-analysis of overall regional trend
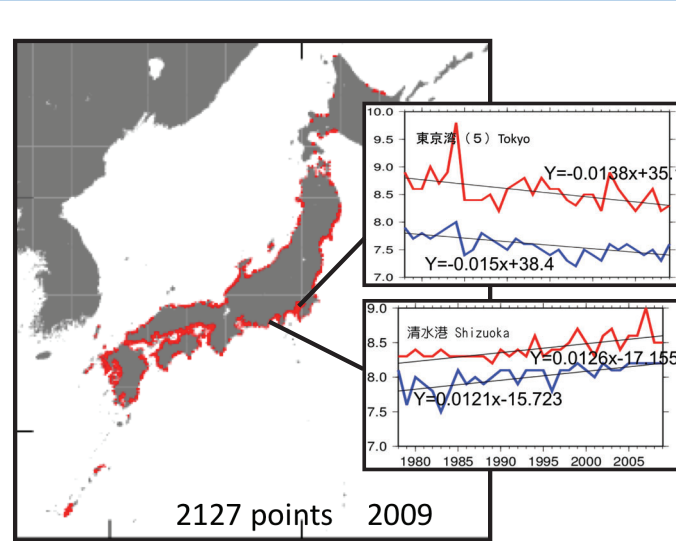
In addition to recent high-precision continuous ocean acidification monitoring sites, Japan has over 2000 coastal pH time series stations operated by the Japan Ministry of the Environment (MOE; Figure 4c-5). These stations were launched in the 1980s and have been maintained for water quality monitoring. Measurement precision of pH is poor, only about 0.1 unit, so the reliability of a long-term pH trend obtained at any individual station is low. In addition, many coastal processes such as eutrophication or artificial alteration of coastlines may affect pH time series at individual stations: many stations even show increasing pH trends. The mean pH trend averaged for all 2000 monitoring stations is -0.0015 per year (Figure 4c-6), almost identical to that observed at open ocean stations like HOT (Bates et al., 2014). So while local processes cause significant variability in ocean acidification trends among the observation points, Japanese coastal waters as a whole show a rate of acidification similar to the global average.

[75]
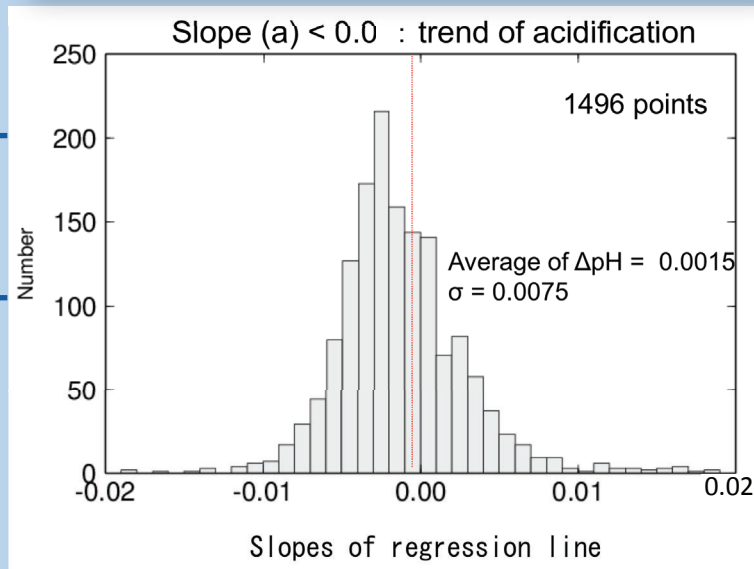
[Figure 4c-4] Location of Akkeshi Bay stations and observed time series (blue: bay; green: estuary) of pH (normalized to a constant temperature of 25°C). Reproduced with permission from Wada and Hama (2013).

[Figure 4c-5] Map of stations for water quality monitoring stations operated by Japan Ministry of the Environment (MOE), and overall linear trends calculated for a meta-analysis of all stations. Red and blue lines indicate annual maximum and minimum pH, respectively. Upper panel shows data from a station in Tokyo Bay; lower panel shows data from a station in Shimizu port, Shizuoka prefecture. Ishizu et al, unpublished data.

[Figure 4c-6] Histogram of pH trends at individual MOE stations. The average is slightly negative, indicating an overall trend towards acidification.
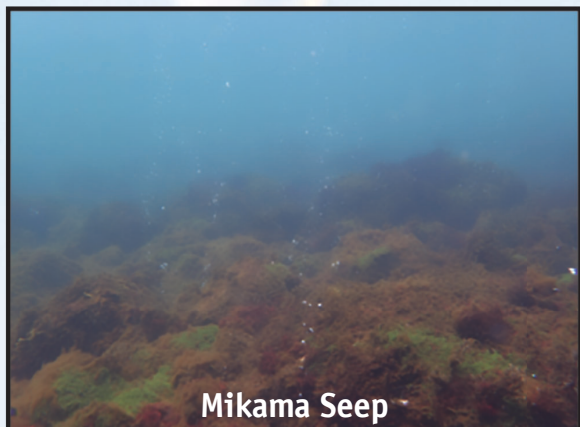
Natural CO$_2$ Seeps

Japan

Shikine Island

Ashitsuke Seep
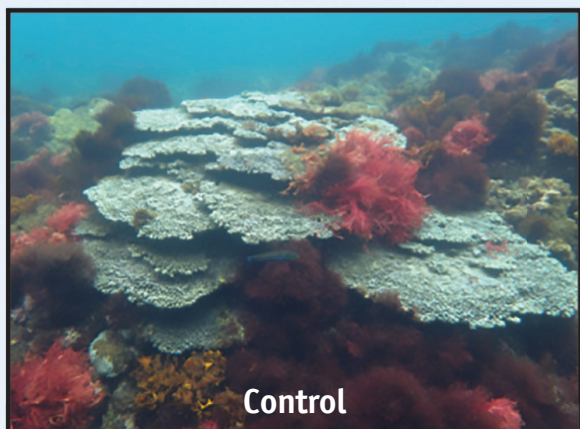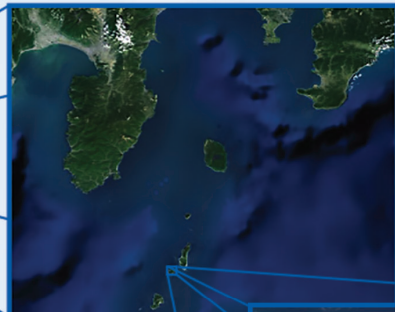
Natural CO$_2$ seeps are an amazing natural laboratory for studying the effects of elevated CO$_2$ on organisms. At natural CO$_2$ seeps, subsurface volcanic activity causes waters to flow out of the seafloor with CO$_2$ concentrations that can be twenty times that of ambient seawater.

Mikama Seep

Control

In 2015, scientists from the University of Tsukuba found two active CO$_2$ seeps at Shikine Island, Japan (Agostini et al., 2018). These seeps are located in a shallow inlet with a depth of less than 10 m, and pH ranges from 8.2 in surrounding natural waters to 6.8 at the center of the seep.

There is a clear transition of bottom vegetation along the pH gradient. In the control area, the seafloor is covered by large brown algae and hard corals. As pH decreases, both two groups disappear and vegetation changes to small brown algae and green algae. The University of Tsukuba created a seep monitoring station in 2016, and variation of flora and fauna along with pH is now being investigated thoroughly.

Coral reefs are usually thought of as being associated primarily with the tropics. But four of the six PICES member countries have them. United States territory extends from Hawaii in the southeast to Midway in the northwest (the linear island chain is the legacy of plate movement across a stationary Hot Spot). The Northwest Hawaiian Islands are coral atolls, uninhabited by humans but home to millions of sea birds and the extremely endangered Hawaiian monk seal (right). Japan has the most northerly coral reefs in the world (Veron and Minchin, 1992). There is concern that ocean acidification will limit the northward migration of Japanese corals with climate change (Yara et al., 2012; 2016): as the climate gets warmer, the region of coral reefs should migrate northward along the coasts of Japan, but ocean CO_2 uptake will make some of this potential new habitat unsuitable. In Korea, corals are found around the southern island of Jeju and along the southernmost reaches of the mainland. And China, of course, extends from the temperate zones into the tropics (Hainan Island is at about the same latitude as Hawaii).
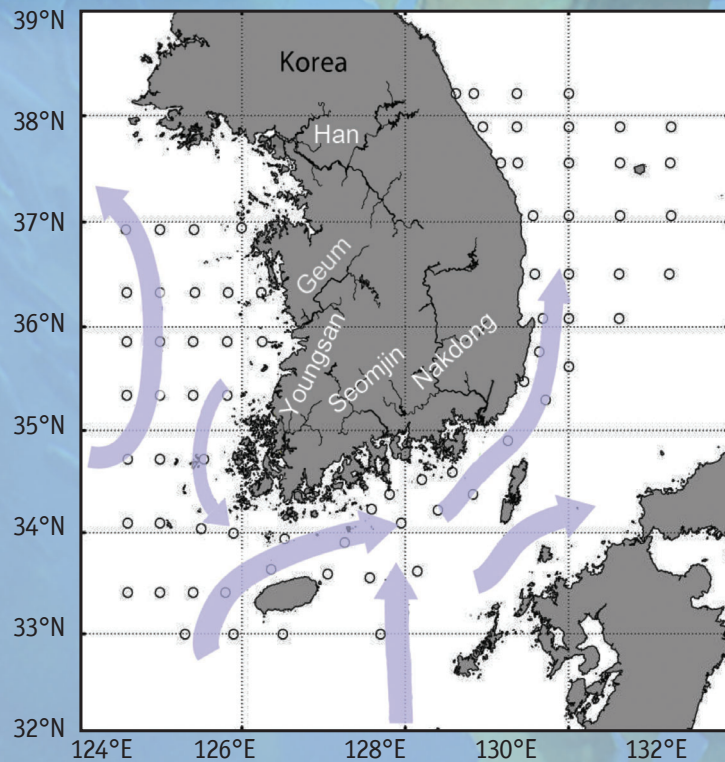
Deep sea corals are distinct from reef building corals, which rely on photosynthetic symbionts for energy and therefore grow only in the sunlit upper ocean. But they also have calcareous skeletons and are therefore vulnerable to acidification. Deep sea corals are found at all latitudes, including the high latitude North Pacific (e.g., Stone, 2006; Jamieson et al., 2007).
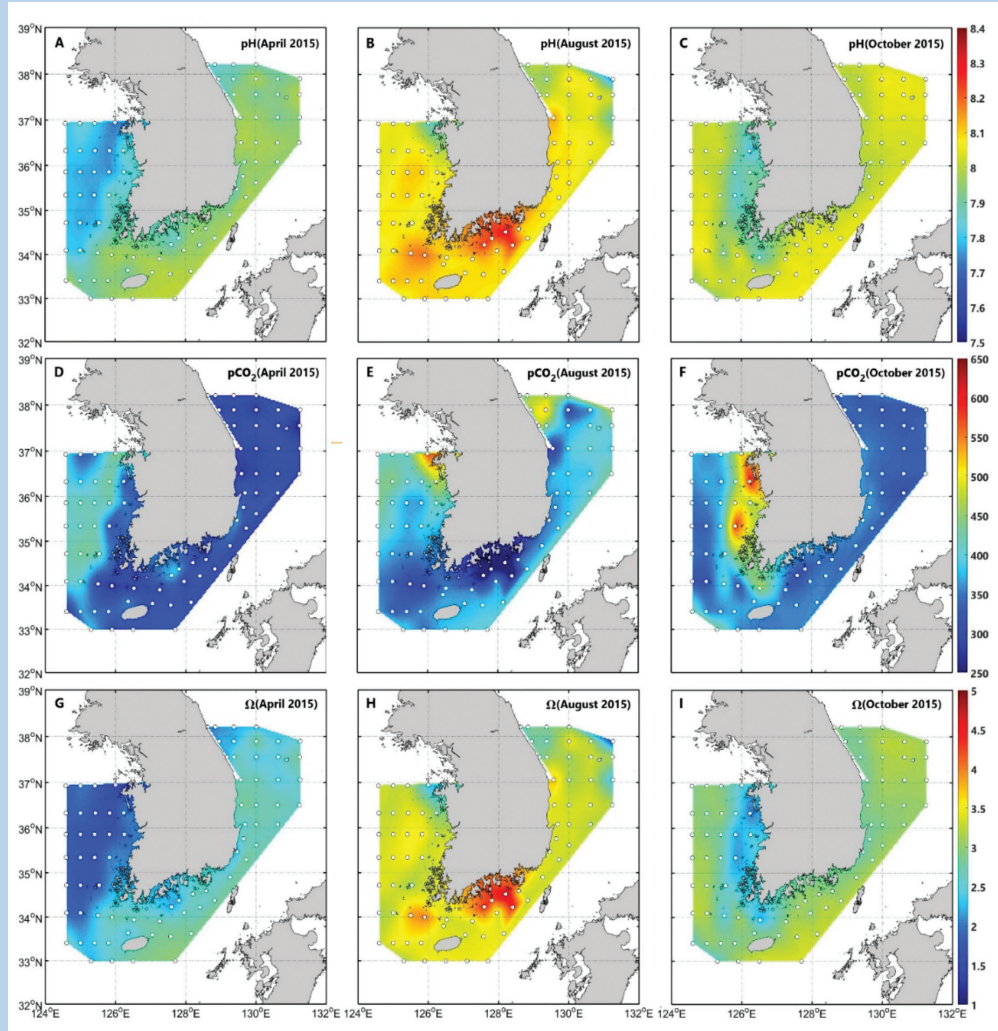
[4d] 「Korea coastal region

[Figure 4d-1] Map of the Korean coastal region. Open circles indicate sampling locations. Grey arrows represent the flow directions of major currents in summer. Courtesy of Pohang University of Science and Technology.

Korea is small country with a great deal of coastline. The east and south coasts border more oceanic waters (see Chapter 4b) while the west coast is adjacent to the more coastal waters of the Yellow Sea. The latter has large tides (4-8 m), strong seasonal phytoplankton blooms and significant river inputs. Three major rivers, the Nakdong, Seomjin and Youngsan, flow into the waters adjacent to the south coast. People and industries are most abundant along the west and south coasts.

Korea has recently introduced a nationwide program for ocean acidification monitoring, with 82 sampling stations along all three coasts, extending far into the ocean (Figure 4d-1). Routine sampling depths are 0, 20, 50, 75, 100, 125, 200, and 500 m, depending on bottom depth. These stations are maintained by the National Institute of Fisheries Science. Samples have been collected during April, August and October since 2015.
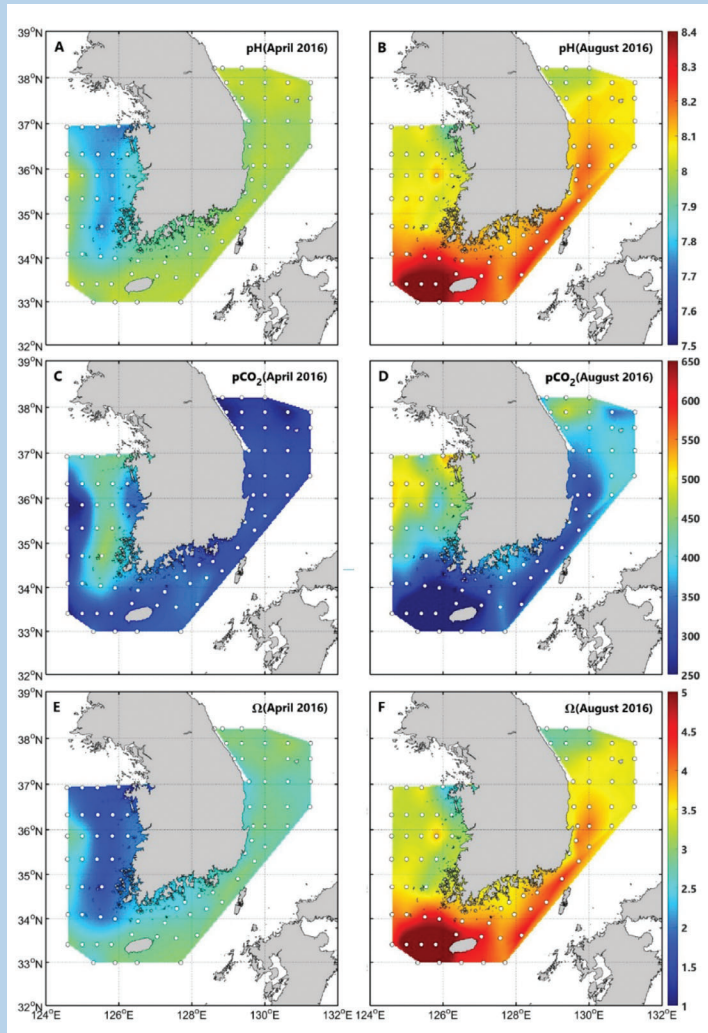
[Figure 4d-2] Spatial distribution of surface seawater pH, pCO_2, and Ω_A (A, D and G, respectively) in April 2015; (B, E and H, respectively) in August 2015; and (C, F and I, respectively) in October 2015. Open circles indicate sampling locations. The colour scales indicate hydrogen ion concentration (pH), gaseous CO_2 (pCO_2) in surface seawater (ppm), and aragonite saturation state (Ω_A).

Results from this sampling show that the ocean is generally supersaturated with respect to aragonite, but with considerable seasonal variation (Figures 4d-2 and 4d-3). In 2015, surface Ω_A ranged from 2.0-3.0 in April, with the Yellow Sea being the least supersaturated region. The range was similar in October. In August, surface saturation reached as high as 4.3, with the highest values observed along the south coast, which suggests substantially higher biological productivity in this region.

Surface pH ranged from 7.8-8.0 in April 2015, 8.1-8.3 in August, and 7.9-8.0 in October. So pH increases in summer by around 0.3 due to higher biological productivity (phytoplankton consume CO_2 in surface waters, which increases Ω_A
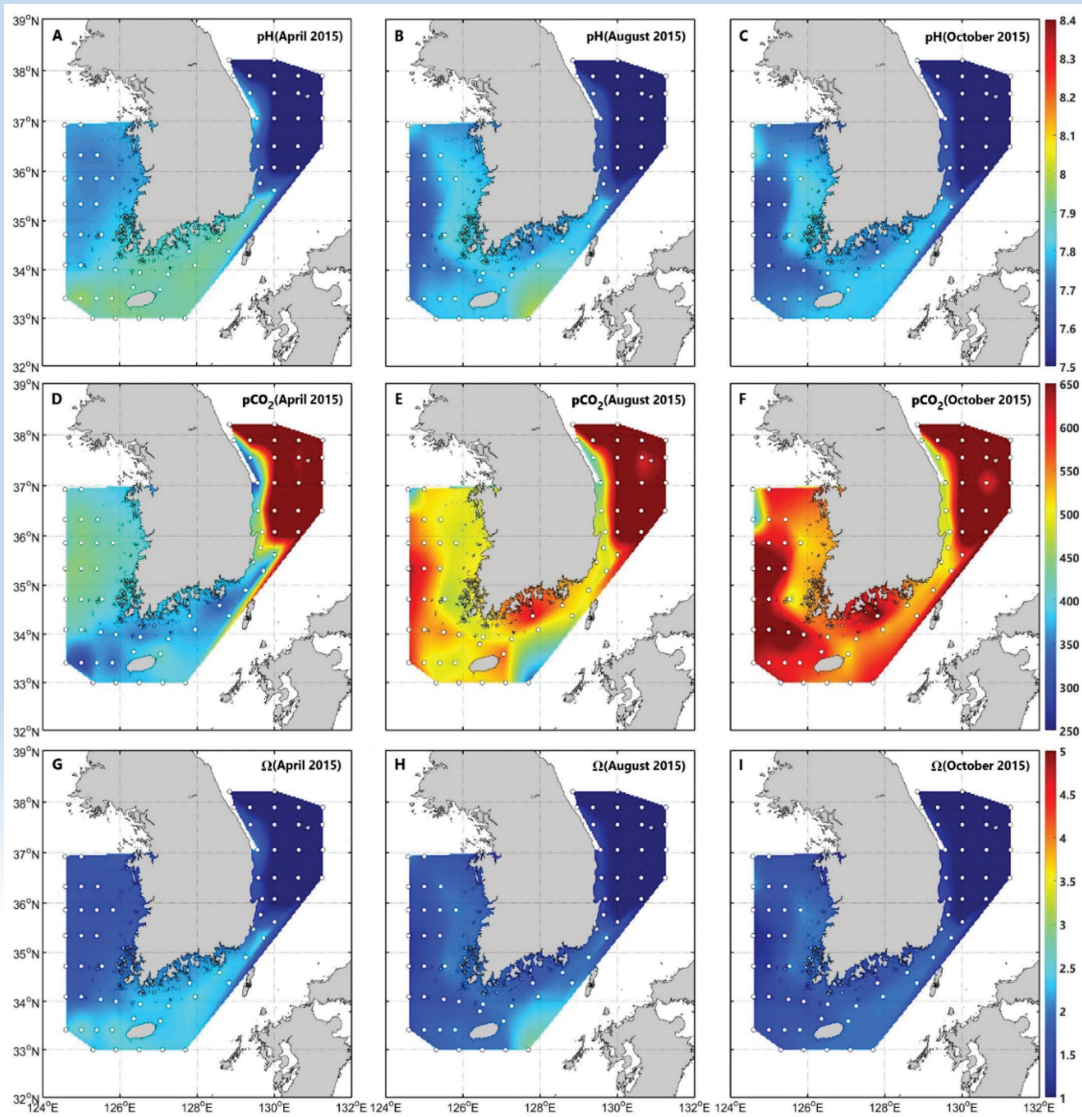
[Figure 4d-3] Spatial distribution of surface seawater pH, pCO_2, and Ω_A (A, C and E, respectively) in April 2016; and (B, D and F, respectively) in August 2016. Open circles indicate sampling locations. The colour scales indicate hydrogen ion concentration (pH), gaseous CO_2 (pCO_2) in surface seawater (ppm), and aragonite saturation state (Ω_A).

and pH while reducing pCO_2). Seasonal changes in water temperature also contribute to these fluctuations.

Coastal waters of the Yellow Sea in April and October showed lower Ω_A and pH relative to the more oceanic waters of the east and south coasts. This can be attributed to the shallow depth (around 50 m) and strong tidal currents that mix

surface waters with bottom waters that have higher DIC.

In 2016, the spatial variations of surface seawater carbonate parameters were mostly similar to 2015, but an anomalous water mass with higher Ω_A and pH and lower pCO_2 relative to the adjacent waters was detected in the southwest. This was thought to be due to the possible

[Figure 4d-4] Spatial distribution of near-bottom seawater pH, pCO_2, and Ω_A (A, D and G, respectively) in April 2015; (B, E and H, respectively) in August 2015; and (C, F and I, respectively) in October 2015. Circles indicate sampling locations. The color scales indicate hydrogen ion concentration (pH), gaseous CO_2 (pCO_2), and aragonite saturation state (Ω_A).

influence of Changjiang River water spreading northeastward (Lee and Kim, 1998; Lie et al., 2003). In general, when the Changjiang River water discharges into the East China Sea, it is diluted as it mixes with seawater. This diluted water plume flows southward along the coast of China in winter, but during the summer monsoon it flows in two directions: one along the southeastern coast of China
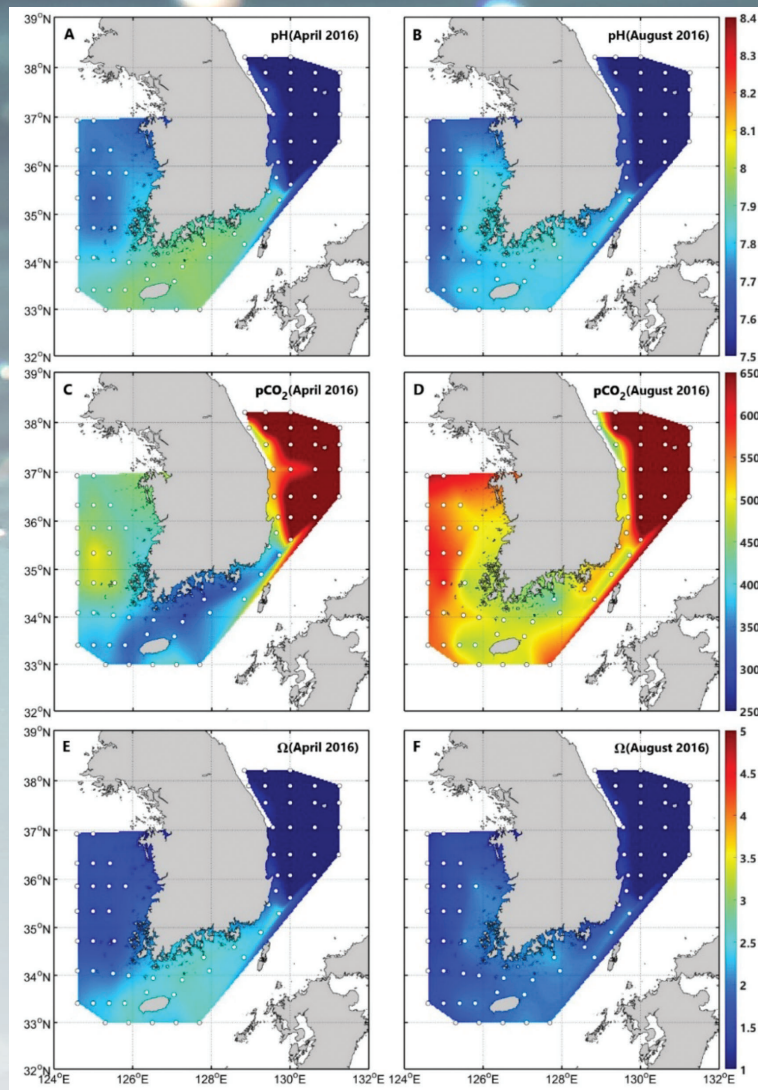
and the other northeastward (Mao et al., 1963; Beardsley et al., 1985). Surface seawater samples collected near Cheju Island in August 2016 showed low salinity (<30); the lowest salinity recorded was 21.8.

The seasonal variations observed in near-bottom waters in 2015 and 2016 were insignificant compared to those in surface

waters (Figures 4d-4 and 4d-5), mainly due to the slower response of deeper waters to changes in near-surface conditions. Distinctive regional variations were observed, but this is mainly due to different bottom depths (and therefore the deepest sampling depth) in each region. The relatively high pH observed in the Yellow Sea is attributable to the shallow depth and large tidal range in this region.

The combined effects of rising sea surface temperature and changes in ocean acidification could have substantial impacts on coastal marine ecosystems. No strong changes in Ω_A between 2015 and 2016 were detected in April. However, in August Ω_A showed large changes when sea surface temperature in some regions increased to around 30°C.

Hypoxia is relatively common in Korean coastal waters, but is primarily associated with local drivers such as nutrient loading (Lee et al., 2018). As in the Russia coastal region (Chapter 4e), there is a decline in pH along with the decline in O_2, but there is a lack of long-term, high-quality pH data for monitoring trends over time. pH as low as 6.6 and Ω_A as low as 1.2 has been observed.

[Figure 4d-5] Spatial distribution of near-bottom seawater pH, pCO_2, and Ω_A (A, C and E, respectively) in April 2016; and (B, D and F, respectively) in August 2016. Open circles indicate sampling locations. The colour scales indicate hydrogen ion concentration (pH), gaseous CO_2 (pCO_2), and aragonite saturation state (Ω_A).

[4e] Russia coastal region
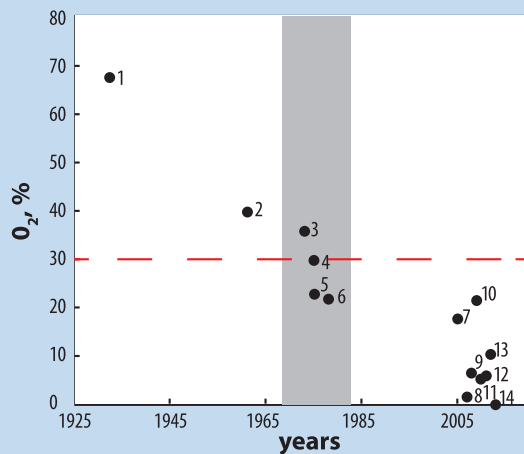
In Russian coastal waters, seasonal hypoxia has been observed in Amursky Bay (part of Peter the Great Bay) every summer since 2007 (Tishchenko et al., 2008; 2011b; 2013). Available historical data show that the lowest dissolved oxygen concentrations observed during the summer season in the bottom waters of Amursky Bay have been systematically decreasing over the last 80 years (Figure 4e-1). There was a period, between 1973 and 1978, during which Amursky Bay became hypoxic during the summer. During the same period, there was an increase in coastal eutrophication globally, in relation to anthropogenic nutrient sources.
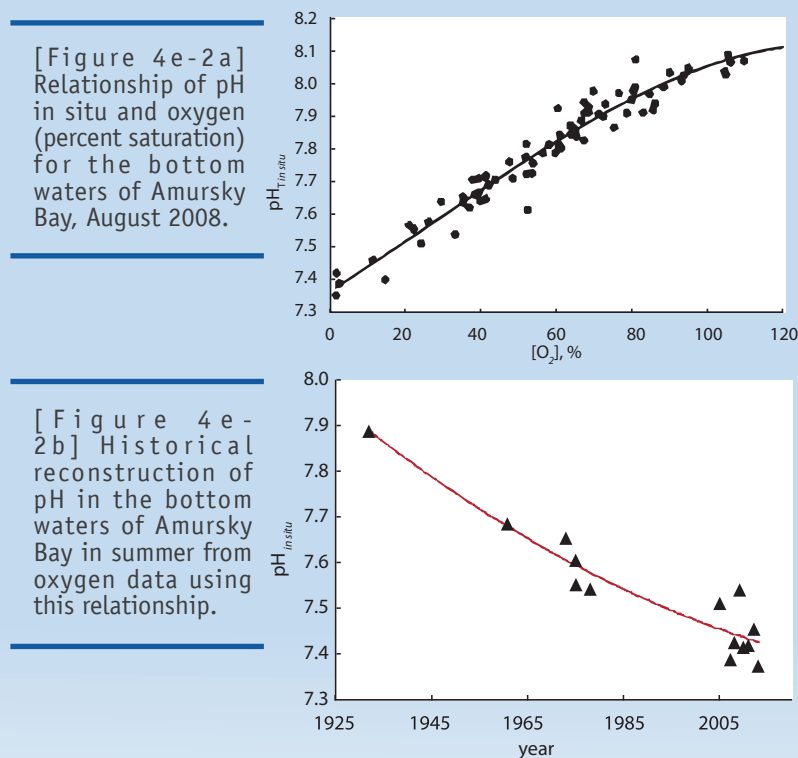
Seasonal hypoxia in the bottom waters of Amursky Bay has occurred since the 1970s, and a strong empirical relationship between O_2 saturation and pH is observed. Using this empirical relationship, we can infer that over the last 80 years the rate of acidification has declined, from 0.008 pH units y^{-1} in 1938 to 0.0032 y^{-1} in 2013. This relationship is based solely on microbial degradation of "excess" organic matter. Increasing atmospheric CO_2 concentration and a decrease of buffering capacity are expected to further enhance acidification of the coastal ocean (Cai et al., 2011; Feely et al., 2018).

Biological observations and historical oxygen data complement each other: maximal changes in composition and structure of bottom fauna in Amursky Bay occurred during the 1970s and 1980s when oxygen concentrations dropped down to the hypoxic state (Tkalin et al., 1993; Belan, 2003). In this period, hypoxia-tolerant animals (including polychaetes, bivalves, and amphipods), which had earlier been observed only occasionally, became common in the Bay and reached maximal abundance (Moshchenko and Belan, 2008). Existing literature attributes observed changes in species structure of benthos in the Bay to processes connected with chronic pollution and eutrophication (Tkalin et al., 1993; Belan, 2003; Moschenko and Belan, 2008). Acidification may also negatively affect benthos in the Bay. However, effects of low oxygen, acidification, and production of H_2S on biota are difficult to distinguish. In terms of seasonal hypoxia on the shelves of the East Asian marginal seas, the deeper waters provide a huge reservoir of oxygenated water. Even with gradually declining midwater oxygen concentration (see Chapter 4b), seasonal upwelling of intermediate waters interrupts hypoxia and increases pH in bottom waters of Peter the Great Bay during the fall and winter seasons.

[Figure 4e-1] Minimal values of dissolved oxygen concentration (percent saturation) observed in bottom waters of Amursky Bay in summer. Data from: 1) Voronkov (1941); 2) Lastovetsky and Veshcheva (1964); 3,5) Redkovskaya (1980); 4) Rodionov (1984); 6) Podorvanova et al. (1989); 7–14) data collected by Pacific Oceanological Institute, Vladivostok.

[Figure 4e-2a] Relationship of pH in situ and oxygen (percent saturation) for the bottom waters of Amursky Bay, August 2008.
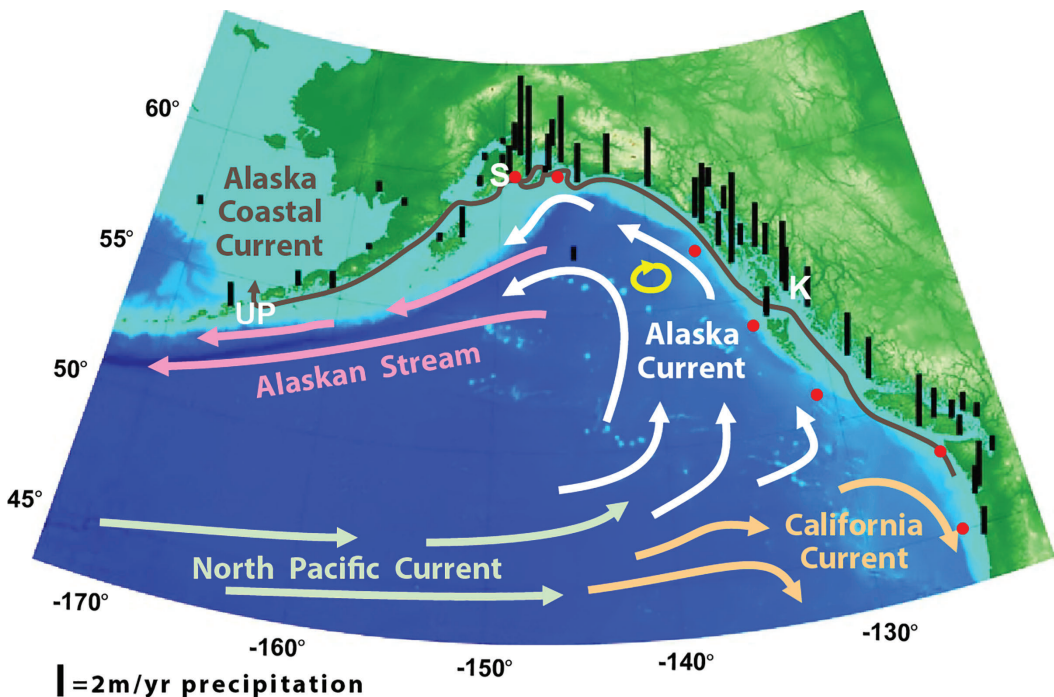
[Figure 4e-2b] Historical reconstruction of pH in the bottom waters of Amursky Bay in summer from oxygen data using this relationship.

[85]

[4f] Coastal Gulf of Alaska

The coastal zone of the Gulf of Alaska extends approximately 3500 km from Queen Charlotte Sound on the British Columbia coast to Alaska's westernmost Aleutian Islands. The eastern and northern shorelines of the basin represent the central and north coasts of British Columbia, the Alexander Archipelago of southeast Alaska, the head of the northern Gulf of Alaska between Yakutat Bay and Prince William Sound, and the Kenai Peninsula on Alaska's south-central coast. The westernmost region is the coasts of the Aleutian Peninsula and the Aleutian Islands. The large-scale circulation flows counterclockwise around the basin, forming a gyre that consists of the North Pacific Current to the south and the northward flowing Alaska Current in the east (see Chapter 2). At the head of the Gulf of Alaska, the Alaska Current turns toward the southwest and becomes the Alaskan Stream (Stabeno et al., 2004). Frequent storms propagate from west to east across the basin between September and May and drive downwelling over the continental shelf (Stabeno et al., 2004). During the summer months, storms are less frequent and downwelling conditions relax (Weingartner et al., 2002). Large-scale climate variability signals can be transmitted to the coastal margin and can induce large changes in coastal ecosystems (Jackson et al., 2018; Sanford et al., 2019).
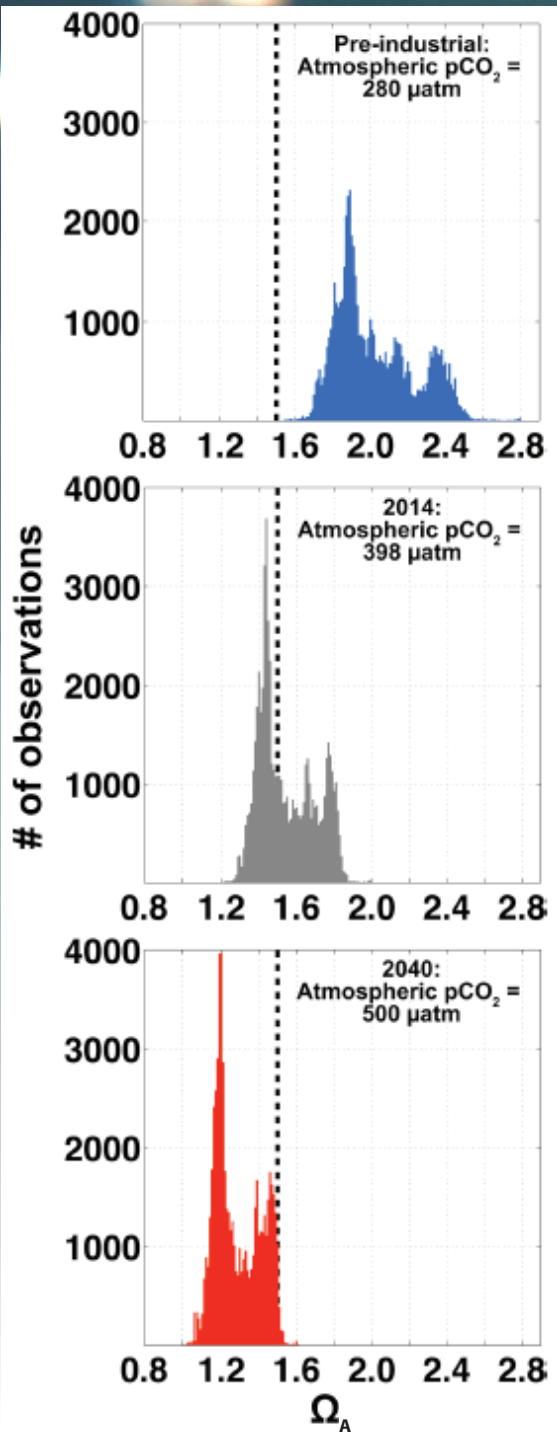
[Figure 4f-1] Schematic of circulation in the Gulf of Alaska. Note the Alaska Coastal Current originating in the region where the North Pacific Current bifurcates. Estimated annual precipitation at coastal sites is shown as vertical bars. Reproduced with permission from Weingartner et al. (2005).

The coastal Gulf of Alaska is a complex geological setting, with areas of broad (~200 km) and narrow (~5 km) continental shelf (depths < 300 m), numerous submarine canyons, numerous inlets and fjords, and tall (~3 km) coastal mountains. North Pacific storms deliver high precipitation, particularly in southeast Alaska (Stabeno et al., 2004). Total runoff for the area spanning the Aleutian Islands and southeast Alaska is 792±120 km^{3}y^{-1} (Hill et al., 2015) and peaks in October (Weingartner et al., 2002). An estimated 370 km^{3}y^{-1} of this runoff is supplied by melt from glaciers and icefields in the area between Prince William Sound and southeast Alaska (Neal et al., 2010). Meltwater input into the coastal zone peaks earlier than total runoff, typically occurring in August (O'Neel et al., 2015). This large freshwater flow

into the Gulf of Alaska coastal zone supports a buoyant nearshore current known as the Alaska Coastal Current that flows northward along the eastern edge of the basin before turning westward and entering the Bering Sea through channels in the Aleutian island chain (Stabeno et al., 2004; Weingartner et al., 2005; 2009).

Over the last decade, ocean observing and modeling efforts aimed at understanding marine CO_2 chemistry have evolved rapidly in the northern Gulf of Alaska (Dugan et al., 2018). Details of the seasonality of air-sea CO_2 exchange (Evans and Mathis, 2013), the influence of meltwater on nearshore CO_2 chemistry (Reisdorph and Mathis, 2014; Evans et al., 2014; Pilcher et al., 2018), and site-specific variability (Evans et al., 2013; 2015) are

[87]

[Figure 4f-2] Shifting variability in aragonite saturation states (Ω_A) at the Alutiiq Pride Shellfish Hatchery in Seward, Alaska. The top panel shows the frequency distribution calculated under pre-industrial atmospheric conditions, the middle panel is observed conditions in 2014, and the lower panel is calculated conditions for 2040. The vertical dashed line marks a sub-optimal Ω_A threshold of 1.5. The window of optimal growth conditions for select shellfish species is estimated to close within the next few decades. Reproduced with permission from Evans et al. (2015).

emerging. In general, surface water CO_2 content is elevated during winter, exceeding atmospheric levels in some areas along the eastern edge of the basin. High primary productivity during the spring phytoplankton bloom (Strom et al., 2006) draws surface CO_2 down to below atmospheric; this condition persists until storm-induced convective mixing occurs in the fall. Trends in aragonite saturation state at the surface are mostly opposite to those of pCO_2, except in areas of high glacial melt. In these settings, pCO_2, pH, and aragonite saturation state can become decoupled, with undersaturation co-occurring with high pH and low pCO_2. Below the surface, relaxed downwelling conditions during summer allow deep North Pacific water to inundate the shelf (Weingartner, 2007), which results in aragonite undersaturation at depth. Modeling results indicate that the depth at which the aragonite saturation state becomes corrosive (the saturation horizon) is deeper and largely off the continental shelf during winter when downwelling is most intense, whereas during summer the saturation horizon is shallower and corrosive water spans the shelf (Siedlecki et al., 2017).

Observational records are still too short to directly resolve long-term changes associated with ocean acidification (Sutton et al., 2019). Estimates of anthropogenic CO_2 content in the upper ocean range from 48 to 55 µmol kg^{-1} (Watanabe et al., 2011; Evans et al., 2015; Feely et al., 2016). This additional CO_2

has shifted the observed variability towards lower pH and $CaCO_3$ saturation state, and will continue to do so as atmospheric CO_2 concentration increases. While contemporary surface aragonite saturation states are largely non-corrosive over the continental shelf, corrosive levels are projected by the end of the century (Mathis et al., 2015). The projected change in the marine CO_2 system, combined with high dependence on potentially impacted fisheries by coastal communities, leads to substantial vulnerability to ocean acidification in northern Gulf of Alaska coastal waters (Ekstrom et al., 2015; Mathis et al., 2015).

Deoxygenation in the coastal Gulf of Alaska has been less of a focus relative to ocean acidification. However, decreasing oxygen content in North Pacific waters below the thermocline (Whitney et al., 2007) may soon become important as this is the source of water on the continental shelf during summer when downwelling conditions are relaxed (Weingartner, 2007). In addition, the California Undercurrent, which flows poleward below the shelf break along the west coast of North America, may reach as far north as Alaska (Thomson and Krassovski, 2010), and oxygen concentrations are reported to be declining within this water (Pierce et al., 2012; Crawford and Peña, 2013). While sub-surface oxygen concentrations are reportedly lower in more southerly regions of the North American continental shelf (Crawford and Peña, 2013; Feely et al., 2018), it is likely that there are undocumented areas of hypoxia in regions of restricted exchange near shore. Such areas could be found within the many inlets and fjords along the eastern and northern portions of the coastal Gulf of Alaska. Future research should address the lack of information on hypoxic conditions in these settings, as well as develop monitoring sites to understand rates of change.

[89]

Credit: Nadja Steiner

[4g] The Salish Sea

The Salish Sea is a large estuarine system on the west coast of North America, which spans the border between the United States and Canada (Figure 4g-1). It includes the Straits of Georgia and Juan de Fuca, and Puget Sound. The name Salish Sea was adopted by Washington in 2009 and by British Columbia in 2010. The Salish Sea region has been inhabited for around 13,000 years (e.g., Trant et al., 2016). However, European settlement came very late compared to many other areas of North America (e.g., Jackson, 2001). Human populations have relied upon and farmed the abundant shellfish along the Salish Sea shoreline for millennia (e.g., Deur et al., 2015; Neudorf et al., 2017).
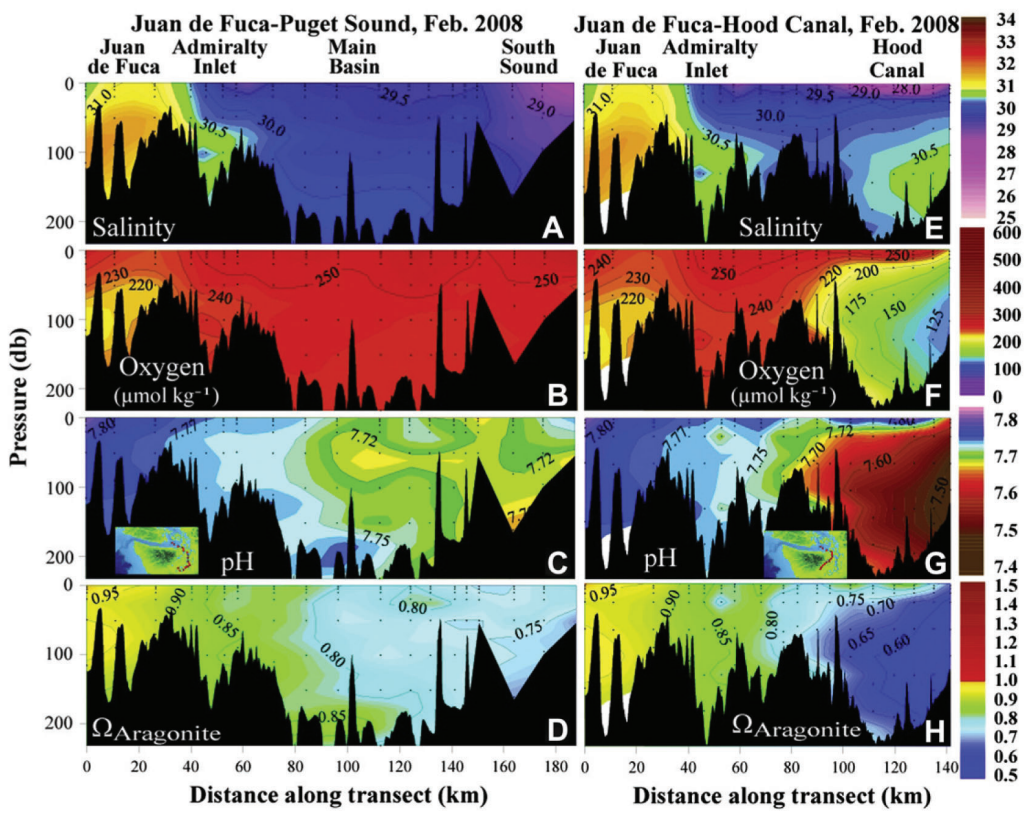
Oceanography is a young science, and oceanographers have been working in the Salish Sea for almost as long as oceanography has existed. The Pacific Biological Station at Nanaimo was founded in 1908 and the University of Washington Oceanographic Laboratories in 1930.

The Salish Sea is characterized by large freshwater inputs, vigorous tidal mixing and seasonally high productivity (e.g., an intense spring phytoplankton bloom). Deep water temperature is about 8°C year-round. Surface water temperatures can reach up to 20°C in summer but are more typically between 12 and 15°C. Glacial sills throughout the Salish Sea inhibit classical estuarine circulation, resulting in lengthy retention of deep water masses in some areas. Deep water renewal time is 1 to 3 years (Pawlowicz et al., 2007). Some regions with weak exchange experience seasonal oxygen depletion.
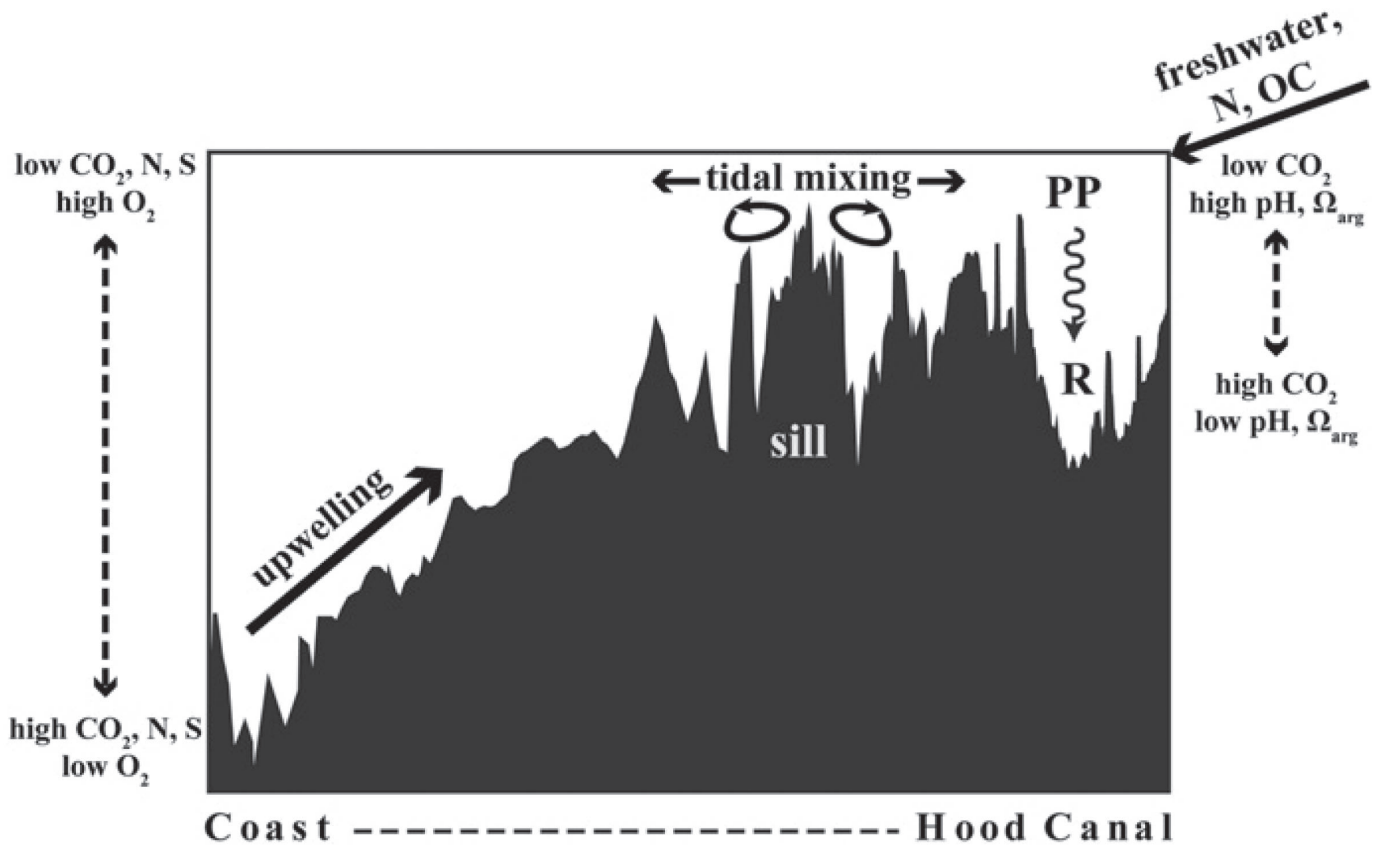
[Figure 4g-1] Map of the Salish Sea and its watershed. Map drawn by Stefan Freelan, Western Washington University. Reproduced with permission.

[Figure 4g-2] Distribution of salinity, oxygen, pH, and aragonite saturation (Ω_A) along a transect of the Strait of Juan de Fuca and Puget Sound (A-D), and a transect from the Strait of Juan de Fuca to the southern end of Hood Canal (E-H), winter 2008. Reproduced with permission from Feely et al. (2010).

Two major reviews of the oceanography of the Strait of Georgia were published in 1957 (Tully and Dodimead, 1957; Waldichuk, 1957). The latter shows a map of temperature and oxygen concentration at a density of 1023.5 kg m^{-3} (~100 m depth) for September 1952 and March 1953. O_2 was generally in excess of 400 µM in spring, and declined to 280 to 380 µM in September. Tully and Dodimead (1957) showed a more extensive set of chemical measurements, including oxygen, pH, and nutrient concentrations. They also established that the seasonal cycle of surface salinity can exceed 10 units, ranging from almost 30 in winter to less than 20 in summer. The pH data were not collected with modern
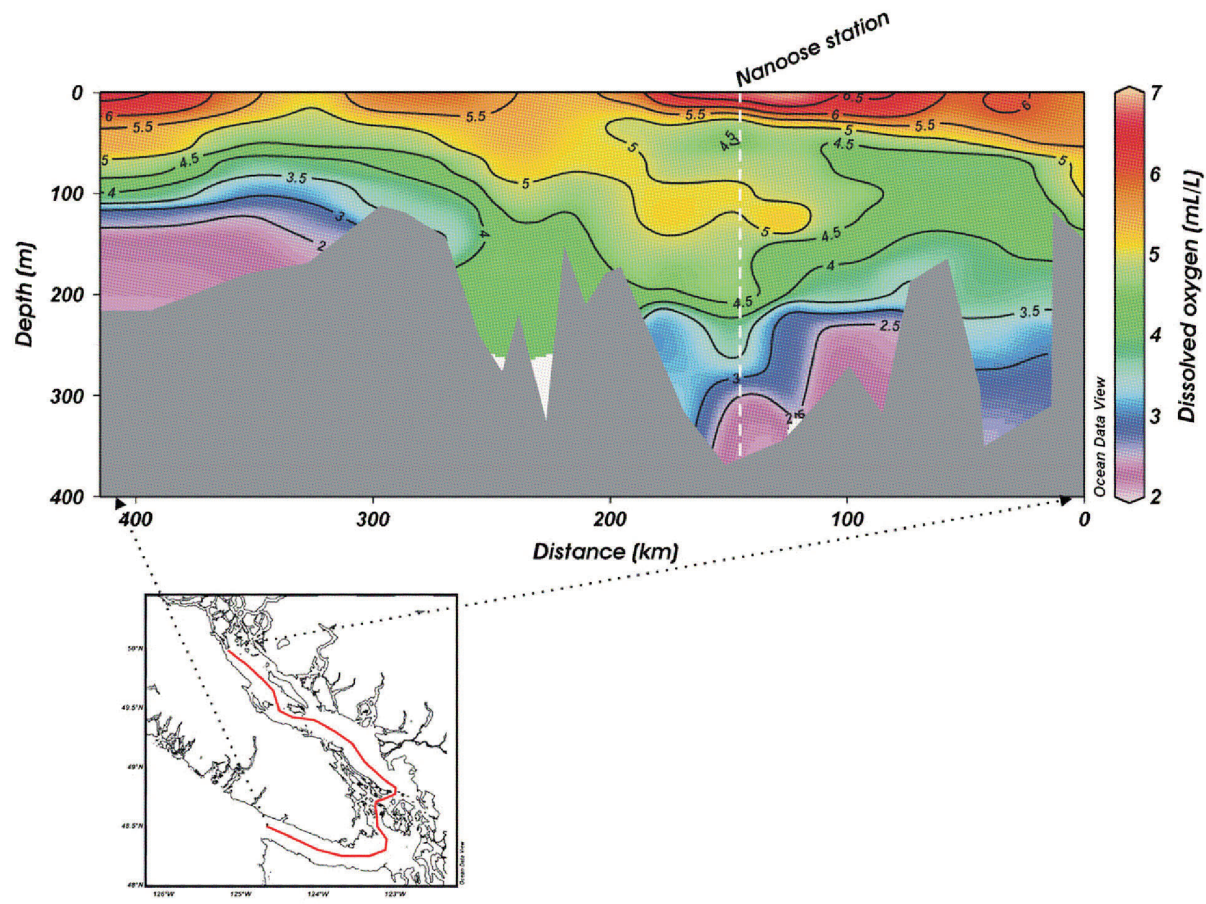
methods, but they show plausible vertical and seasonal distributions, with large increases in surface waters in summer. There is very little literature on oxygen or carbon in the Salish Sea over the next half century. Johnson et al. (1979) observed declining O_2 and a commensurate increase in total CO_2 (calculated from measurements of pH and alkalinity) over a 14-day period in the summer of 1976, but their sampling was spatially and temporally limited. A special volume of the *Canadian Journal of Fisheries and Aquatic Sciences* was published in 1983 with major reviews of the physical and biological oceanography of the Strait of Georgia, but very little about chemistry.

[Figure 4g-3] Schematic illustration of physical and biological processes determining the chemical composition of seawater within different regions of the Salish Sea. Reproduced with permission from Feely et al. (2010).

Starting in the 1990s, regular surveys of oxygen, salinity, and temperature revealed the seasonality of water mass properties, oxygen concentration, and hypoxia in Puget Sound (e.g., Newton et al., 2002; 2011; Moore et al., 2008). More recently, systematic surveys and syntheses of carbonate chemistry in the Salish Sea have revealed that large parts of the Sea experience naturally low pH, O_2, and $CaCO_3$ saturation states, and high pCO_2. Strong seasonal drawdown of CO_2 by phytoplankton greatly increases the pH and $CaCO_3$ saturation state in surface waters in summer throughout the Salish Sea (e.g., Feely et al., 2010; Ianson et al., 2016; Evans et al., 2019), although wind-induced mixing with subsurface waters can disrupt these surface layers in some regions (Evans et al., 2019). In contrast, deep waters are acidified by decomposition of organic matter from surface production, resulting in the formation of low saturation state and pH hot spots where retention times are longest (e.g., Feely et al., 2010; Pelletier et al., 2018). This natural acidification is made more intense by anthropogenic CO_2 uptake.

[93]

[Figure 4g-4] Dissolved oxygen concentration along the thalweg of the Strait of Juan de Fuca and Strait of Georgia. The thalweg is the line that follows the deepest point in a cross-section of the strait at each point along its length. Reproduced with permission from Masson and Cummins (2007).

Tidal currents are extremely strong in Juan de Fuca Strait. Waters entering the Sea are generally well mixed and phytoplankton production in Juan de Fuca Strait is not nutrient-limited. Tidal currents regularly exceed 1 m s^{-1} and sea surface temperature is rarely greater than 12°C (Thomson, 1981). Mackas and Harrison (1997), attempting to put anthropogenic nitrogen inputs into oceanographic context, noted that more than 90% of the nitrate brought into the Strait by the tidal currents is carried out again on the ebb tide. Mixing intensifies over rough topography at the inshore end of the Strait, so that the salinity is generally nearly constant from surface to bottom in all seasons (Thomson, 1981). The inflow from the Pacific has relatively low oxygen concentration, high DIC, low $CaCO_3$ saturation state (Ω), and low pH, compared to coastal surface waters. In the region of intense tidal mixing, surface ocean pCO_2 is generally very high, averaging almost twice the atmosphere concentration, because the topographically driven mixing brings subsurface DIC to the surface (Nemcek et al., 2008; Evans et al., 2012; Murray et al., 2015). The subsurface waters of the Strait of Georgia have low pH and Ω_A relative to open ocean waters at similar depths (Ianson et al., 2016; Evans et al., 2019).

Strait of Georgia

The Strait of Georgia is open at both ends, but most of the exchange with the open ocean occurs at the southern end (Waldichuk, 1957; Thomson, 1981). The waters within the Salish Sea are a mixture of saline inflow from the Pacific and freshwater runoff; the Fraser River is by far the largest of the rivers flowing into the Sea. The Strait of Georgia is strongly stratified in summer, with intense phytoplankton blooms occurring within a well-mixed surface layer that is rarely more than 5 m thick. These blooms play an important role in determining the oxygen and DIC concentration in subsurface waters and the seasonal cycle of $CaCO_3$ saturation in surface waters (Johannessen et al., 2014; Ianson et al., 2016; Moore-Maley et al., 2016). The surface waters of the southern Strait of Georgia are also strongly influenced by the chemistry of the river water, such that pH and saturation state can become decoupled in ways that would not be expected simply from dilution of seawater with fresh (Moore-Maley et al., 2018)

Puget Sound, by contrast, is open only at Admiralty Inlet. While the water column is generally well mixed there, relatively dense marine water incursions spill over the sill and fill the deeper parts of the fjordal basins within Puget Sound (typically during neap tides in early fall), refreshing the bottom water masses. Fourteen major rivers within Puget Sound, along with the Fraser River to the north, are the dominant surface freshwater sources to Puget Sound, with the Puget Sound rivers dominating in winter, and the Fraser in summer (Banas et al., 2015). Nutrients in Puget Sound are predominantly of marine origin (~70–98%, depending on the basin). River nutrient loads are dominated by human sources (Mohamedali et al., 2011; Steinberg et al., 2011). Like the Strait of Georgia, the water column in all basins of Puget Sound is stratified and experiences intense surface phytoplankton blooms in summer, with the strongest and most persistent stratification in Hood Canal (Hood Canal is the westermost arm of Puget Sound (see Figure 4g-1)). Water column profiles of oxygen, pH, and $CaCO_3$ saturation state show the effects of this stratification (e.g., Moore et al., 2008; Feely et al., 2010; Reum et al., 2014).

The southern portions of the Salish Sea (Puget Sound, including Hood Canal) consist of much narrower channels than the Strait of Georgia, but have similar circulation, with strong tidal mixing at the entrance. Seasonal stratification, with oxygen drawdown and DIC accumulation in the subsurface waters, is particularly apparent in the strongly stratified southern region (Feely et al., 2010). The southernmost parts of Hood Canal experience the most extreme seasonal oxygen depletion of any part of the Salish Sea, except for some isolated deep basins such as Saanich Inlet. The residence time of deep water in the Strait of Georgia is on the order of one year, and oxygen depletion in the deep water is unlikely (Johannessen et al., 2014; Ianson et al., 2016). In contrast, oxygen depletion has been observed in parts of Puget Sound with restricted circulation, such as southern Hood Canal. Seasonal hypoxia develops frequently in subsurface waters, with near anoxic conditions observed occasionally.
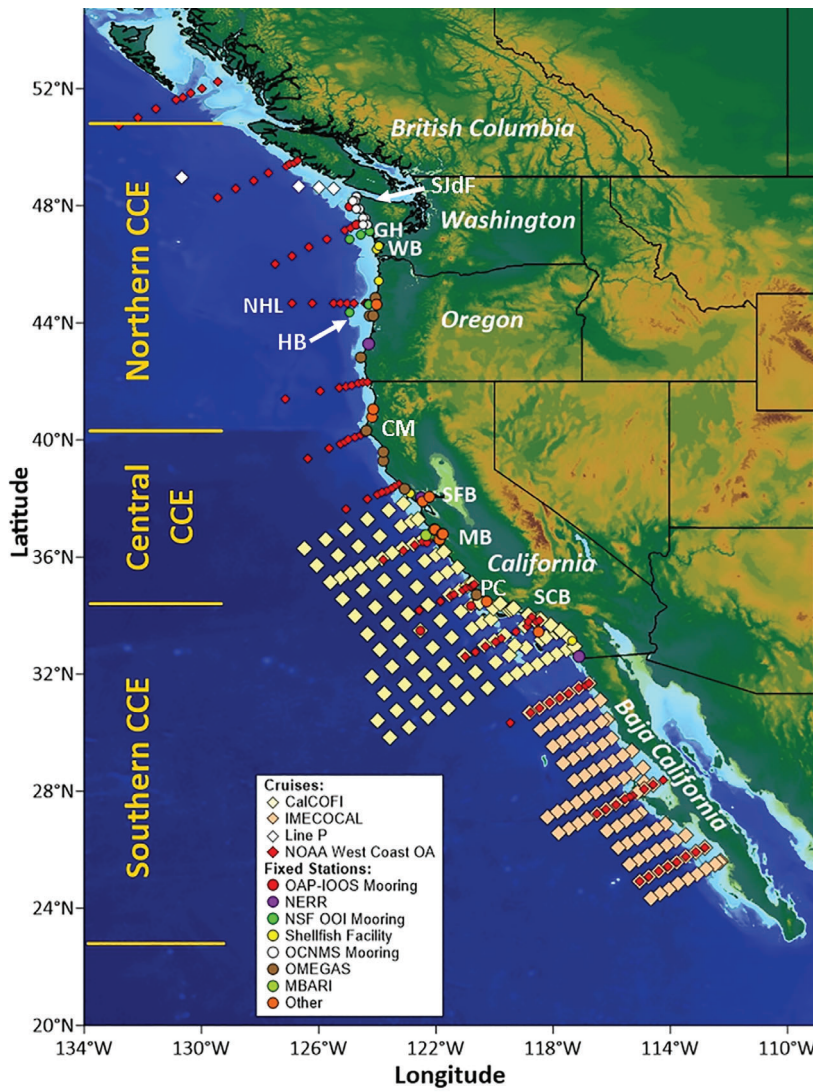
[4h] The California Current

The California Current Ecosystem (CCE) is an upwelling ecosystem along the Pacific coast of North America from British Columbia, Canada, to Baja California, Mexico. Upwelling brings cold, nutrient- and CO_2-rich, and oxygen-poor water into the surface layer from late spring to early fall.

The CCE encompasses both the California Current, which flows southward at the surface and up to 1000 km offshore, and the subsurface California Undercurrent, which flows northward at depth along the upper continental slope. The surface current is relatively fresh, cold, and oxygen-rich, while the undercurrent contains warm, salty, oxygen-poor water originating in the Eastern Tropical Pacific. The California Current begins where the North Pacific Current diverges into the northward-flowing Alaska Current and the southward California Current (Figure 2-2). In this chapter, we consider the northern and southern limits of the California Current to be the northern end of Vancouver Island (50.8°N) and the southern tip of Baja California (22.8°N). As is common practice, we divide the CCE into northern, central, and southern subregions, with the boundaries at Cape Mendocino and Point Conception (Figure 4h-1). Physical, climatic, and human population density gradients from north to south within the CCE set the stage for strong gradients in coastal carbon cycling and acidification variability. Freshwater inputs are stronger to the north, reflecting wetter climate conditions and having a strong influence on the stratification and nutrient input to coastal surface waters.
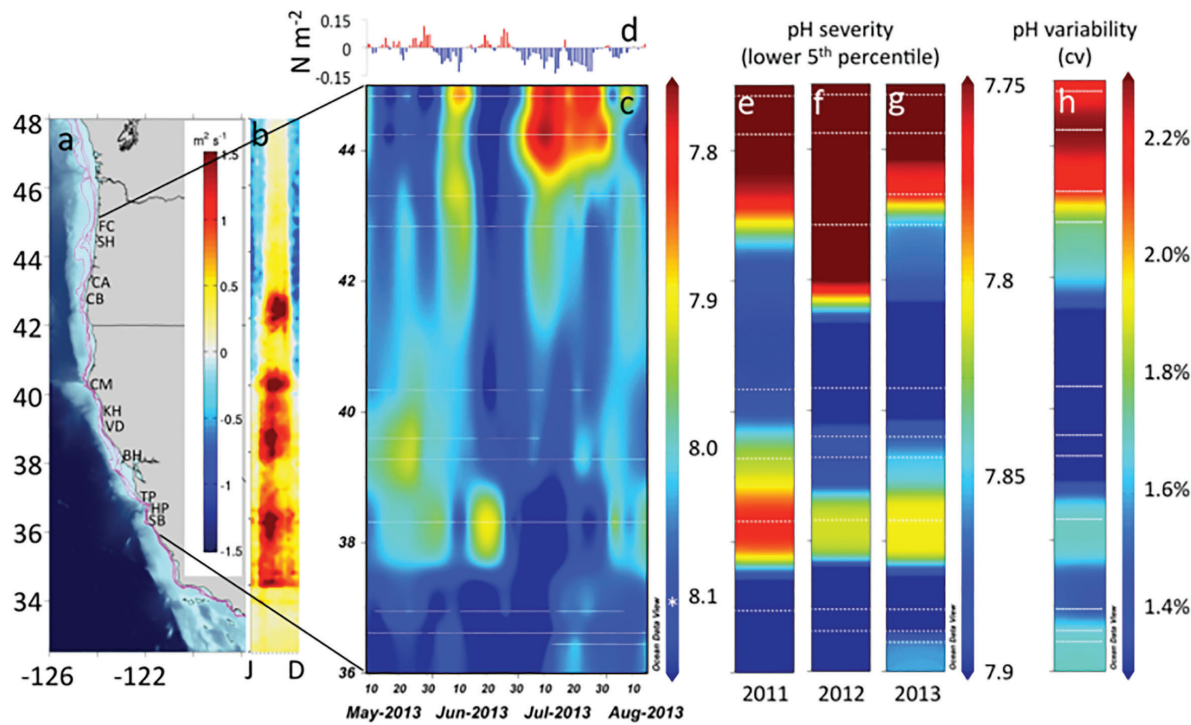
[Figure 4h-1] Map of California Current ocean acidification observing assets. SJdF=Strait of Juan de Fuca, GH=Grays Harbor, WB=Willapa Bay, NHL= Newport Hydrographic Line, HB=Heceta Bank, CM=Cape Mendocino, SFB=San Francisco Bay, MB=Monterey Bay, PC=Point Conception, SCB=Southern California Bight. Map courtesy of Dana Greeley, National Oceanic and Atmospheric Administration (US).

The CCE has a wealth of observing assets and programs in place that have yielded insight into the range of carbon chemistry conditions within this system (Figure 4h-1). In addition to direct carbon chemistry observations, empirical relationships developed for the CCE utilize proxy oceanographic variables, (e.g., oxygen, temperature, salinity) to estimate carbon system parameters where direct measurements are not available (e.g., Juranek et al., 2009; Alin et al., 2012). Many data are from pelagic coastal waters, but a growing number of studies represent benthic, intertidal, kelp, or embayment waters as well.

[Figure 4h-2] Intertidal pH total variation across the California Current Large Marine Ecosystem. (a, b) Study domain with average wind-driven cross-shelf surface flow (m²s⁻¹) from June to December. (c, d) Variation in pH during summer 2013 and daily wind stress (N m⁻²) at 44.65°N. (e–g) Low pH exposure (average of lowest 5% of data) across three years of observation. (h) pH variability (% of mean). White dotted lines in pH panels denote observation station locations. Reproduced with permission from Chan et al. (2017).

The first synoptic West Coast Ocean Acidification (WCOA) cruise demonstrated that undersaturated water was present at the surface of the central CCE, decades earlier than had been expected (Feely et al., 2008) (see Chapter 1). The three-year OMEGAS study showed a persistent spatial distribution of acidification hotspots and relative refuges, with the lowest pH (and inferred CaCO₃ saturation state) and highest variability seen in nearshore habitats along the Oregon coast with a secondary locus at Bodega Head, California (Chan et al., 2017, Figure 4h-2). From these and other studies (e.g., Bednaršek et al., 2017), we have learned that conditions are consistently more undersaturated in the northern and central CCE than in the southern CCE, and worse in the nearshore compared to offshore. Based on oxygen and carbon observations and models, we know that persistent hotspots of hypoxia and CaCO₃ undersaturation exist, from north to south, in the areas of the Juan de Fuca Eddy, the central Washington coast, the central Oregon coast (Heceta Bank), and northern California (Cape Mendocino to Monterey Bay) (Chan et al., 2008; 2017; Feely et al., 2008; 2016; 2018; Connolly et al., 2010; Gruber et al., 2012; Hauri et al., 2013ab; Peterson et al., 2013; Siedlecki et al., 2015; 2016).
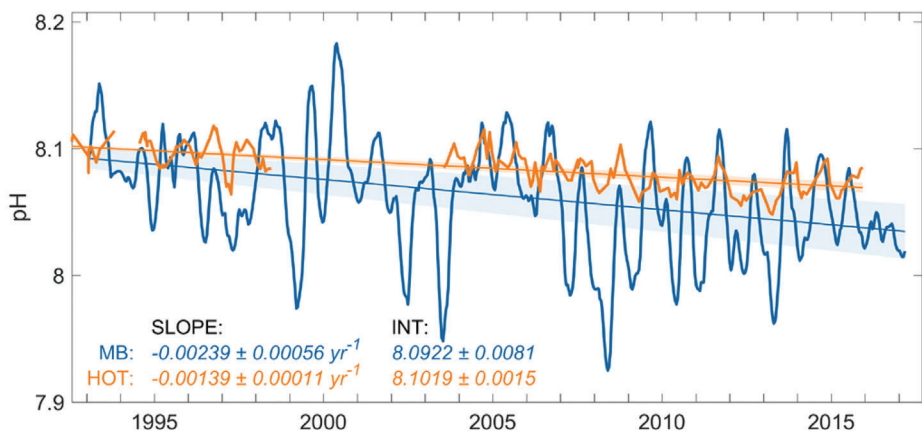
Moored and other stationary time-series can best document the full dynamic range of conditions at a given site. The NOA-ON, MBARI, and IMECOCAL moorings deployed from Washington to northern Baja California provide ranges of pCO_2 variability that are largest along the Oregon and Baja California shelves (pCO_2 range of 800 ppm at the shelf break to 1100 ppm at the surface off Oregon, and 733 ppm at the surface off Baja California). Intermediate pCO_2 variability is seen on the Washington shelf (550 and 590 ppm at the Cape Elizabeth and Chá bǎ moorings, respectively) and at CCE2 off Point Conception in southern California, which is an upwelling locus (500 ppm). The narrowest pCO_2 ranges measured at CCE moorings are 265 ppm at M1 (Monterey Bay, California), 320 ppm at CCE1 (offshore California Current waters, considered open ocean), and 120 ppm at the Santa Monica Bay Observatory (this is a very short data record and probably does not represent the full range). The full range of pCO_2 found in the upper 20 m of all WCOA cruises, spanning British Columbia to Baja California, is 141-1396 ppm (each cruise represents a snapshot of conditions during 3-5 weeks of a single upwelling season). For pH, the full range is 7.513-8.545, excluding the Columbia River plume. The Ω_A and Ω_C ranges were 0.53-5.06 and 0.93-7.93, respectively.

Underway observations augment spatial coverage of hydrographic profiles and fill gaps in the space-time tradeoffs between moored and cruise-based observations. Such "gap-filling" observations have proven critical for generating high-resolution climatologies of carbon system variables (pH, pCO_2, TA, DIC, Ω_A) at 0.1° x 0.1° resolution in Washington state marine waters (Fassbender et al., 2018). As reliable autonomous sensors for the carbon system become available, we should eventually have profiling gliders and moorings that can resolve the full water-column across habitat types within the CCE (Martz et al., 2015; Chavez et al., 2017).

Northern and nearshore parts of the CCE are changing more rapidly than offshore and southern areas, and faster than most other regions of the global ocean (Feely et al., 2016; 2018; Sutton et al., 2016; Turi et al., 2016; Chavez et al., 2017) (Figure 4h-3). Observations in pelagic, benthic, and rocky intertidal environments across a broad swath of the CCE (e.g., Hauri et al., 2013a; Chan et al., 2017) suggest that change will accelerate over the coming decades. This is a consequence of both rapidly increasing atmospheric CO_2 concentration and reductions in the ocean's buffering capacity (Feely et al., 2018).
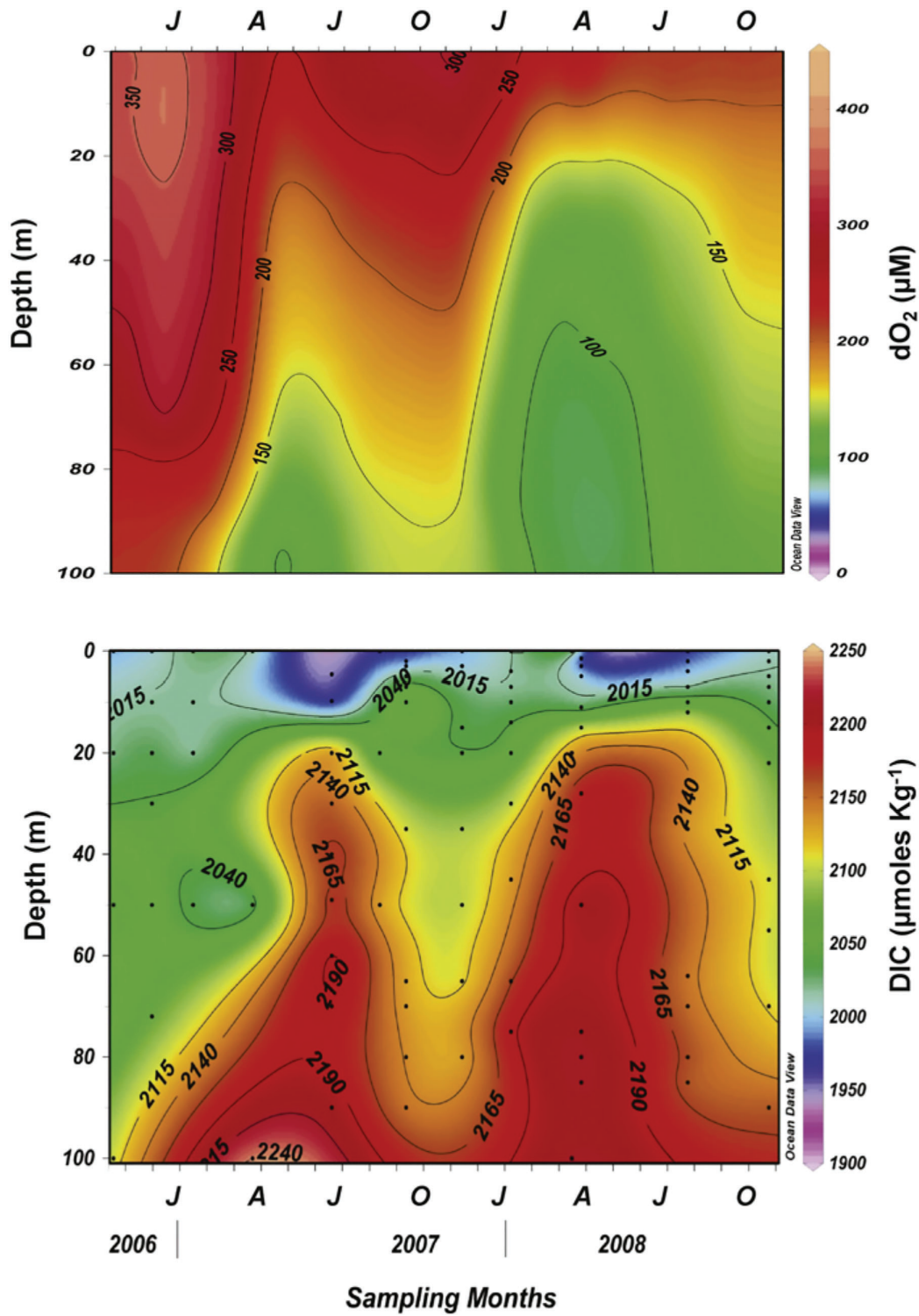
[Figure 4h-3] Time series of pH from 1992-2017 from Monterey Bay (MB) and the open ocean Station HOT (see Chapter 2). The coastal station shows slightly faster acidification. Reproduced with permission from Chavez et al. (2017).
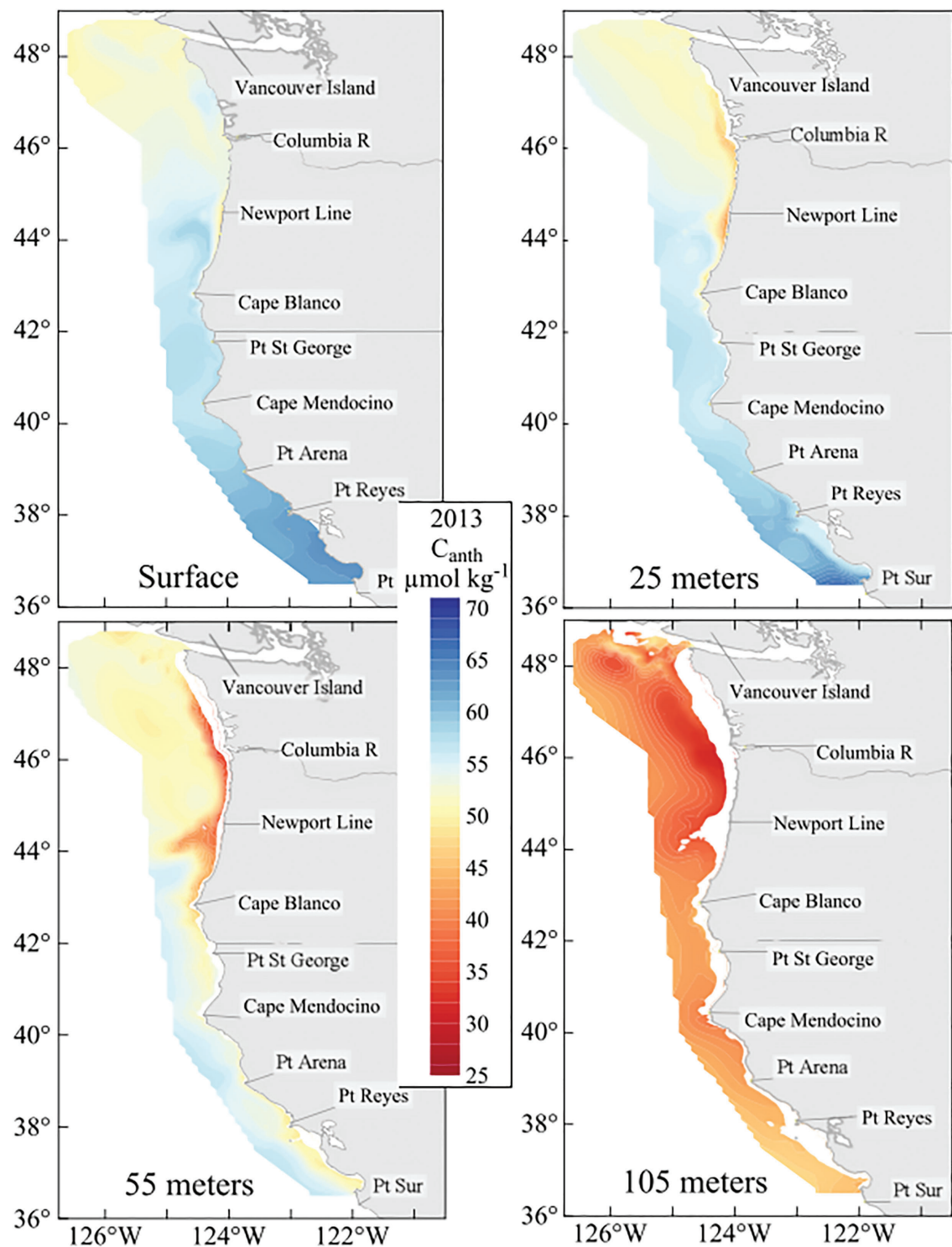
Since 2006, the Universidad Autónoma de Baja California and the Centro de Investigación Científica y de Educación Superior de Ensenada have conducted time-series observations at a site close to two areas where oysters and mussels are cultured, in a location that is considered to represent the transitional region between tropical/subtropical and subarctic systems of the California Current System (Linacre et al., 2010). This station is located near the inshore end of the second (from north) IMECOCAL line (Figure 4h-1). These observations show that the coastal waters reflect the chemistry of open shelf waters, and the seasonal and interannual variability of upwelling of oxygen-poor and DIC-rich waters originating in the eastern tropical Pacific (Figure 4h-4). These observations show the potential impacts of large-scale oceanographic variability on nearshore waters, and suggest that DIC-rich upwelled water will become more corrosive in the future.

Three sets of natural processes play critical roles in structuring the spatial and temporal variability of carbon chemistry. First, *metabolism*,
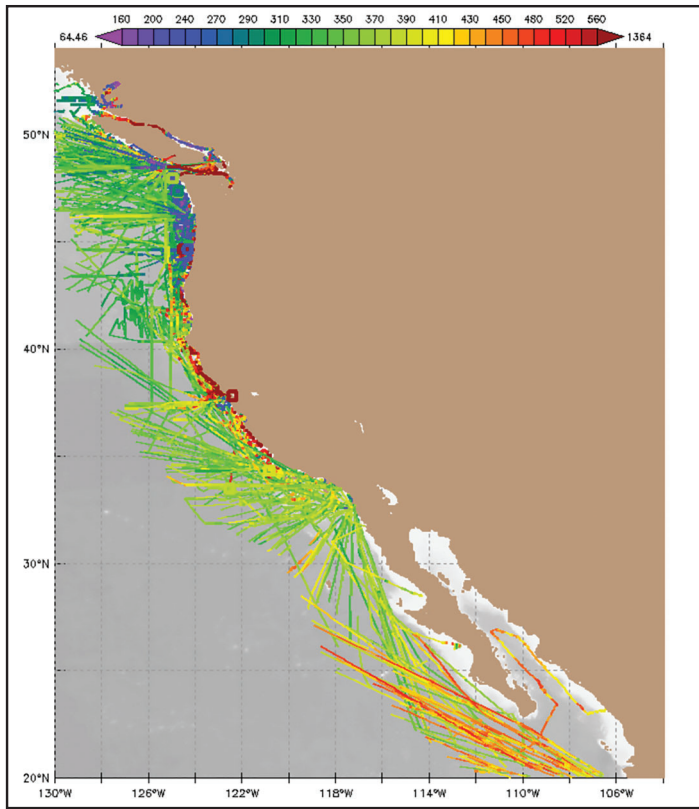
i.e., photosynthetic production of organic matter at the surface and decomposition at depth. Second, *circulation*: variability in the strength of upwelling and northward transport of the California Undercurrent controls the chemical composition of water upwelling onto the shelves. Finally, *river inputs* affect photosynthesis, stratification, and buffering capacity. Anthropogenic effects on carbon chemistry are superimposed on this natural background. Anthropogenic CO_2 is taken up both during remote ventilation (uptake by distant waters that are subducted and then upwelled years or decades later into productive CCE habitats) and by direct, local uptake. Other anthropogenic effects on coastal ocean carbon chemistry include sewage, pollutants in storm runoff, and excess nutrients from agriculture. Natural and human-caused processes interact to determine coastal carbon chemistry, which may (locally) exacerbate or ameliorate the degree of acidification in specific CCE habitats. Near-surface concentrations of anthropogenic CO_2 are greatest in the southern part of the CCE (Figure 4h-5).

[101]

[Figure 4h-4] Depth-time evolution of (a) dissolved oxygen (mmol m⁻³) and (b) dissolved inorganic carbon (μmol kg⁻¹) at station ENSENADA from October 2006 to November 2008. Reproduced with permission from Linacre et al. (2010).

[Figure 4h-5] Distribution of anthropogenic CO_2 (C_{anth}) at various depths in the northern and central CCE from the 2013 West Coast Ocean Acidification cruise. Reproduced with permission from Feely et al. (2016).

[103]

[Figure 4h-6] Surface underway (linear traces) and moored (open squares) CO_2 (ppm) within the California Current and adjacent embayments. Data from SOCAT version 5.

Physical circulation processes also shape the distribution of oxygen and acidification throughout the CCE. Wind-driven upwelling, which can be enhanced by capes and submarine canyons, is strongest in the central CCE, and increases from north to south within the northern CCE. Remote effects from central CCE winds can even be observed in water properties in the northern CCE, due to propagation of coastally trapped planetary waves (e.g., Hickey et al., 2016). Variability in the intensity of upwelling and the strength of the California Undercurrent affect hypoxia and acidification hotspots that develop on the Pacific Northwest shelf during the upwelling season (Durski et al. ,

2017). The California Undercurrent also affects nearshore oxygen and carbon chemistry in the Southern California Bight (Nam et al., 2015). In the Pacific Northwest, both along-shelf and cross-shelf advection affect the distribution of hypoxic and undersaturated conditions (Connolly et al., 2010). Intermittency of upwelling in the northern CCE means that phytoplankton blooms may either remain over the shelf, so that the organic matter is respired locally (forming hotspots of hypoxic and undersaturated conditions), or be transported off the shelf to the open ocean (Barth et al., 2005; Hales et al., 2006; Siedlecki et al., 2015).

GLOSSARY

Advection- Transport of chemical species or organisms by ocean currents.

Benthos - Organisms that live on the sea floor or along rocky shorelines, such as clams, mussels, crabs, starfish, and sea cucumbers.

Bivalve - Molluscs with two symmetrical shells held together by a 'hinge' muscle. The most commonly harvested shellfish are bivalves: clams, mussels, and oysters. The shell are made of calcium carbonate and are therefore vulnerable to dissolution under acidic conditions.

Buffering capacity - Buffering capacity is the ability of a solution to absorb inputs of acid without large changes in pH. In a strongly buffered solution, the pH will change only a bit, whereas in a weakly buffered solution it will change much more. Seawater is much more strongly buffered than fresh water (see "What is pH?" box). Seawater buffering capacity in some regions of the North Pacific is low because of large freshwater inputs.

Calcareous - Calcareous organisms are those that have calcium carbonate ($CaCO_3$) minerals in their shells or exoskeletons. While the most familiar of these are the bivalves that live along our shores (clams, mussels, oysters), there are many other kinds in the sea. In the open ocean there are calcareous phytoplankton, such as coccolithophores (see Figure 4a-4) and calcareous zooplankton, such as foraminiferans and pteropods (see Pteropods Box, Chapter 3). Exoskeletons made predominantly of organic matter, like those of crabs or sea urchins, also contain some $CaCO_3$.

Calcite - The most common crystalline form of calcium carbonate ($CaCO_3$). Calcite can withstand a lower carbonate ion concentration than its cousin Aragonite. The chemical composition of the different $CaCO_3$ minerals is the same: only the crystal structures differ.

Convective mixing - In fall, the sea surface loses heat to the atmosphere, which makes the surface water more dense and the water column less stable. This allows the wind to mix the surface water down to much greater depths than in summer, when the water column is stable and stratified. Convective mixing is much deeper in the North Atlantic than in the North Pacific, but can reach as deep as 350 m in some areas of the western North Pacific.

Diurnal - Strictly speaking, diurnal is the opposite of nocturnal, designating animals that are active in the daytime. But it is often used in a more general sense to refer to day-night fluctuations of water properties like temperature or pH. In coastal waters, the pH of seawater can fluctuate greatly between day and night (see Chapter 4c).

Eutrophication - Increased productivity in coastal waters due to anthropogenic nutrient sources, often accompanied by oxygen depletion in subsurface waters.

Hypoxia - A condition of low oxygen concentration that limits the ability of some organisms to inhabit that water. Hypoxic waters are those less with than 60 µM oxygen, which will become inhospitable for fish and some other higher organisms. Below about 10 µM only microbial life can exist. *Anoxic* waters contain less than 1 µM.

Phytoplankton - Phytoplankton are the microscopic single-celled algae that are the base of open ocean food chains. Common types include Bacillariophytes (diatoms), Dinophytes (dinoflagellates), and Haptophytes. Phytoplankton range from 1-100 µm in diameter and there can be from 1 million to >100 million cells per litre of seawater.

Primary production - Transformation of inorganic carbon and nutrients into organic matter by photosynthetic algae. In the open ocean these will be almost exclusively phytoplankton; in coastal waters primary production is partly phytoplankton and partly macroalgae such as kelp.

Remineralization - Oxidation of organic matter to inorganic by respiration of animals, bacteria, and protists. Essentially the reverse of primary production. Occurs throughout the water column, whereas photosynthesis occurs only in the lighted surface layer.

Saturation state - The saturation state of seawater with respect to calcium carbonate determines whether the solid minerals can precipitate. Higher values are more favourable to shell formation; values less than one imply dissolution (see Chapters 1 and 3). Saturation states are different for different forms of $CaCO_3$ with different crystal structures, such as calcite and aragonite, even though the chemical composition is the same.

Ventilation - Introduction of oxygen-rich near surface waters into the subsurface ocean by subduction or mixing.

Zooplankton - Zooplankton are the next step up the food chain from phytoplankton. They eat phytoplankton and smaller zooplankton.

Abbreviations

CalCOFI	California Cooperative Oceanic Fisheries Investigations
CCE	California Current Ecosystem
CDIAC	Carbon Dioxide Information Analysis Centre (U.S.)
CMAP	CPC Merged Analysis of Precipitation (CPC is the NOAA Climate Prediction Center)
CTD	Conductivity-Temperature-Depth probe
CZCS	Coastal Zone Colour Scanner
DIC	dissolved inorganic carbon
DO	dissolved oxygen
DOC	dissolved organic carbon
ESTOC	European Station for Time Series in the Ocean
FRA	Fisheries Research Agency (Japan)
FRRF	Fast repetition rate fluorometer
GLOBEC	Global Ocean Ecosystem Dynamics
GOA-ON	Global Ocean Acidification Observing Network
GPCP	Global Precipitation Climatology Project
IMECOCAL	Investigaciones Mexicanas de la Corriente de California
JSPS	Japan Society for the Promotion of Science
MBARI	Monterey Bay Aquarium Research Institute
MERI	Marine Ecology Research Institute
MODIS	Moderate Resolution Imaging Spectrometer
MOE	Ministry of the Environment (Japan)
NASA	National Aeronatics and Space Administration (U.S.)
NBS	National Bureau of Standards (now known as the National Institute of Standards and Technology - NIST)
NERR	National Estuarine Research Reserve
NGO	Non-governmental Organization
NIES	National Institute of Environmental Studies (Japan)
NOAA	National Oceanic and Atmospheric Administration
NOA-ON	NOAA Ocean Acidification Observing Network
NSF OOI	National Science Foundation Ocean Observatories Initiative
OAP-IOOS	Ocean Acidification Program Integrated Ocean Observing System
OCNMS	Olympic Coast National Marine Sanctuary
OMEGAS	Ocean Margin Ecosystems Group for Acidification Studies
PAR	photosynthetically active radation
SeaWiFS	Sea-viewing Wide Field-of-View Sensor
SOCAT	Surface Ocean CO_2 Atlas
TDN	total dissolved nitrogen
TUMSAT	Tokyo University of Marine Science and Technology
WCOA	West Coast Ocean Acidification
WOCE	World Ocean Circulation Experiment

REFERENCES

Agostini, S., Harvey, B.P., Wada, S., Kon, K., Milazzo, M., Inaba, K., Hall-Spencer, J.M. 2018. Ocean acidification drives community shifts towards simplified non-calcified habitats in a subtropical-temperate transition zone. *Scientific Reports* 8: doi: 10.1038/s41598-018-29251-7.

Alexander, M.A., Scott, J.D., Friedland, K.D., Mills, K.E., Nye, J.A., Pershing, A.J., Thomas, A.C. 2018. Projected sea surface temperatures over the 21st century: Changes in the mean, variability and extremes for large marine ecosystem regions of northern oceans. *Elementa - Science of the Anthropocene* 6: doi:10.1525/elementa.191.

Alin, S.R., Feely, R.A., Dickson, A.G., Hernández-Ayón, J.M., Juranek, L.W., Ohman, M.D., Goericke, R. 2012. Robust empirical relationships for estimating the carbonate system in the southern California Current System and application to CalCOFI hydrographic cruise data (2005-2011). *Journal of Geophysical Research* 117: doi:10.1029/2011JC007511.

Andreev, A.G., Baturina, V.I. 2006. Impacts of tides and atmospheric forcing variability on dissolved oxygen in the subarctic North Pacific. *Journal of Geophysical Research* 111: doi:10.1029/2005JC003103.

Aydin, K.Y., McFarlane, G.A., King, J.R., Megrey, B.A., Myers, K.W. 2005. Linking oceanic food webs to coastal production and growth rates of Pacific salmon (*Oncorhynchus* spp.), using models on three scales. *Deep-Sea Research Part II - Topical Studies in Oceanography* 52: 757-780.

Banas, N.S., Conway-Cranos, L., Sutherland, D.A., MacCready, P., Kiffney, P., Plummer, M. 2015. Patterns of river influence and connectivity among subbasins of Puget Sound, with application to bacterial and nutrient loading. *Estuaries and Coasts* 38: 735-753.

Banse, K., English, D.C. 1999. Comparing phytoplankton seasonality in the eastern and western subarctic Pacific and the western Bering Sea. *Progress in Oceanography* 43: 235-288.

Barth, J.A., Pierce, S.D., Castelao, R.M. 2005. Time-dependent, wind-driven flow over a shallow midshelf submarine bank. *Journal of Geophysical Research* 110: doi:10.1029/2004JC002761.

Barton, A., Hales, B., Waldbusser, G.G., Langdon, C., Feely, R.A. 2012. The Pacific oyster, *Crassostrea gigas*, shows negative correlation to naturally elevated carbon dioxide levels: Implications for near-term ocean acidification effects. *Limnology and Oceanography* 57: 698-710.

*B*ates, N.R., Astor, Y.M., Church, M.J., Currie, K., Dore, J.E., González-Dávila, M., Lorenzoni, L., Muller-Karger, F., Olafsson, J., Santana-Casiano, J.M. 2014. A time-series view of changing surface ocean chemistry due to ocean uptake of anthropogenic CO_2 and ocean acidification. *Oceanography* 27: 126-141.

Beardsley, R., Limeburner, R., Yu, H., Cannon, G. 1985. Discharge of the Changjiang (Yangtze River) into the East China Sea. *Continental Shelf Research* 4: 57-76.

Bednaršek, N., Tarling, G.A., Bakker, D.C.E., Fielding, S., Jones, E.M., Venables, H.J., Ward, P., Kuzirian, A., Leze, B., Feely, R.A., Murphy, E.J. 2012. Extensive dissolution of live pteropods in the Southern Ocean. *Nature Geoscience* 5: 881-885.

Bednaršek, N., Tarling, G.A., Bakker, D.C.E., Fielding, S., Feely, R.A. 2014. Dissolution dominating calcification process in polar pteropods close to the point of aragonite undersaturation. *PLoS One* 9: doi: 10.1371/journal.pone.0109183.

Bednaršek, N., Feely, R.A., Tolimieri, N., Hermann, A.J., Siedlecki, S.A., Waldbusser, G.G., McElhany, P., Alin, S.R., Klinger, T., Moore-Maley, B., Pörtner, H.O. 2017. Exposure history determines pteropod vulnerability to ocean acidification along the US West Coast. *Scientific Reports* 7: doi: 10.1038/s41598-017-03934-z.

Belan, T.A. 2003. Benthos abundance pattern and species composition in conditions of pollution in Amursky Bay (the Peter the Great Bay, the Sea of Japan). *Marine Pollution Bulletin* 46: 1111-1119.

Bond, N.A., Cronin, M.F., Freeland, H., Mantua, N. 2015. Causes and impacts of the 2014 warm anomaly in the NE Pacific. *Geophysical Research Letters* 42: 3414-3420.

Broerse, A.T.C., Ziveri, P., Honjo, S. 2000. Coccolithophore ($CaCO_3$) flux in the Sea of Okhotsk: seasonality, settling and alteration processes. *Marine Micropaleontology* 39: 179-200.

Bubenshchikova, N., Nürnberg, D., Lembke-Jene, L., Pavlova, G. 2008. Living benthic foraminifera of the Okhotsk Sea: Faunal composition, standing stocks and microhabitats. *Marine Micropaleontology* 69: 314-333.

Cai, W., Hu, X., Huang, W., Murrell, M.C., Lehrter, J.C., Lohrenz, S.E., Chou, W., Zhai, W., Hollibaugh, J.T., Wang, Y., Zhao, P., Guo, X., Gundersen, K., Dai, M., Gong, G. 2011. Acidification of subsurface coastal waters enhanced by eutrophication. *Nature Geoscience* 4: 766-770.

Chan, F., Barth, J.A., Lubchenco, J., Kirincich, A., Weeks, H., Peterson, W.T., Menge, B.A. 2008. Emergence of anoxia in the California current large marine ecosystem. *Science* 319: 920, doi: 10.1126/science.1149016.

Chan, F., Barth, J.A., Blanchette, C.A., Byrne, R.H., Chavez, F., Cheriton, O., Feely, R.A., Friederich, G., Gaylord, B., Gouhier, T., Hacker, S., Hill, T., Hofmann, G., McManus, M.A., Menge, B.A., Nielsen, K.J., Russell, A., Sanford, E., Sevadjian, J., Washburn, L. 2017. Persistent spatial structuring of coastal ocean acidification in the California Current System. *Scientific Reports* 7: doi: 10.1038/s41598-017-02777-y.

Chavez, F.P., Pennington, J.T., Michisaki, R.P., Blum, M., Chavez, G.M., Friederich, J., Jones, B., Herlien, R., Kieft, B., Hobson, B., Ren, A.S., Ryan, J., Sevadjian, J.C., Wahl, C., Walz, K.R., Yamahara, K., Friederich, G.E., Messié, M. 2017. Climate variability and change response of a coastal ocean ecosystem. *Oceanography* 30: 128-145.

Chen, C.-C., Gong, G.-C., Shiah, F.-K. 2007. Hypoxia in the East China Sea: One of the largest coastal low-oxygen areas in the world. *Marine Environmental Research* 64: 399-408.

Chen, C.-T.A., Bychkov, A.S., Wang, S.L, Pavlova, G.Yu. 1999. An anoxic Sea of Japan by the year 2200? *Marine Chemistry* 67: 249-265.

Chen, C.-T.A., Andreev, A., Kim, K.-R., Yamamoto, M. 2004a. Roles of continental shelves and marginal seas in the biogeochemical cycles of the North Pacific Ocean. *Journal of Oceanography* 60: 17-44.

Chen, C. -T.A, Lui, H.-K., Hsieh, C.-H., Yanagi, T., Kosugi, N., Ishii, M., Gong, G.-C. 2017. Deep oceans may acidify faster than anticipated due to global warming. *Nature Climate Change* 7: 890-894.

Chen, L., Gao, Z. 2007. Spatial variability in the partial pressures of CO_2 in the northern Bering and Chukchi seas. *Deep-Sea Research Part II-Topical Studies in Oceanography* 54: 2619-2629.

Chen, L., Gao, Z., Wang, W., Yang, X. 2004b. Characteristics of pCO_2 in surface water of the Bering Abyssal Plain and their effects on carbon cycle in the western Arctic Ocean. *Science in China Series D-Earth Sciences* 47: 1035-1044.

Christian, J.R. 2014. Timing of the departure of ocean biogeochemical cycles from the preindustrial state. *PLoS One* 9: doi: 10.1371/journal.pone.0109820.

Codispoti, L.A., Friederich, G.E., Iverson, R.L., Hood, D.W. 1982. Temporal changes in the inorganic carbon system of the southeastern Bering Sea during spring 1980. *Nature* 296: 242-245.

Connolly, T.P., Hickey, B.M., Geier, S.L., Cochlan, W.P. 2010. Processes influencing seasonal hypoxia in the northern California Current System. *Journal of Geophysical Research* 115: doi: 10.1029/2009JC005283.

Crawford, W., Peña, M. 2013. Declining oxygen on the British Columbia continental shelf. *Atmosphere-Ocean* 51: 88-103.

Cross, J.N., Mathis, J.T., Bates, N.R. 2012. Hydrographic controls on net community production and total organic carbon distributions in the eastern Bering Sea. *Deep-Sea Research Part II-Topical Studies in Oceanography* 65-70: 98-109.

Deur, D., Dick (Kwaxsistalla), A., Recalma-Clutesi (Ogwi'low'qua), K., Turner, N.J. 2015. Kwakwaka'wakw "Clam Gardens": Motive and agency in traditional northwest coast mariculture. *Human Ecology* 43: 201-212.

Diaz, R., Eriksson-Hägg, H., Rosenberg, R. 2013. Hypoxia, pp. 67-96, In Noone, K., Sumaila, U.R., Diaz, R. (eds.), Managing Ocean Environments in a Changing Climate, Elsevier, Amsterdam.

Dore, J.E., Lukas, R., Sadler, D.W., Church, M.J., Karl, D.M. 2009. Physical and biogeochemical modulation of ocean acidification in the central North Pacific. *Proceedings of the National Academy of Sciences of the United States of America* 106: 12,235-12,240.

Dugan, D., Janzen, C., McCammon, M., Evans, W., Bidlack, A. 2018. The evolution of ocean acidification observing efforts in Alaska and the development of an Alaska Ocean Acidification Network, OCEANS 2017, Anchorage, AK, 18-21 September 2017. available at https://ieeexplore.ieee.org/document/8232393

Durski, S.M., Barth, J.A., McWilliams, J.C., Frenzel, H., Deutsch, C. 2017. The influence of variable slope-water characteristics on dissolved oxygen levels in the northern California Current System. *Journal of Geophysical Research* 122: 7674-7697.

Ekstrom, J.A., Suatoni, L., Cooley, S.R., Pendleton, L.H., Waldbusser, G.G., Cinner, J.E., Ritter, J., Langdon, C., Van Hooidonk, R., Gledhill, D., Wellman, K., Beck, M.W., Brander, L.M., Rittschof, D., Doherty, C., Edwards, P.E.T., Portela, R. 2015. Vulnerability and adaptation of US shellfisheries to ocean acidification. *Nature Climate Change* 5: 207-214.3

Ellis, R.P., Davison, W., Queirós, A.M., Kroeker, K.J., Calosi, P., Dupont, S., Spicer, J.I., Wilson, R.W., Widdicombe, S., Urbina, M.A. 2017. Does sex really matter? Explaining intraspecies variation in ocean acidification responses. *Biology Letters* 13: doi: 10.1098/rsbl.2016.0761.

England, M.H. 1995. The age of water and ventilation timescales in a global ocean model. *Journal of Physical Oceanography* 25: 2756-2777.

Evans, W., Mathis, J. 2013. The Gulf of Alaska coastal ocean as an atmospheric CO_2 sink. *Continental Shelf Research* 65: 52-63.

Evans, W., Mathis, J., Cross, J. 2014. Calcium carbonate corrosivity in an Alaskan inland sea. *Biogeosciences* 11: 365-379.

Evans, W., Mathis, J., Ramsay, J., Hetrick, J. 2015. On the frontline: tracking ocean acidification in an Alaskan shellfish hatchery. *PLoS One* 10: doi:10.1371/journal.pone.0130384.

Evans, W., Mathis, J., Winsor, P., Statscewich, H., Whitledge, T. 2013. A regression modeling approach for studying carbonate system variability in the northern Gulf of Alaska. *Journal of Geophysical Research* 118: 476-489.

Evans, W., Hales, B., Strutton, P., Ianson, D. 2012. Sea-air CO_2 fluxes in the western Canadian coastal ocean. *Progress in Oceanography* 101: 78-91.

Evans, W., Pocock, K., Hare, A., Weekes, C., Hales, B., Jackson, J., Gurney-Smith, H., Mathis, J.T., Alin, S.R., Feely, R.A. 2019. Marine CO_2 patterns in the northern Salish Sea. *Frontiers in Marine Science* 5: doi: 10.3389/fmars.2018.00536.

Fabry, V. 1989. Aragonite production by pteropod mollusks in the sub-arctic Pacific. *Deep-Sea Research Part A - Oceanographic Research Papers* 36: 1735-1751.

Fassbender, A.J., Sabine, C.L., Lawrence-Slavas, N., De Carlo, E.H., Meinig, C., Maenner Jones, S. 2015. Robust sensor for extended autonomous measurements of surface ocean dissolved inorganic carbon. *Environmental Science and Technology* 49: 3628-3635.

Fassbender, A.J., Alin, S.R., Feely, R.A., Sutton, A.J., Newton, J.A., Krembs, C., Bos, J., Keyzers, M., Devol, A., Ruef, W., Pelletier, G. 2018. Seasonal carbonate chemistry variability in marine surface waters of the US Pacific Northwest. *Earth System Science Data* 10: 1367-1401.

Feely, R.A., Sabine, C.L., Lee, K., Berelson, W., Kleypas, J., Fabry, V.J., Millero, F.J. 2004. Impact of anthropogenic CO_2 on the $CaCO_3$ system in the oceans. *Science* 305: 362-366.

Feely, R.A., Sabine, C.L., Hernández-Ayón, J.M., Ianson, D., Hales, B. 2008. Evidence for upwelling of corrosive "acidified" water onto the continental shelf. *Science* 320: 1490-1492.

Feely, R., Alin, S., Newton, J., Sabine, C., Warner, M., Devol, A., Krembs, C., Maloy, C. 2010. The combined effects of ocean acidification, mixing, and respiration on pH and carbonate saturation in an urbanized estuary. *Estuarine, Coastal and Shelf Science* 88: 442-449.

Feely, R.A., Alin, S.R., Carter, B., Bednaršek, N., Hales, B., Chan, F., Hill, T.M., Gaylord, B., Sanford, E., Byrne, R.H., Sabine, C.L., Greeley, D., Juranek, L. 2016. Chemical and biological impacts of ocean acidification along the west coast of North America. *Estuarine, Coastal and Shelf Science* 183: 260-270.

Feely, R.A., Okazaki, R.R., Cai, W.-J., Bednaršek, N., Alin, S.R., Byrne, R.H., Fassbender, A. 2018. The combined effects of acidification and hypoxia on pH and aragonite saturation in the coastal waters of the California current ecosystem and the northern Gulf of Mexico. *Continental Shelf Research* 152: 50-60.

Freeland, H.J., Bychkov, A.S., Whitney, F., Taylor, C., Wong, C.S., Yurasov, G.I. 1998. WOCE section P1W in the Sea of Okhotsk - 1. Oceanographic data description. *Journal of Geophysical Research* 103: 15613-15623.

Gamo, T. 1999. Global warming may have slowed down the deep conveyor belt of a marginal sea of the northwestern Pacific: Japan Sea. *Geophysical Research Letters* 26: 3137-3140.

Gamo, T., Nozaki, Y., Sakai, H., Nakai, T., Tsubota, H. 1986. Spatial and temporal variations of water characteristics in the Japan Sea bottom layer. *Journal of Marine Research* 44: 781-793.

Gamo, T., Nakayama, N., Takahata, N., Sano, Y., Zhang, J., Yamazaki, E., Taniyasu, S., Yamashita, N. 2014. The Sea of Japan and its unique chemistry revealed by time-series observations over the last 30 years. *Monographs on Environment, Earth and Planets* 2: 1-22.

Gao, Z., Sun, H., Chen, L., Zhang, F. 2012. Summertime freshwater fractions in the surface water of the western Arctic Ocean evaluated from total alkalinity. *Advances in Polar Science* 2: 95-102.

Gazeau, F., Parker, L., Comeau, S., Gattuso, J., O'Connor, W., Martin, S., Pörtner, H., Ross, P. 2013. Impacts of ocean acidification on marine shelled molluscs. *Marine Biology* 160: 2207-2245.

Gewin, V. 2010. Dead in the water. *Nature* 466: 812-814.

Grantham, B., Chan, F., Nielsen, K., Fox, D., Barth, J., Huyer, A., Lubchenco, J., Menge, B. 2004. Upwelling-driven nearshore hypoxia signals ecosystem and oceanographic changes in the northeast Pacific. *Nature* 429: 749-754.

Gruber, N., Hauri, C., Lachkar, Z., Loher, D., Frölicher, T.L., Plattner, G.K. 2012. Rapid progression of ocean acidification in the California Current system. *Science* 337: 220-223.

Haigh, R., Ianson, D., Holt, C., Neate, H., Edwards, A. 2015. Effects of ocean acidification on temperate coastal marine ecosystems and fisheries in the northeast Pacific. *PLoS One* 10: doi: 10.1371/journal.pone.0117533.

Hales, B., Karp-Boss, L., Perlin, A., Wheeler, P.A. 2006. Oxygen production and carbon sequestration in an upwelling coastal margin. *Global Biogeochemical Cycles* 20: doi:10.1029/2005GB002517.

Harris, R.M.B., Beaumont, L.J., Vance, T.R., Tozer, C.R., Remenyi, T.A., Perkins-Kirkpatrick, S.E., Mitchell, P.J., Nicotra, A.B., McGregor, S., Andrew, N.R., Letnic, M., Kearney, M.R., Wernberg, T., Hutley, L.B., Chambers, L.E., Fletcher, M.-S., Keatley, M.R., Woodward, C.A., Williamson, G., Duke, N.C., Bowman, D.M.J.S. 2018. Biological responses to the press and pulse of climate trends and extreme events. *Nature Climate Change* 8: 579-587.

Hauri, C., Gruber, N., McDonnell, A.M.P., Vogt, M. 2013a. The intensity, duration, and severity of low aragonite saturation state events on the California continental shelf. *Geophysical Research Letters* 40: 3424-3428.

Hauri, C., Gruber, N., Vogt, M., Doney, S.C., Feely, R.A., Lachkar, Z., Leinweber, A., McDonnell, A.M.P., Munnich, M., Plattner, G.-K. 2013b. Spatiotemporal variability and long-term trends of ocean acidification in the California Current System. *Biogeosciences* 10: 193-216.

Hickey, B., Geier, S., Kachel, N., Ramp, S., Kosro, P.M., Connolly, T.P. 2016. Alongcoast structure and interannual variability of seasonal midshelf water properties and velocity in the Northern California Current System. *Journal of Geophysical Research* 121: 7408-7430.

Hill, D., Bruhis, N., Calos, S., Arendt, A., Beamer, J. 2015. Spatial and temporal variability of freshwater discharge into the Gulf of Alaska. *Journal of Geophysical Research* 120: 634-646.

Hill, K.I., Weaver, A.J., Freeland, H.J., Bychkov, A. 2003. Evidence of change in the Sea of Okhotsk: Implications for the North Pacific. *Atmosphere-Ocean* 41: 49-63.

Holsman, K., Hollowed, A., Ito, S.-I., Bograd. S., Hazen. E., King, J., Mueter, F., Perry, R.I. 2018. Climate change impacts, vulnerabilities and adaptations: North Pacific and Pacific Arctic marine fisheries. pp. 113-138, In Barange, M., Bahri, T., Beveridge, M.C.M., Cochrane, K.L., Funge-Smith, S., Poulaine, F. (eds.), Impacts of climate change on fisheries and aquaculture: synthesis of current knowledge, adaptation and mitigation options. *FAO Fisheries and Aquaculture Technical Paper* 627.

Ianson, D., Allen, S.E., Moore-Maley, B.L., Johannessen, S.C., Macdonald, R.W. 2016. Vulnerability of a semienclosed estuarine sea to ocean acidification in contrast with hypoxia. *Geophysical Research Letters* 43: 5793-5801.

Iida, Y., Kojima, A., Takatani, Y., Nakano, T., Sugimoto, H., Midorikawa, T., Ishii, M. 2015. Trends in pCO_2 and sea-air CO_2 flux over the global open oceans for the last two decades. *Journal of Oceanography* 71: 637-661.

Imbrie, J., Boyle, E., Clemens, S., Duffy, A., Howard, W., Kukla, G., Kutzbach, J., Martinson, D., McIntyre, A., Mix, A., Molfino, B., Morley, J., Peterson, L., Pisias, N., Prell, W., Raymo, M., Shackleton, N., Toggweiler, J. 1992. On the structure and origin of major glaciation cycles 1. Linear responses to Milankovitch forcing. *Paleoceanography* 7: 701-738.

Ishii, M., Kosugi, N., Sasano, D., Saito, S., Midorikawa, T., Inoue, H. Y. 2011. Ocean acidification off the south coast of Japan: A result from time series observations of CO_2 parameters from 1994 to 2008. *Journal of Geophysical Research* 116: doi:10.1029/2010JC006831 .

Itaki, T., Ikehara, K., Motoyama, I., Hasegawa, S. 2004. Abrupt ventilation changes in the Japan Sea over the last 30 ky: evidence from deep-dwelling radiolarians. *Palaeogeography, Palaeoclimatology, Palaeoecology* 208: 263-278.

Jackson, J.B.C. 2001. What was natural in the coastal oceans? Proceedings of the *National Academy of Sciences of the United States of America* 98: 5411-5418.

Jackson, J., Johnson, G., Dosser, H., Ross, T. 2018. Warming from recent marine heatwave lingers in deep British Columbia fjord. *Geophysical Research Letters* 45: 9757-9764.

Jamieson, G.S., Pellegrin, N., Jesson, S. 2007. Taxonomy and zoogeography of cold-water corals in coastal British Columbia, pp. 215-229, In George, R.Y. Cairns, S.D. (eds.), Conservation and adaptive management of seamount and deep-sea coral ecosystems. *Bulletin of Marine Science*, Volume 81, Supplement 1.

Johannessen, S.C., Masson, D., Macdonald, R.W. 2014. Oxygen in the deep Strait of Georgia, 1951-2009. The roles of mixing, deep-water renewal, and remineralization of organic carbon. *Limnology and Oceanography* 59: 211-222.

Johnson, K.M., King, A.E., Sieburth, J.McN. 1985. Coulometric TCO_2 analyses for marine studies - an introduction. *Marine Chemistry* 16: 61-82.

Johnson, K.S., Pytkowicz, R.M., Wong, C.S. 1979. Biological production and the exchange of oxygen and carbon-dioxide across the sea-surface in Stuart Channel, British Columbia. *Limnology and Oceanography* 24: 474-482.

Johnson, K.S., Plant, J.N., Coletti, L.J., Jannasch, H.W., Sakamoto, C.M., Riser, S.C., Swift, D.D., Williams, N.L., Boss, E., Haentjens, N., Talley, L.D., Sarmiento, J.L. 2017. Biogeochemical sensor performance in the SOCCOM profiling float array. *Journal of Geophysical Research* 122: 6416-6436.

Juranek, L.W., Feely, R.A., Peterson, W.T., Alin, S.R., Hales, B., Lee, K., Sabine, C.L., Peterson, J. 2009. A novel method for determination of aragonite saturation state on the continental shelf of central Oregon using multi-parameter relationships with hydrographic data. *Geophysical Research Letters* 36: doi:10.1029/2009GL040778.

Kang, D.-J., Kim, J.-Y., Lee, T., Kim, K.-R. 2004. Will the East/Japan Sea become an anoxic sea in the next century? *Marine Chemistry* 91: 77-84.

Kashiwase, H., Ohshima, K., Nihashi, S. 2014. Long-term variation in sea ice production and its relation to the intermediate water in the Sea of Okhotsk. *Progress in Oceanography* 126: 21-32.

Kayanne, H. 2017. Validation of degree heating weeks as a coral bleaching index in the northwestern Pacific. *Coral Reefs* 36: 63-70.

Keeling, R.F., Körtzinger, A., Gruber, N. 2010. Ocean deoxygenation in a warming world. *Annual Review of Marine Science* 2: 199-229.

Kim, J.-Y., Kang, D.-J., Lee, T., Kim, K.-R. 2014. Long-term trend of CO_2 and ocean acidification in the surface water of the Ulleung Basin, the East/Japan Sea inferred from the underway observational data. *Biogeosciences* 11: 2443-2454.

Kim, K., Kim, K.-R., Min, D.-H., Volkov, Y., Yoon, J.-H., Takematsu, M. 2001. Warming and structural changes in the East (Japan) Sea: A clue to future changes in global oceans? *Geophysical Research Letters* 28: 3293-3296.

Kim, K., Kim, K.-R., Kim, Y.-G., Cho, Y.-K., Kang, D.-J., Takematsu, M., Volkov, Y. 2004. Water masses and decadal variability in the East Sea (Sea of Japan). *Progress in Oceanography* 61: 157-174.

Kim, K.-R., Kim, K. 1996. What is happening in the East Sea (Japan Sea)?: Recent chemical observations from CREAMS 93-96. *Journal of the Korean Society of Oceanography* 31: 164–172.

Kim, K.-R., Kim, K., Kang, D.-J., Park, S.Y., Park, M.-K., Kim, Y.-G., Min, H.S., Min, D. 1999. The East Sea (Japan Sea) in change: A story of dissolved oxygen. *Marine Technology Society Journal* 33: 15-22.

Kim, T.-W., Lee, K., Feely, R.A., Sabine, C.L., Chen, C.-T.A., Jeong, H.J., Kim, K.Y. 2010. Prediction of Sea of Japan (East Sea) acidification over the past 40 years using a multiparameter regression model. *Global Biogeochemical Cycles* 24: doi:10.1029/2009GB003637.

Koslow, J.A., Goericke, R., Lara-Lopez, A., Watson, W. 2011. Impact of declining intermediate-water oxygen on deepwater fishes in the California Current. *Marine Ecology Progress Series* 436: 207-218.

Kroeker, K.J., Kordas, R.L., Harley, C.D.G. 2017. Embracing interactions in ocean acidification research: confronting multiple stressor scenarios and context dependence. *Biology Letters* 13: doi: 10.1098/rsbl.2016.0802.

Land, P.E., Shutler, J.D., Findlay, H.S., Girard-Ardhuin, F., Sabia, R., Reul, N., Piolle, J.F., Chapron, B., Quilfen, Y., Salisbury, J., Vandemark, D., Bellerby, R., Bhadury, P. 2015. Salinity from space unlocks satellite-based assessment of ocean acidification. *Environmental Science and Technology* 49: 1987-1994.

Lastovetsky, E.I., Veshcheva, V.M. 1964. Hydrometeorological description of Amursky and Ussurijsky Bays, In Zaokopnij, K.N. (ed.), Primorskoye Management of Hydrometeorological Service, Vladivostok (in Russian).

Lee, J., Park, K.-T., Lim, J.-H., Yoon, J.-E., Kim, I.-N. 2018. Hypoxia in Korean coastal waters: A case study of the natural Jinhae Bay and artificial Shihwa Bay. *Frontiers in Marine Science* 5: doi:10.3389/fmars.2018.00070.

Lee, T., Kim, K.H. 1998. A study on the origin of anomalous low saline Tsushima Current water using [228]Ra. *Journal of the Korean Society of Oceanography* 3: 175-182.

Lie, H., Cho, C., Lee, J., Lee, S. 2003. Structure and eastward extension of the Changjiang River plume in the East China Sea. *Journal of Geophysical Research* 108: doi:10.1029/2001JC001194.

Linacre, L., Durazo, R., Hernández-Ayón, J., Delgadillo-Hinojosa, F., Cervantes-Diaz, G., Lara-Lara, J., Camacho-Ibar, V., Siqueiros-Valencia, A., Bazan-Guzman, C. 2010. Temporal variability of the physical and chemical water characteristics at a coastal monitoring observatory: Station ENSENADA. Continental Shelf Research 30: 1730-1742.

Lui, H., Chen, C., Lee, J., Wang, S., Gong, G., Bai, Y., He, X. 2015. Acidifying intermediate water accelerates the acidification of seawater on shelves: An example of the East China Sea. *Continental Shelf Research* 111: 223-233.

Lyakhin, Y.I. 1970. Saturation of water of Sea of Okhotsk with calcium carbonate. *Oceanology* 10: 789-795.

Maas, A.E., Wishner, K.F., Seibel, B.A. 2012. The metabolic response of pteropods to acidification reflects natural CO_2-exposure in oxygen minimum zones. *Biogeosciences* 9: 747-757.

Mackas, D.L., Harrison, P.J. 1997. Nitrogenous nutrient sources and sinks in the Juan de Fuca Strait/Strait of Georgia/Puget Sound estuarine system: Assessing the potential for eutrophication. *Estuarine, Coastal and Shelf Science* 44: 1-21.

Mao, H.-L., Kan, T.-C., Lan, S.-F. 1963. A preliminary study of the Yangtze diluted water and its mixing processes. *Oceanologia et Limnologia Sinica* 5: 183-206. (in Chinese)

Martz, T.R., Daly, K.L., Byrne, R.H., Stillman, J.H., Turk, D. 2015. Technology for ocean acidification research: needs and availability. *Oceanography* 28: 40-47.

Masson, D., Cummins, P.F. 2007. Temperature trends and interannual variability in the Strait of Georgia, British Columbia. *Continental Shelf Research* 27: 634-649.

Masuzawa, T., Kitano, Y. 1984. Appearance of H_2S-bearing bottom waters during the last glacial period in the Japan Sea. *Geochemical Journal* 18: 167-172.

Mathis, J., Cooley, S., Lucey, N., Colt, S., Ekstrom, J., Hurst, T., Hauri, C., Evans, W., Cross, J., Feely, R. 2015. Ocean acidification risk assessment for Alaska's fishery sector. *Progress in Oceanography* 136: 71-91.

Mathis, J.T., Cross, J.N., Monacci, N., Feely, R.A., Stabeno, P. 2014. Evidence of prolonged aragonite undersaturations in the bottom waters of the southern Bering Sea shelf from autonomous sensors. *Deep-Sea Research Part II-Topical Studies in Oceanography* 109: 125-133.

Mohamedali, T., Roberts, M., Sackmann, B., Kolosseus, A. 2011. Puget Sound dissolved oxygen model nutrient load summary for 1999-2008. Washington Department of Ecology. Olympia, Washington. Publication No. 11-03-057.

Moore, S., Mantua, N.J., Newton, J.A., Kawase, M., Warner, M.J., Kellogg, J.P. 2008. A descriptive analysis of temporal and spatial patterns of variability in Puget Sound oceanographic properties. *Estuarine, Coastal and Shelf Science* 80: 545-554.

Moore-Maley, B.L., Allen, S.E., Ianson, D. 2016. Locally driven interannual variability of near-surface pH and Ω_A in the Strait of Georgia. *Journal of Geophysical Research* 121: 1600-1625.

Moore-Maley, B.L., Ianson, D., Allen, S.E. 2018. The sensitivity of estuarine aragonite saturation state and pH to the carbonate chemistry of a freshet-dominated river. *Biogeosciences* 15: 3743-3760.

Moshchenko, A.V., Belan, T.A. 2008. Ecological state and long–term changes of macrozoobenthos in the northern part of Amursky Bay (Sea of Japan), pp. 61-91, In Lutaenko, K.A., Vaschenko, M.A. (eds.), Ecological Studies and the State of Ecosysytems of Amursky Bay and Estuarine Zone of Razdolnaya River. Dalnauka, Vladivostok.

Murray, J.W., Roberts, E., Howard, E., O'Donnell, M., Bantam, C., Carrington, E., Foy, M., Paul, B., Fay, A. 2015. An inland sea high nitrate-low chlorophyll (HNLC) region with naturally high pCO_2. *Limnology and Oceanography* 60: 957-966.

Nakaoka, S., Telszewski, M., Nojiri, Y., Yasunaka, S., Miyazaki, C., Mukai, H., Usui, N. 2013. Estimating temporal and spatial variation of ocean surface pCO_2 in the North Pacific using a self-organizing map neural network technique. *Biogeosciences* 10: 6093-6106.

Nam, S., Takeshita, Y., Frieder, C.A., Martz, T., Ballard, J. 2015. Seasonal advection of Pacific equatorial water alters oxygen and pH in the Southern California Bight. *Journal of Geophysical Research* 120: 5387-5399.

Neal, E., Hood, E., Smikrud, K. 2010. Contribution of glacier runoff to freshwater discharge into the Gulf of Alaska. *Geophysical Research Letters* 37: doi: 10.1029/2010GL042385.

Nemcek, N., Ianson, D., Tortell, P. 2008. A high-resolution survey of DMS, CO_2, and O_2/Ar distributions in productive coastal waters. *Global Biogeochemical Cycles* 22: doi: 10.1029/2006GB002879.

Neudorf, C.M., Smith, N., Lepofsky, D., Toniello, G., Lian, O.B. 2017. Between a rock and a soft place: Using optical ages to date ancient clam gardens on the Pacific Northwest. *PLoS One* 12: doi: 10.1371/journal.pone.0171775.

Newton, J.A., Albertson, S.L., Van Voorhis, K., Maloy, C., Siegel, E. 2002. Washington State Marine Water Quality, 1998 through 2000. Environmental Assessment Program, Washington State Department of Ecology, Olympia, Washington. Publication No. 02-03-056.

Newton, J.A., Bassin, C.J., Devol, A., Richey, J., Kawase, M., Warner, M. 2011. Hood Canal dissolved oxygen program integrated assessment and modeling report. Chapter 1: Overview and results synthesis. http://www.hoodcanal.washington.edu/news-docs/publications.jsp.

Nimmergut, A., Abelmann, A. 2002. Spatial and seasonal changes of radiolarian standing stocks in the Sea of Okhotsk. *Deep-Sea Research Part I-Oceanographic Research Papers* 49: 463-493.

Ning, X., Lin, C., Su, J., Liu, C., Hao, Q., Le, F. 2011. Long-term changes of dissolved oxygen, hypoxia, the responses of the ecosystems in the East China Sea from 1975 to 1995. *Journal of Oceanography* 67: 59-75.

Nishioka, J., Mitsudera, H., Yasuda, I., Liu, H., Nakatsuka, T., Volkov, Y. 2014. Biogeochemical and physical processes in the Sea of Okhotsk and the linkage to the Pacific Ocean - Preface. *Progress in Oceanography* 126: 1-7.

Oba, T., Kato, M., Kitazato, H., Koizumi, I., Omura, A., Sakai, T., Takayama, T. 1991. Paleoenvironmental changes in the Japan Sea during the last 85,000 years. *Paleoceanography* 6: 499-518.

Ohshima, K.I., Nakanowatari, T., Riser, S., Volkov, Y., Wakatsuchi, M. 2014. Freshening and dense shelf water reduction in the Okhotsk Sea linked with sea ice decline. *Progress in Oceanography* 126: 71-79.

Oka, E., Ishii, M., Nakano, T., Suga, T., Kouketsu, S., Miyamoto, M., Nakano, H., Qiu, B., Sugimoto, S., Takatani, Y. 2018. Fifty years of the 137°E repeat hydrographic section in the western North Pacific Ocean. *Journal of Oceanography* 74: 115-145.

O'Neel, S., Hood, E., Bidlack, A., Fleming, S., Arimitsu, M., Arendt, A., Burgess, E., Sergeant, C., Beaudreau, A., Timm, K., Hayward, G., Reynolds, J., Pyare, S. 2015. Icefield-to-ocean linkages across the northern Pacific coastal temperate rainforest ecosystem. *Bioscience* 65: 499-512.

Onitsuka, T., Takami, H., Muraoka, D., Matsumoto, Y., Nakatsubo, A., Kimura, R., Ono, T., Nojiri, Y. 2018. Effects of ocean acidification with pCO_2 diurnal fluctuations on survival and larval shell formation of Ezo abalone, *Haliotis discus hannai*. *Marine Environmental Research* 134: 28-36.

Ono, T., Midorikawa, T., Watanabe, Y., Tadokoro, K., Saino, T. 2001. Temporal increases of phosphate and apparent oxygen utilization in the subsurface waters of western subarctic Pacific from 1968 to 1998. *Geophysical Research Letters* 28: 3285-3288.

Pavlova, G.Yu., Tishchenko, P.Ya., Nedashkovskii, A.P. 2008. Distribution of alkalinity and dissolved calcium in the Sea of Okhotsk. *Oceanology* 48: 23-32.

Pawlowicz, R., Riche, O., Halverson, M. 2007. The circulation and residence time of the Strait of Georgia using a simple mixing-box approach. *Atmosphere-Ocean* 45: 173-193.

Pelletier, G., Roberts, M., Keyzers, M., Alin, S.R. 2018. Seasonal variation in aragonite saturation in surface waters of Puget Sound - a pilot study. *Elementa - Science of the Anthropocene* 6: doi: 10.1525/elementa.270.

Peterson, J.O., Morgan, C.A., Peterson, W.T., Di Lorenzo, E. 2013. Seasonal and interannual variation in the extent of hypoxia in the northern California Current from 1998-2012. *Limnology and Oceanography* 58: 2279-2292.

Pierce, S., Barth, J., Shearman, R., Erofeev, A. 2012. Declining oxygen in the northeast Pacific. *Journal of Physical Oceanography* 42: 495-501.

Pierrot-Bults, A.C., Peijnenburg, K.T.C.A. 2015. Pteropods, pp. 1-10, In Harff, J., Meschede, M., Petersen, S., Thiede, J. (eds.), Encyclopedia of Marine Geosciences, Springer, Dordrecht, doi 10.1007/978-94-007-6644-0_88-1.

Pilcher, D., Siedlecki, S., Hermann, A., Coyle, K., Mathis, J., Evans, W. 2018. Simulated impact of glacial runoff on CO_2 uptake in the Gulf of Alaska. *Geophysical Research Letters* 45: 880-890.

Podorvanova, N.F., Ivashinnikova, T.S., Petrenko, V.C., Khomichuk, L.S. 1989. Main features of hydrochemistry of Peter the Great Bay (Japan Sea). DVO AN SSSR, DVGU, Vladivostok, 201 pp.

Ponomarev V.I., Salyuk A.N. 2001. The climate regime shifts and heat accumulation in the Sea of Japan. Proceedings of CREAMS'97 International Symposium, January 26-31, 1997, Fukuoka, Japan, pp.129-136.

Redkovskaya, Z.P. 1980. Influence of chemical pollutants on oxygen regime of Peter the Great Bay, pp. 94-103, In Belen'ky, V.S. (ed.), Estimations of Pollutant Migrations and Their Impact on Environment, FERHRI Report 73, Vladivostok (in Russian).

Reisdorph, S., Mathis, J. 2014. The dynamic controls on carbonate mineral saturation states and ocean acidification in a glacially dominated estuary. *Estuarine, Coastal and Shelf Science* 144: 8-18.

Reum, J.C.P., Alin, S.R., Feely, R.A., Newton, J., Warner, M., McElhany, P. 2014. Seasonal carbonate chemistry covariation with temperature, oxygen, and salinity in a fjord estuary: implications for the design of ocean acidification experiments. *PLoS One* 9: doi: 10.1371/journal.pone.0089619.

Rodionov, N.P. 1984. Impact of chemical pollutants on dissolved oxygen in Peter the Great Bay, pp. 118-150, In Kotlyakov, V.M. (ed.), Japan Sea. Forecast Pollutions of Seas of USSR. GIMIZ, Leningrad (in Russian).

Sabine, C., Feely, R., Gruber, N., Key, R., Lee, K., Bullister, J., Wanninkhof, R., Wong, C., Wallace, D., Tilbrook, B., Millero, F., Peng, T., Kozyr, A., Ono, T., Rios, A. 2004. The oceanic sink for anthropogenic CO_2. *Science* 305: 367-371.

Sabine, C.L., Mackenzie, F.T., Winn, C.W., Karl, D.M. 1995. Geochemistry of carbon-dioxide in seawater at the Hawaii Ocean Time-Series Station, ALOHA. *Global Biogeochemical Cycles* 9: 637-651.

Saitoh, S., Kishino, M., Kiyofuji, H., Taguchi, S., Takahashi, M. 1996. Seasonal variability of phytoplankton pigment concentration in the Okhotsk Sea. *Journal of the Remote Sensing Society of Japan* 16: 86-92.

Sanford, E., Sones, J., Garcia-Reyes, M., Goddard, J., Largier, J. 2019. Widespread shifts in the coastal biota of northern California during the 2014-2016 marine heatwaves. *Scientific Reports* 9: doi:10.1038/s41598-019-40784-3.

Sasano, D., Takatani, Y., Kosugi, N., Nakano, T., Midorikawa, T., Ishii, M. 2018: Decline and bidecadal oscillations of dissolved oxygen in the Oyashio region and their propagation to the western North Pacific. *Global Biogeochemical Cycles* 32, doi: 10.1029/2017GB005876.

Sergeant, C.J., Bellmore, J.R., McConnell, C., Moore, J.W. 2017. High salmon density and low discharge create periodic hypoxia in coastal rivers. *Ecosphere* 8: e01846. 10.1002/ecs2.1846.

Siedlecki, S.A., Banas, N.S., Davis, K.A., Giddings, S., Hickey, B.M., MacCready, P., Connolly, T., Geier, S. 2015. Seasonal and interannual oxygen variability on the Washington and Oregon continental shelves. *Journal of Geophysical Research* 120: 608-633.

Siedlecki, S.A., Kaplan, I.C., Hermann, A.J., Nguyen, T.T., Bond, N.A., Newton, J.A., Williams, G.D., Peterson, W.T., Alin, S.R., Feely, R.A. 2016. Experiments with seasonal forecasts of ocean conditions for the northern region of the California Current upwelling system. *Scientific Reports* 6: doi:10.1038/srep27203.

Siedlecki, S., Pilcher, D., Hermann, A., Coyle, K., Mathis, J. 2017. The importance of freshwater to spatial variability of aragonite saturation state in the Gulf of Alaska. *Journal of Geophysical Research* 122: 8482-8502.

Sorokin, Y., Sorokin, P. 1999. Production in the Sea of Okhotsk. *Journal of Plankton Research* 21: 201-230.

Stabeno, P., Bond, N., Hermann, A., Kachel, N., Mordy, C., Overland, J. 2004. Meteorology and oceanography of the northern Gulf of Alaska. *Continental Shelf Research* 24: 859-897.

Steinberg, P.D., Brett, M.T., Bechtold, J.S., Richey, J.E., Porensky, L.M., Smith, S.N. 2011. The influence of watershed characteristics on nitrogen export to and marine fate in Hood Canal, Washington, USA. *Biogeochemistry* 106: 415-433.

Stone, R.P. 2006. Coral habitat in the Aleutian Islands of Alaska: depth distribution, fine scale species associations, and fisheries interactions. *Coral Reefs* 25: 229-238.

Strom, S., Olson, M., Macri, E., Mordy, C. 2006. Cross-shelf gradients in phytoplankton community structure, nutrient utilization, and growth rate in the coastal Gulf of Alaska. *Marine Ecology Progress Series* 328: 75-92.

Sunday, J.M., Calosi, P., Dupont, S., Munday, P.L., Stillman, J.H., Reusch, T.B. 2014. Evolution in an acidifying ocean. *Trends in Ecology and Evolution* 29: 117-125.

Sutton, A., Feely, R., Maenner-Jones, S., Musielwicz, S., Osborne, J., Dietrich, C., Monacci, N., Cross, J., Bott, R., Kozyr, A., Andersson, A., Bates, N., Cai, W., Cronin, M., De Carlo, E., Hales, B., Howden, S., Lee, C., Manzello, D., McPhaden, M., Melendez, M., Mickett, J., Newton, J., Noakes, S., Noh, J., Olafsdottir, S., Salisbury, J., Send, U., Trull, T., Vandemark, D., Weller, R. 2019. Autonomous seawater pCO_2 and pH time series from 40 surface buoys and the emergence of anthropogenic trends. *Earth System Science Data* 11: 421-439.

Sutton, A.J., Sabine, C.L., Feely, R.A., Cai, W.-J., Cronin, M.F., McPhaden, M.J., Morell, J.M., Newton, J.A., Noh, J.-H., Ólafsdóttir, S.R., Salisbury, J.E., Send, U., Vandemark, D.C., Weller, R.A. 2016. Using present-day observations to detect when anthropogenic change forces surface ocean carbonate chemistry outside preindustrial bounds. *Biogeosciences* 13: 5065-5083.

Suzuki, T. and the PACIFICA Group 2013. PACIFICA Data Synthesis Project. NDP-092, ORNL/CDIAC-159.

Takao, S., Fujii, M. 2015. Ocean monitoring for evaluation of the impacts of ocean acidification to subarctic coastal ecosystem - diurnal pH variation in Oshoro Bay, Hokkaido Island, Japan. AORI Joint Research Meeting on "Forefront of marine ecological modeling: their outcome, cooperation and development for the next stage", March 3-4, 2015, Kashiwa, http://cesd.aori.u-tokyo.ac.jp/MEM/DL/sympo_marineeco2014/P20150304_fujii.pdf (in Japanese).

Takao, S., Kumagai, N., Yamano, H., Fujii, M., Yamanaka, Y. 2015. Projecting the impacts of rising seawater temperatures on the distribution of seaweeds around Japan under multiple climate change scenarios. *Ecology and Evolution* 5: 213-223.

Takatani, Y., Enyo, K., Iida, Y., Kojima, A., Nakano, T., Sasano, D., Kosugi, N., Midorikawa, T., Suzuki, T., Ishii, M. 2014. Relationships between total alkalinity in surface water and sea surface dynamic height in the Pacific Ocean. *Journal of Geophysical Research* 119: 2806-2814.

Talley, L.D. 1991. An Okhotsk Sea-water anomaly - implications for ventilation in the North Pacific. *Deep-Sea Research Part A-Oceanographic Research Papers* 38: S171-S190.

Talley, L.D. 2001. Okhotsk Sea circulation, pp. 2007-2015, In Steele, J.H., Thorpe, S.A., Turekian, K.K. (eds.), Encyclopedia of Ocean Sciences, Academic, San Diego.

Tanaka, K., Taino, S., Haraguchi, H., Prendergast, G., Hiraoka, M. 2012. Warming off southwestern Japan linked to distributional shifts of subtidal canopy-forming seaweeds. *Ecology and Evolution* 2: 2854-2865.

Thomson, R.E., Krassovski, M.V. 2010. Poleward reach of the California Undercurrent extension. *Journal of Geophysical Research* 115, doi: 10.1029/2010JC006280

Thomson, R.E. 1981. Oceanography of the British Columbia coast. Canadian Special Publication of Fisheries and Aquatic Sciences 56. 291 pp.

Tishchenko, P.Ya., Kang, D.-J., Chichkin, R.V., Lazaryuk, A.Yu., Wong, C.S., Johnson, W.K. 2011a. Application of potentiometric method using a cell without liquid junction to underway pH measurements in surface seawater. *Deep-Sea Research Part I - Oceanographic Research Papers* 58: 778–786.

Tishchenko, P.P., Tishchenko, P.Ya., Zvalinskii, V.I., Sergeev, A.F. 2011b. The carbonate system of Amur Bay (Sea of Japan) under conditions of hypoxia. *Oceanology* 51: 235-246.

Tishchenko, P.Y., Talley, L.D., Lobanov, V.B., Zhabin, I.A., Luchin, V.A., Nedashkovskii, A.P., Sagalaev, S.G., Chichkin, R.V., Shkirnikova, E.M., Ponomarev, V.I., Masten, D., Kang, D.J., Kim, K.R. 2003. Seasonal variability of the hydrochemical conditions in the Sea of Japan. *Oceanology* 43: 643-655.

Tishchenko P.Ya., Sergeev, A.F., Lobanov, V.B., Zvalinsky, V.I., Koltunov, A.M., Mikhajlik, T.T., Tishchenko, P.P., Shevtsova, M.G. 2008. Hypoxia in near-bottom waters of the Amursky Bay. *Bulletin of the Far Eastern Branch of the Russian Academy of Science* 6: 115-125 (in Russian).

Tishchenko, P.Ya., Lobanov, V.B., Zvalinsky, V.I., Sergeev, A.F., Koltunov, A., Mikhailik, T.A., Tishchenko, P.P., Shvetsova, M.G., Sagalaev, S., Volkova, T. 2013. Seasonal hypoxia of Amursky Bay in the Japan Sea: Formation and destruction. *Terrestrial Atmospheric and Oceanic Sciences* 24: 1033-1050.

Tkalin, A.V., Belan, T.A., Shapovalov, E.N. 1993. The state of the marine-environment near Vladivostok, Russia. *Marine Pollution Bulletin* 26: 418-422.

Trant, A.J., Nijland, W., Hoffman, K.M., Mathews, D.L., McLaren, D., Nelson, T.A., Starzomski, B.M. 2016. Intertidal resource use over millennia enhances forest productivity. *Nature Communications* 7: doi: 10.1038/ncomms12491.

Tully, J.P., Dodimead, A.J. 1957. Properties of the water in the Strait of Georgia, British Columbia, and influencing factors. *Journal of the Fisheries Research Board of Canada* 14: 241-319

Turi, G., Lachkar, Z., Gruber, N., Nunnich, M. 2016. Climatic modulation of recent trends in ocean acidification in the California Current system. *Environmental Research Letters* 11: doi:10.1088/1748-9326/11/1/014007.

Uehara, H., Kruts, A., Volkov, Y., Nakamura, T., Ono, T., Mitsudera, H. 2012. A new climatology of the Okhotsk Sea derived from the FERHRI database. *Journal of Oceanography* 68: 869-886

Veron, J.E.N., Minchin, P.R. 1992. Correlations between sea surface temperature, circulation patterns and the distribution of hermatypic corals of Japan. *Continental Shelf Research* 12: 835-857.

Voronkov, P.P. 1941. Hydrochemical state of the Peter the Great Bay of the Japan Sea, pp. 42-102, In Voronkov, P.P. (ed.), Problems of Marine Chemistry, Gidrometeoizdat, Leningrad.

Wada, S., Hama, T. 2013. The role of macroalgae as a factor controlling spatial variation of pH in coastal environment. Abstracts of 60th Annual Meeting of the Geochemical Society of Japan, https://www.jstage.jst.go.jp/article/geochemproc/60/0/60_159/_pdf (in Japanese).

Wakita, M., Watanabe, S., Murata, A., Tsurushima, N., and Honda, M. 2010. Decadal change of dissolved inorganic carbon in the subarctic western North Pacific Ocean. *Tellus B* 62: 608–620.

Wakita, M., Watanabe, S., Honda, M., Nagano, A., Kimoto, K., Matsumoto, K., Kitamura, M., Sasaki, K., Kawakami, H., Fujiki, T., Sasaoka, K., Nakano, Y., Murata, A. 2013. Ocean acidification from 1997 to 2011 in the subarctic western North Pacific Ocean. *Biogeosciences* 10: 7817-7827.

Wakita, M., Nagano, A., Fujiki, T., Watanabe, S. 2017. Slow acidification of the winter mixed layer in the subarctic western North Pacific. *Journal of Geophysical Research* 122: 6923-6935.

Waldbusser, G.G., Hales, B., Langdon, C.J., Haley, B.A., Schrader, P., Brunner, E.L., Gray, M.W., Miller, C.A., Gimenez, I. 2015. Saturation-state sensitivity of marine bivalve larvae to ocean acidification. *Nature Climate Change* 5: 273-280.

Waldichuk, M. 1957. Physical oceanography of the Strait of Georgia, British Columbia. *Journal of the Fisheries Research Board of Canada* 14: 321-486.

Wall-Palmer, D., Hart, M.B., Smart, C., Sparks, R.S.J., Le Friant, A., Boudon, G., Deplus, C., Komorowski, J.C. 2012. Pteropods from the Caribbean Sea: variations in calcification as an indicator of past ocean carbonate saturation. *Biogeosciences* 9: 309-315.

Walsh, J.J. 1991. Importance of continental margins in the marine biogeochemical cycling of carbon and nitrogen. *Nature* 350: 53-55.

Warner, M.J., Roden, G.I. 1995. Chlorofluorocarbon evidence for recent ventilation of the deep Bering Sea. *Nature* 373: 409-412.

Watanabe, Y., Chiba, T., Tanaka, T. 2011. Recent change in the oceanic uptake rate of anthropogenic carbon in the North Pacific subpolar region determined by using a carbon-13 time series. *Journal of Geophysical Research* 116: doi: 10.1029/2010JC006199.

Weingartner, T.J., Coyle, K., Finney, B., Hopcroft, R., Whitledge, T., Brodeur, R., Dagg, M., Farley, E., Haidvogal, D., Haldorson, L., Hermann, A., Hinckley, S., Napp, J., Stabeno, P.J., Kline, T., Lee, C., Lessard, E.J., Royer, T.C., Strom, S. 2002. The Northeast Pacific GLOBEC program: coastal Gulf of Alaska. *Oceanography* 15: 48-63.

Weingartner, T., Danielson, S., Royer, T. 2005. Freshwater variability and predictability in the Alaska Coastal Current. *Deep-Sea Research Part II - Topical Studies in Oceanography* 52: 169-191.

Weingartner, T. 2007. The physical environment of the Gulf of Alaska, pp. 12-47 In Spies, R.B., (ed.), Long-term ecological change in the northern Gulf of Alaska. Elsevier, Amsterdam.

Weingartner, T., Eisner, L., Eckert, G., Danielson, S. 2009. Southeast Alaska: oceanographic habitats and linkages. *Journal of Biogeography* 36: 387-400.

Weiss, R.F. 1970. Solubility of nitrogen, oxygen and argon in water and seawater. *Deep-Sea Research* 17: 721-735.

Whitney, F.A., Freeland, H.J., Robert, M. 2007. Persistently declining oxygen levels in the interior waters of the eastern subarctic Pacific. *Progress in Oceanography* 75: 179-199.

Yara, Y., Vogt, M., Fujii, M., Yamano, H., Hauri, C., Steinacher, M., Gruber, N., Yamanaka, Y. 2012. Ocean acidification limits temperature-induced poleward expansion of coral habitats around Japan. *Biogeosciences* 9: 4955-4968.

Yara, Y., Fujii, M., Yamano, H., Yamanaka, Y. 2014. Projected coral bleaching in response to future sea surface temperature rises and the uncertainties among climate models. *Hydrobiologia* 733: 19-29.

Yara, Y., Yamano, H., Steinacher, M., Fujii, M., Vogt, M., Gruber, N., Yamanaka, Y. 2016. Potential future coral habitats around Japan depend strongly on anthropogenic CO_2 emissions, pp. 41-56, In Nakano, S., Yahara, T., Nakashizuka, T. (eds.), Aquatic Biodiversity Conservation and Ecosystem Services, Springer, Tokyo.

Zachos, J.C., Röhl, U., Schellenberg, S.A., Sluijs, A., Hodell, D.A., Kelly, D.C., Thomas, E., Nicolo, M., Raffi, I., Lourens, L.J., McCarren, H., Kroon, D. 2005. Rapid acidification of the ocean during the Paleocene-Eocene thermal maximum. *Science* 308: 1611-1615.

North Pacific Marine Science Organization (PICES)